An-Najah National University

Faculty of Graduate Studies

Efficiency Improvement of Solar Water Heater by Using PV-Powered Pump

By

Mahmoud Abu Arrah

Supervisor

Prof. Marwan Mahmoud

This Thesis is Submitted in Partial Fulfillment of the Requirements for the Degree of Master of Engineering in Clean Energy and Conservation Strategy, Faculty of Graduate Studies, An-Najah National University, Nablus – Palestine.

2017

Efficiency Improvement of Solar Water Heater by Using PV-Powered Pump

By

Mahmoud Abu Arrah

This thesis was defended successfully on 29/1/2017 and approved by:

Defense committee Members	**Signature**
– **Prof. Marwan Mahmoud /Supervisor**	**…..……………..**
– **Prof. Afif Hasan /External Examiner**	**…………………**
– **Dr. Abdelrahim Abusafa /Internal Examiner**	**…………………**

Acknowledgments

All praises are due to Allah. Peace and blessing be upon His Messengers.

I would like to thank my supervisor, Professor Marwan Mahmoud for his guidance and support. His encouragement and constructive criticism made the completion of this study possible. Special thanks go to Eng. Luqman Herzollah and Eng. Ramiz Khaldi for their valuable comments.

My mother, I will never forget you always reminding me: “your study…your study”. My father you lived my academic life more than me. Both of you as if you were me working hard and waiting for this moment. Thank you. Special thanks go to Dr. Sufyan; my older brother for supporting me in this work. This work is all yours.

This work would have never been accomplished without the continues support of my family. My dear wife ‘Fatima’ and my little baby ‘Aya’. Fatima, you waited so long for this moment and I will never forget your co question: Mahmoud, how many tasks are left to go. This thesis is all yours. Thank you.

My brothers and sisters, you all lived my work. this thesis is all yours. Thank you.

Mahmoud Abu Arrah

الإقرار

أنا الموقع أدناه مقدم الرسالة التي تحمل العنوان:

Efficiency Improvement of Solar Water Heater by Using PV-Powered Pump

أقر بأن ما اشتملت عليه هذه الرسالة إنما هو نتاج جهدي الخاص، باستثناء ما تمّت الإشارة إليه حيثما ورد، وإنّ هذه الرسالة ككل، أو أي جزء منها لم يُقدّم من قبل لنيل أيّة درجة علمية أو لقب علمي أو بحثي لدى أيّة مؤسسة تعليمية أو بحثية أخرى.

Declaration

The work provided in this thesis -unless otherwise referenced- is the researcher's own work, and has not been submitted from elsewhere for any other degree or qualification.

Student's name:	**اسم الطّالب:**
Signature:	**التوقيع:**
Date:	**التاريخ:**

List of Contents

List of Figures

List of Tables

Abbreviations

Ac	Area collector (m^2)
C_p	Specific heat (J/ (Kg. K))
D	Diameter of the collector tube (mm)
h	Heat transfer coefficient ($W/(m^2.K)$)
k	Thermal conductivity (W/(m.K))
$\dot{m}$	Mass flow rate (Kg/s)
W	Tube spacing (mm)
δ	Plate thickness (mm)
T	Temperature (°C)
V	Volume (m^3)
v	Flow velocity (m/s)
α	Absorption coefficient
β	Collector inclination angle (deg)
ε	Emissivity
ρ	Density (Kg/m3)
σ	Stefan-Boltzmann constant ($W/ (m^2 K^4)$)
$(\tau\alpha)$	Effective transmittance-absorption coefficient
I	Solar intensity
G_t	Threshold radiation
R_e	Reynold number
Q	Energy
H	Head losses
P	Friction losses

Efficiency Improvement of Solar Water Heater by Using PV-Powered Pump

By
Mahmoud Abu Arrah
Supervisor
Prof. Marwan Mahmoud

Abstract

The main objective of this research is to analyze the impact of using solar driven pump to circulate the liquid on the overall efficiency of flat plate collector. To achieve this goal, accurate and practical mathematical models for flat plate collectors, storage tank and PV-pump were selected. These models were analyzed by using Matlab software. SWHSs in Palestine are thermosyphon systems. This thesis suggests adding a solar driven pump to the systems to circulate the fluid in order to increase their efficiency and this is the main contribution of the study. The study concludes that adding the circulation pump to thermosyphon system raises the annual efficiency of collectors from 33% to 37%. The study also concludes that by adding a PV pump with two panel of flat plate collector, this gives the same annual energy by using three panels of flat plate collector. Adding a solar pump also increases the solar fraction from 76 % to 86 % particularly in winter and the absorbed energy from the sun which means less electrical energy consumption.

Chapter One

Introduction

1 Introduction:

Solar domestic hot water (SDHW) systems are ranked among the most promising solar energy technologies. However, despite this optimistic view, several technical obstacles remain. Among these obstacles is that SDHW system requires an auxiliary electric source to operate a pump to circulate the fluid through the thermal collector. Also, the collector at a constant fluid flows need an ON/OFF deferential temperature sensing controller; this controller is the weakest component in SDHW systems which make the pump cycle between ON and OFF. As an alternative, PV cells can be used to power the SDHW system's pump and provide a continual adjustment of fluid flow [1], and possibly improving the system performance.

The use of PV cells to power the pumps of SDHW systems is an attractive concept because it serves two purposes. Firstly, a PV pumping system can act as a fast-response sensor to solar energy and therefore pumping will only be working at the times when the thermal collector is also receiving solar radiation. Secondly, using the PV cells can neglect the auxiliary power source to operate the pump [1].

In Palestine, energy sources consist of (i) the energy generated by petroleum and natural gas derivatives; (ii) electricity; and (iii) renewable energy (including solar power, and energy generated from burning wood, biogas, peat, etc.). With the exception of renewable energy, the Palestinian energy sector is distinctive of scarce sources and inability to exploit these sources, because it is fully dependent on importation of energy from Israel.

Residential electric water heating is considered as one of the higher energy intensive items; it accounts for approximately 18.2 % of the total energy consumption in Palestine [2]. Solar water heating (SWH) is the conversion of sunlight into thermal energy for water heating using a solar thermal collector. Solar water heating systems comprise various technologies that are used worldwide increasingly. Nowadays, more than 62.4% of households in Palestine are utilizing solar energy by using solar water heaters [3]. This percentage differs within the Palestinian regions. Figure (1.1) shows the percentage of households in Palestine using solar water heaters by region in 2005. The total area of installed SWH in Palestine is more than 1,500,000 square meters [4]. The PV Powered Pump could increase the efficiency of the solar collector, therefore decreasing the electrical energy consumption. The main type of solar collector used in Palestine is called flat plate collectors. Used SWH type depends on natural circulation of the fluid in the system. The reasons for using this system in residential places is cheapest, simple and requires less maintenance. The main purpose for this thesis is to increase the overall efficiency in solar water heater used in Palestine by using PV-powered pump to circulate the liquid in the system.

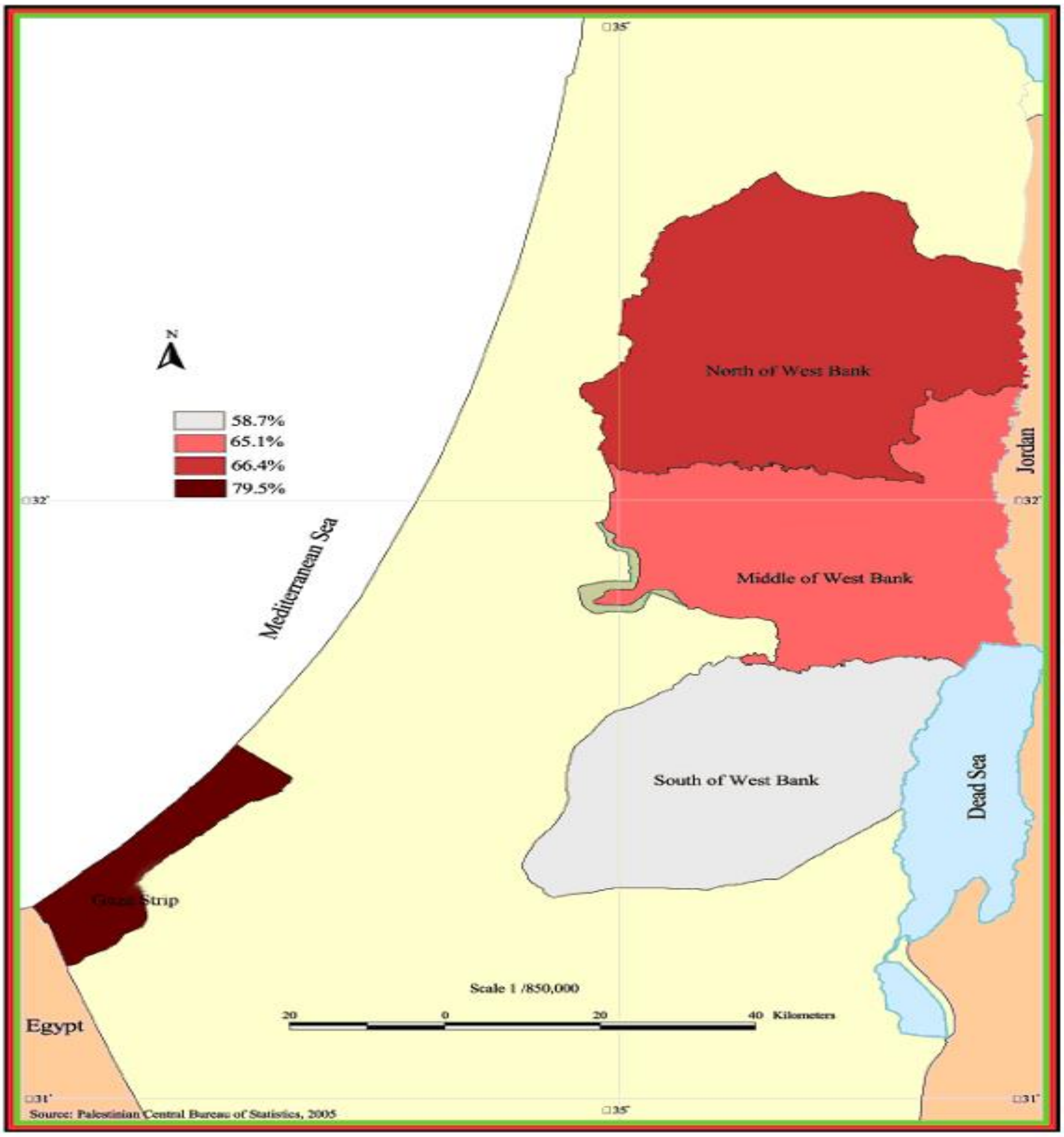

Figure 1.1: Percentage of households in Palestine using solar water heaters by region (PCBS, 2011)

Objectives:

The main goals for this thesis are:

- To analyze the effect of using solar pump to circulate the liquid on the overall efficiency of SWH systems.
- To Optimize and simulate SWH system by using MATLAB software.

- To compare the electric energy savings of the new solar water heater with the conventional SWH and the electric water heater.
- To analyze the economic feasibility of the new investigated PV-supported solar water system in comparison with the usually utilized thermosiphon type.

Methodology:

To achieve the goals of this research, accurate and practical mathematical models were selected for flat plat collectors, storage tank and PV-pump. These models will be solved by using MATLAB software. The theoretical results in this thesis are obtained from MATLAB code.

Chapter Tow

Solar Water Heater (SWH)

2 What is SWH?

Many types of solar water heater (SWH) are not used in Palestine. They are nevertheless many with different types as used in different parts of the world. In this section, we will review the general types of SWH. There are two types of SWH; the first type is the active solar water heater, which has circulating pumps and controllers; the second type is the passive solar water heater, which depends on natural circulation for the fluid without any external force [5].

2.1 Active solar water heating system

Active systems use electric pumps, valves, and controllers to circulate water or other heat-transfer fluids in the collectors. So, the active system is also called forced circulation systems. There are two types of active solar water heating systems:

2.1.1 Open loop (Direct) active system:

this type uses a pump to circulate household water through the collectors and into the home. This design is good because it lowers initial cost. However, this type is not appropriate if the fluid is acidic which causes pipe corrosion and quickly disables the system. This type of collector works well in climates where it rarely freezes [6].

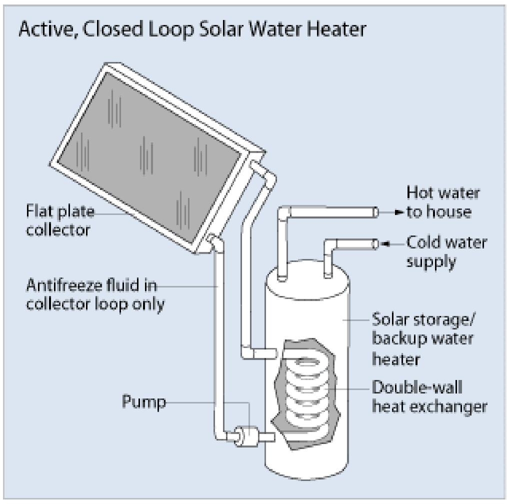

Figure 2.1: Schematic diagram for Active closed loop solar water heater [5]

2.1.2 Closed loop (indirect) active system:

A pump circulates a non-freezing fluid as illustrated in Figure 2-1. The heat transfers to the fluid by a heat exchanger from the collectors. This heats the water which then flows into the home. Closed loop systems are popular in high freezing temperatures because they offer good freeze protection [7].

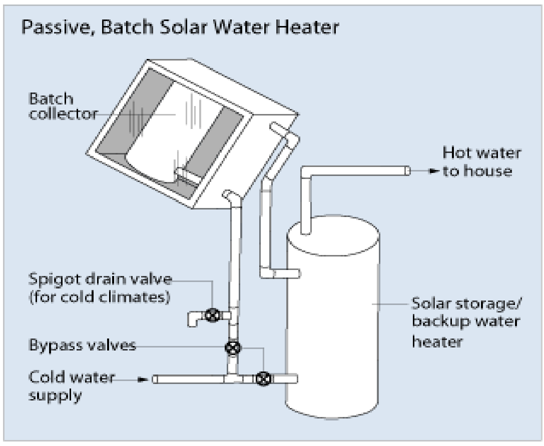

Figure 2.2: Schematic diagram for passive, batch solar water heater [5]

2.2 Passive solar water heating systems

Passive solar water heating systems are typically less expensive than active systems, but they are usually not as efficient. However, passive systems can be more reliable and may last longer. There are two basic types of passive systems:

2.2.1 Batch solar water heaters:

Batch solar water heaters, also called integral collector-storage (ICS) Systems are made up of a water tank or tubes inside an insulated, glazed box. Cold water flows through the solar collector as illustrated in Figure 2.2. The water is heated and then continues on to the backup water heating storage tank. There is no requirement for a pump. It has a simple design, few components, less maintenance and fewer failure chances [7].

2.2.2 Thermosyphon systems:

Water flows from the overhead tank to the bottom of the solar collector by natural circulation. Water circulates from the collector to a storage tank as long as the collector absorbs heat from the sun. The cold water in the bottom of the collector replaces the hot water, then the hot water is forced inside the insulated hot water storage tank. This process of thermosiphon systems is stopped when there is no solar radiation. Thermosiphon is simple and requires less maintenance. The efficiency of thermosiphon depends on the difference between the temperature of hot water and ambient temperature. However, thermosiphon system is not suitable for large systems; those with more than 10 m^2 of collector surface [9]. Furthermore, it's difficult to place the tank above the collector on buildings with sloping roofs. Figure 2.3 shows how thermosiphon systems work. The height difference between the top of the collector and the bottom of storage tank is usually 30cm in most cases [10]

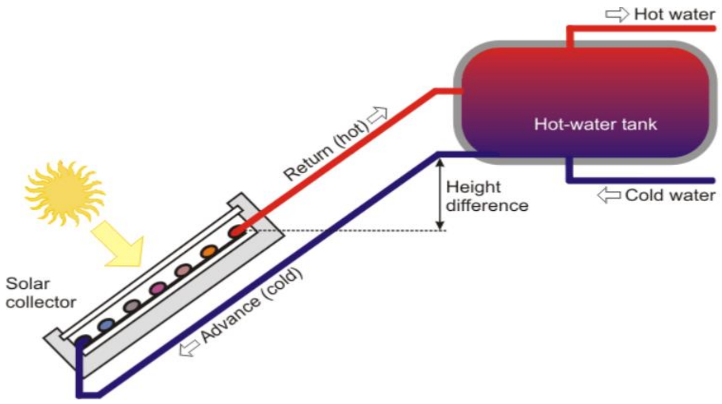

Figure 2.3: Thermosyphone system [5]

There are two types of solar collectors used for residential applications; namely flat plate collector and evacuated tube collector.

Flat-plate collector:

Glazed flat-plate collectors are insulated. They are weatherproofed boxes that contain a dark absorber plate under one or more glass or plastic (polymer) covers. There are two types of flat plate collectors.

- Header/Riser-Flat plate collector
- Serpentine Flat-plate Collector

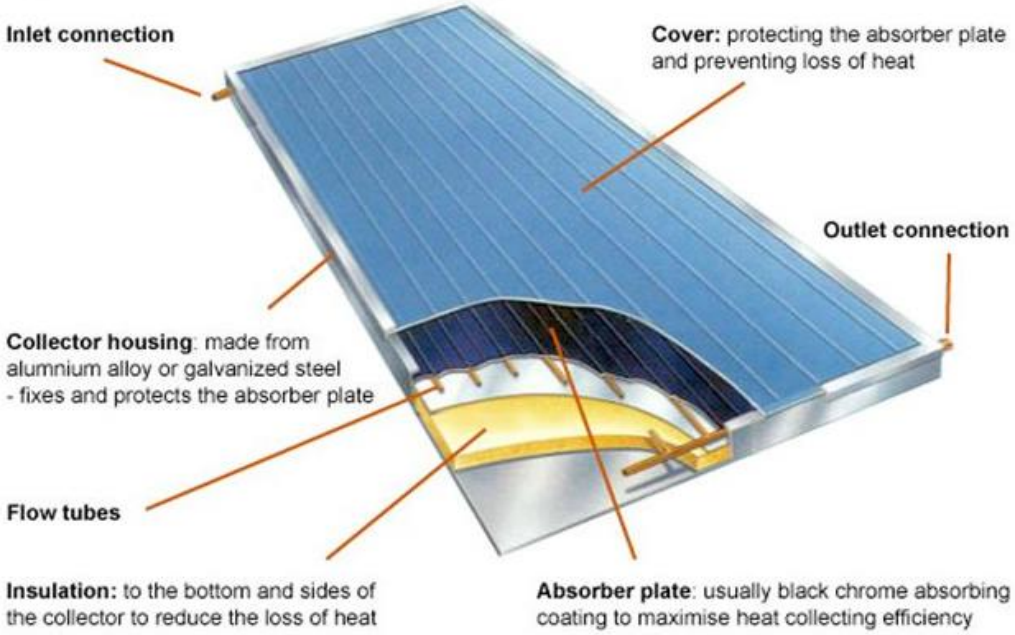

Figure 2.4: Main parts of flat plate collector [11]

Header/Riser-flat plate collector

This type of collectors consists of two headers and a series of parallel vertical risers (Figure 2.5) The diameter of the header is larger than the diameter of the riser. Such collectors normally have 7, 9 or 12 risers. To model the collector, there are some of assumptions that can be made without any change of physical situation, these assumptions are as follows [8]:

1. Performance is in steady state.
2. The headers cover a small area of collector and can be neglected.

3. The headers provide uniform flow to tubes.
4. No heat absorption by cover of the collector.
5. Negligible temperature drops through a cover.
6. Dust and dirt on the collector are negligible.
7. Shading of the collector absorber is negligible.
8. The temperature gradient through the sheet is negligible.

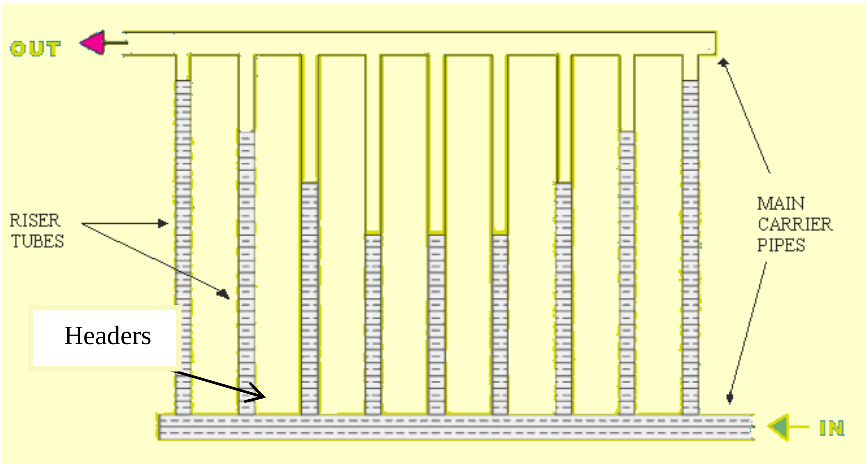

Figure 2.5: Header-Riser flat plat collector schematic diagram

Serpentine flat-Plate collector

It is made of flow duct bonded with absorber plate in a serpentine or zigzag fashion as shown in Figure 2.6**.** It is used in low-flow systems, and the initial cost is lower than header/riser flat plate collector.

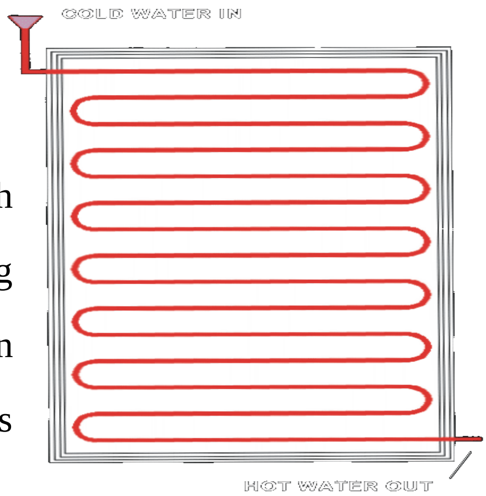

Figure 2.6: Serpentine flat-plate collector

Evacuated-tube solar collectors:

They feature parallel rows of transparent glass tubes. Each tube contains a glass outer tube and metal absorber tube attached to a fin. The fin's coating absorbs solar energy but inhibits radioactive heat loss. These collectors are used more frequently for U.S. commercial applications.

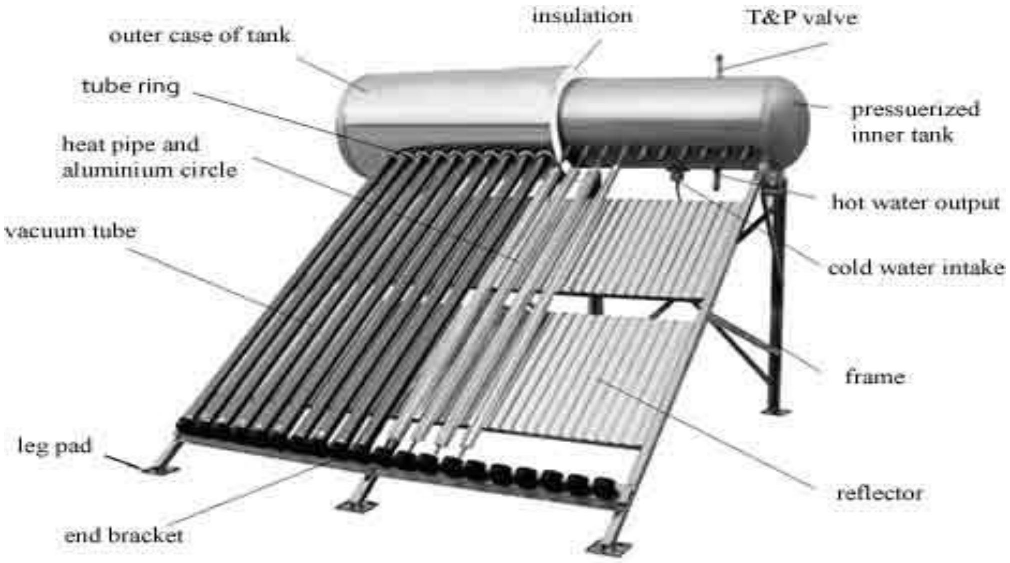

Figure 2.7: Evacuated tube solar collector [12]

2.3 Solar domestic hot water systems (SDHWS) in Palestine

The basic component of SDHWS are a solar collector, tank. Some of them have electrical heaters inside the tank. The main function of the collector is to absorb the

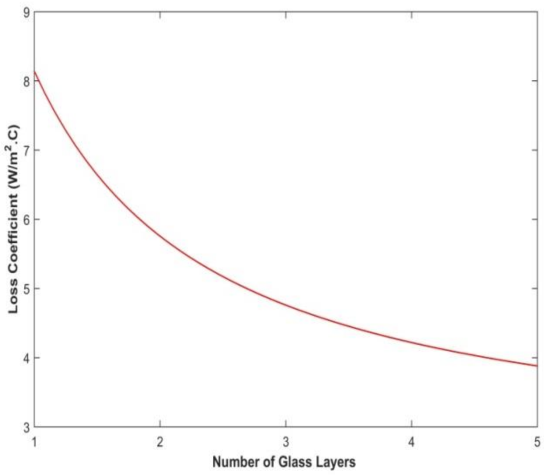

Figure 2.8: Effect of increasing number of glass layers on loss coefficient factor for collector

solar intensity by absorber surface (usually black steel plate), and convert it into thermal energy. The heated fluid is usually water flowing through steel tubes placed on the absorber plates. The collector is protected from convection losses by glass cover; in some of cases they have multi glass layers to reduce the heat losses in the SWHSs. However, this is not usually used in Palestine. Figure 2.8 shows the relation of increasing the layers of glass on the loss coefficient factor in the collector.

The insulation material is usually located in the back and sides of the collector. Storage tank is a medium to store the heated water. Some of storage tanks contain auxiliary electrical heaters to compensate the reduction in solar energy content. In thermosiphon systems, the tank should be on the roof. Other systems like active collector, which is driven with pump, can be placed anywhere. A pump is normally controlled by a differential temperature sensing unit. If the inlet water temperature to the tank is higher than the stored water temperature, the pump runs. In other conditions, the pump is shut down. The temperature of water can be measured by thermocouple sensors.

In Palestine the collector material is usually formed from steel sheet which has good conductivity for heating. In some countries, the collector material formed from copper sheet gives high collector efficiency; however, the initial cost for copper material is higher.

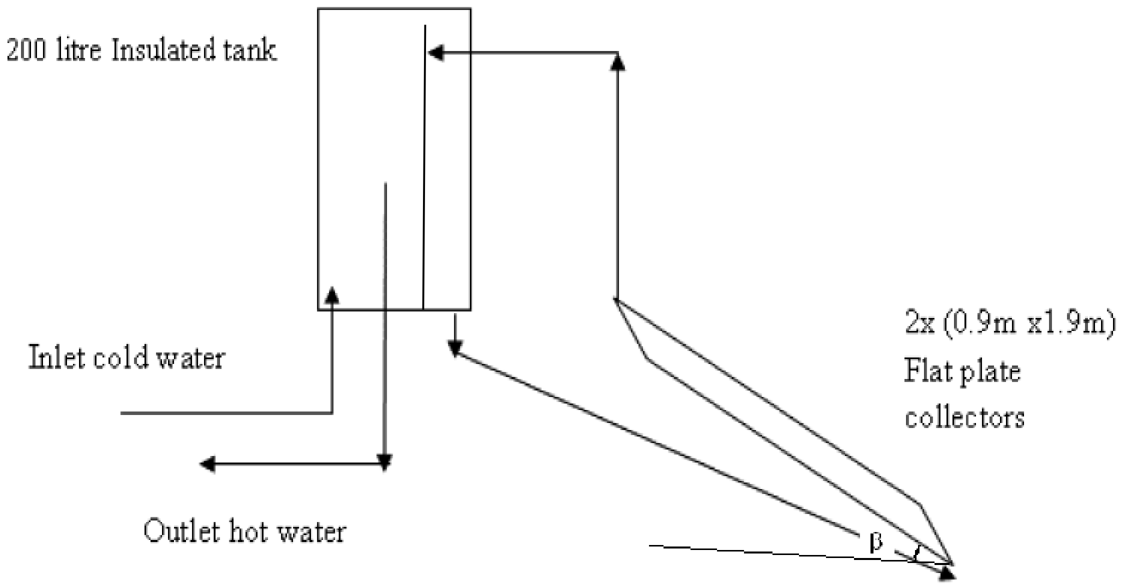

Figure 2.9: Typical diagram of open loop system used in Palestine for solar water heating

SWH systems that use thermosiphon systems are dominant in Palestine. Some other systems have been introduced to the market such as evacuated tube system. Yet, those systems failed in the market due to their higher price, more frequent maintenance, and hard water intolerance. The local manufacturing of SWH systems in Palestine is relatively developed and effective; more than 90% of the installed systems are manufactured locally. Table (2.1) gives an idea about these factories and their production rate per day [14]. Figure (2.9) shows a typical open loop system in Palestine. Their efficiency ranges between 29-45% [14]. The average price of the locally produced solar water heating systems, with two or three flat plates collectors (90cmX190cm each) and from 150 to 200 liter insulated storage tank, is between 250 and 400$. According to the PCBS (Palestine Central Bureau of Statistics) energy department the average total number of solar collectors produced is around 35,000 units annually with more than 59,000 square meter area installed every year.

Table 2.1: Solar Water Heater Producers in Palestine (2008) [14]

Factory Name	Location	Average Daily Production
Niroukh for SWH	Hebron	12
Al-Nimr for SWH	Hebron	6
Al-Sadder for metals and SWH	Hebron	7
Lafi brothers for SWH	Hebron	3
Al-Ofuq for SWH	Hebron	3
Super crystals for SWH	Hebron	8
Al-Itimad Heaters	Ramallah	12
Ibrahim original for SWH	Ramallah	7
Original for SWH	Ramallah	4
Abu-Shosheh for SWH	Ramallah	8
Mansour for SWH	Nablus	10
Dweikat for SWH	Nablus	6
Ashour for SWH	Nablus	5
Toubasi for SWH	Nablus	5
Al-Sakka for SWH	Nablus	3
Al-aqsa for SWH	Jenin	3
Jamal Al-Sabbagh for SWH	Jenin	2
llayyan Ridwan for SWH	Jenin	3
Al-Iktisad for SWH	Tulkarem	3
Abu-Tammam for SWH	Tulkarem	2
Al-Ittimad for SWH	Gaza	8
Al-Qadiseyya for SWH	Gaza	10
Aristol for SWH	Gaza	6

According to some manufacturers the maximum temperature of the water is 70-90°C. In picture (2-10) a typical flat plate collector produced by a local manufacturer is illustrated.

Figure 2.10: Typical flat plat collector produced by local manufacturers

As shown in Figure 2.9 the tilted angle of the collector (β) should be 45°, Table 2.2 shows the useful and auxiliary energy from the collector at different titled angle in Palestine [13]. From this table, using the tilt angle (45°) represent the best one which requires the least auxiliary heating throughout the year and higher useful energy particularly in October through March.

Table 2.2: Optimization of tilt angles [13]

Tilt angle	**Useful energy (kWh)**			**Auxiliary energy (kWh)**
	Annual	***Oct-Mar***	***Nov-Feb***	
25	4014	1666	997	263
32	4000	1719	1042	221
45	3839	1768	1090	198
55	3731	1766	1097	199
60	3600	1751	1095	206

2.4 Efficiency of flat-plate collectors

Flat-plate collectors can be designed for applications requiring energy delivery at moderate temperatures, up to 100°C above ambient temperature. They use both beam and diffuse solar radiation [8], do not require tracking of the sun, and require little maintenance. They are mechanically simpler than other types of collectors,

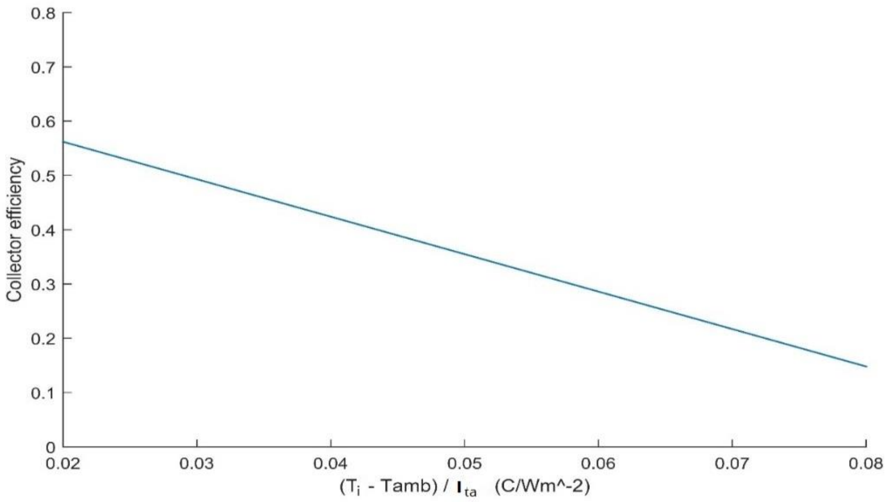

Figure 2.11: Performance curve of a typical flat-plate thermal collector

Figure 2.11 shows the performance curve of a typical flat-plate thermal collector The curve shows the performance as a function of the variables on the x-axis, whereby:

T_{in}: Inlet water temperature to the collector in ˚C

T_{amb}: Ambient temperature in ˚C

$I_{t,a}$: Solar radiation intensity in W/m^2

Chapter Three

Solar Energy Potential in Palestine

3 Solar Energy Potential in Palestine

3.1 Solar radiation in Palestine:

Palestine is located between the longitudes 34.15° and 35.40° east and between the latitudes 29.30° and 33.15° north. Palestine has a considerably high exposure to solar radiation; it has around 2860 hours of sunshine per year. Solar radiation in Palestine reaches about 8000Wh/m^2-day in June and July. This is the highest radiation during the year. In January and December, the least radiation is estimated at 2800Wh/m^2-day. In average the daily solar radiation around the year in Palestine is 5400Wh/m^2-day [15]. Figure (3.1) shows the measured value on the different areas by three meteorological stations in Palestine. Bait Dajan, Jericho and Jerusalem station. The values demonstrate that the annual average insolation values are about 5.25 kWh/m^2-day, 5.69 kWh/m^2-day, and 5.39 kWh/m^2-day in the Bait Dajan, Jericho, and Jerusalem respectively.

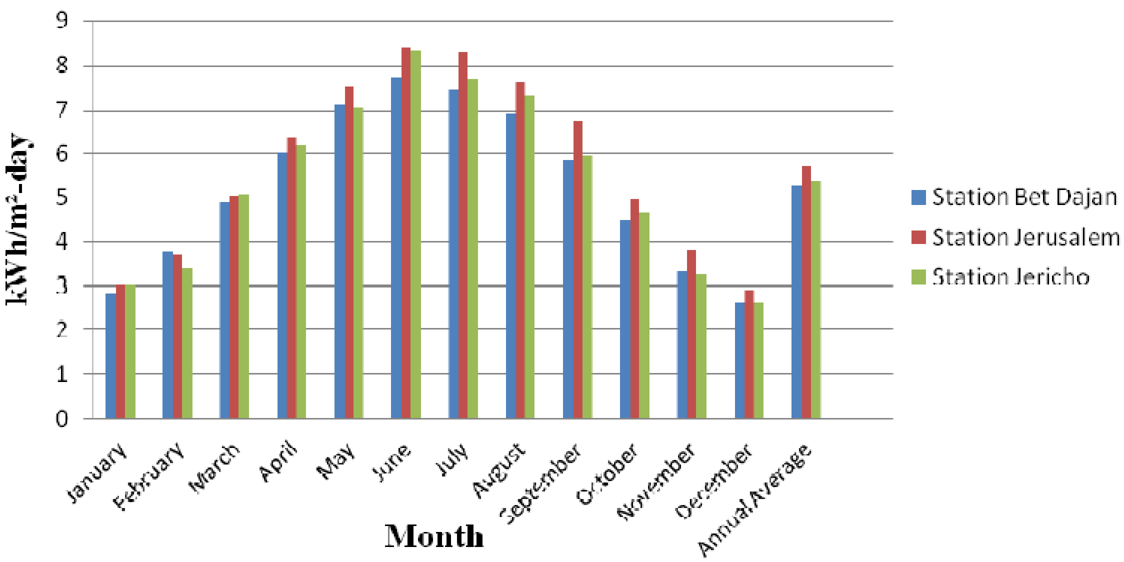

Figure 3.1: Daily average of global solar radiation on horizantal surface on the three geographical locations (Bait Dajan, Jericho, and Jerusalem) [14].

Most of the available solar radiation data are based on hourly measurements [8]. They point out that using the average daily solar radiation for calculation may lead to serious errors if non-linearity's are not taken into account. The results for hourly solar radiation in Palestine are illustrated in Figure (3.2). They are achieved through a preliminary design using the PVSYS software; this software is able to import meteorological data from many different sources.

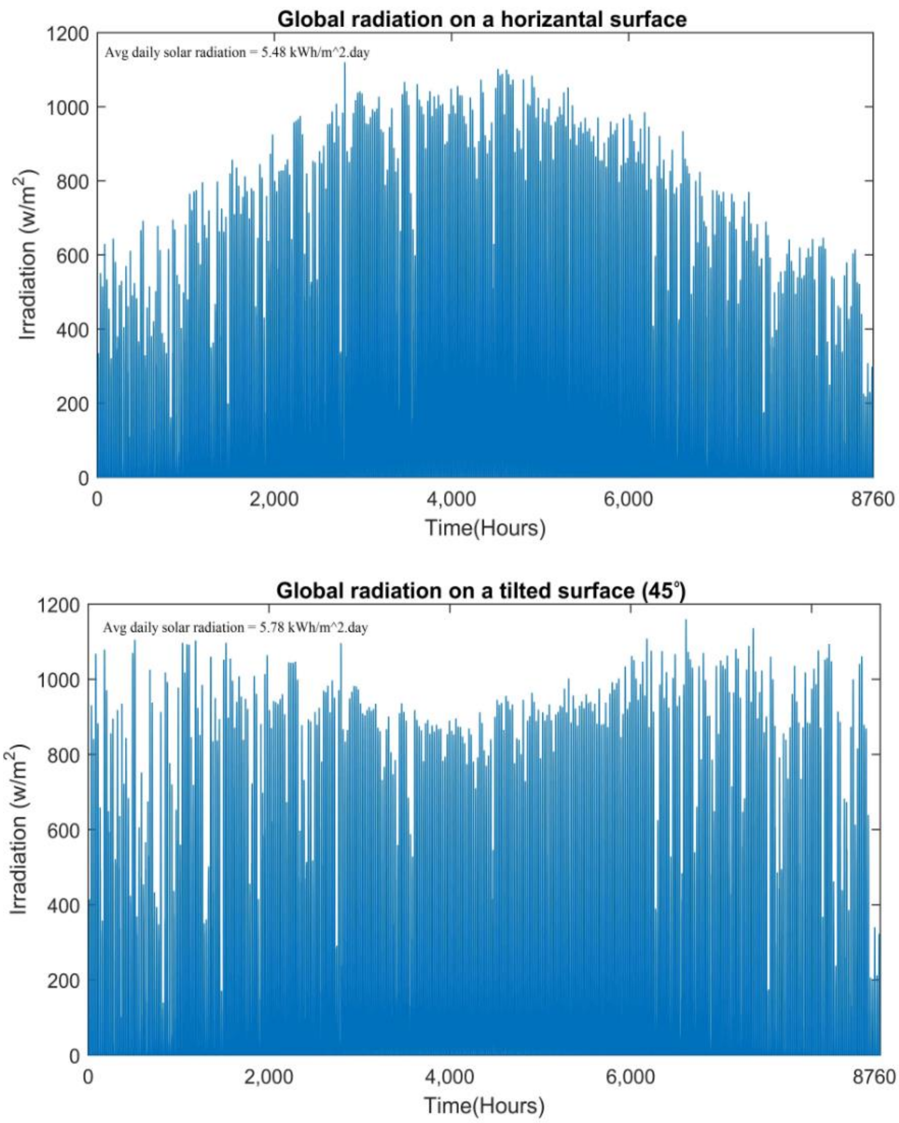

Figure 3.2: Hourly irradiation on a horizantal and tilted plane

3.2 Ambient temperatures

Ambient temperature affects Solar collector's efficiency. The relation between efficiency and ambient temperature is direct proportional. Figure (3.3) shows the mean of air temperature in the Palestinian territory for some stations.

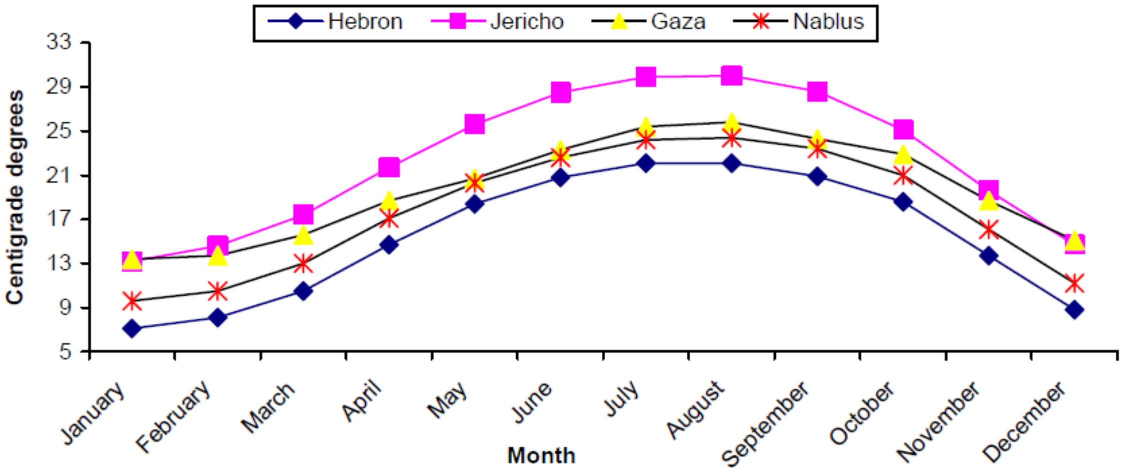

Figure 3.3: Monthly Mean of Air Temperature in Palestine for some Stations[16]

From PV SYS software, the hourly ambient temperature is used for mathematical calculations in solar collectors. Figure (3.4) shows the average hourly ambient temperature in Palestine.

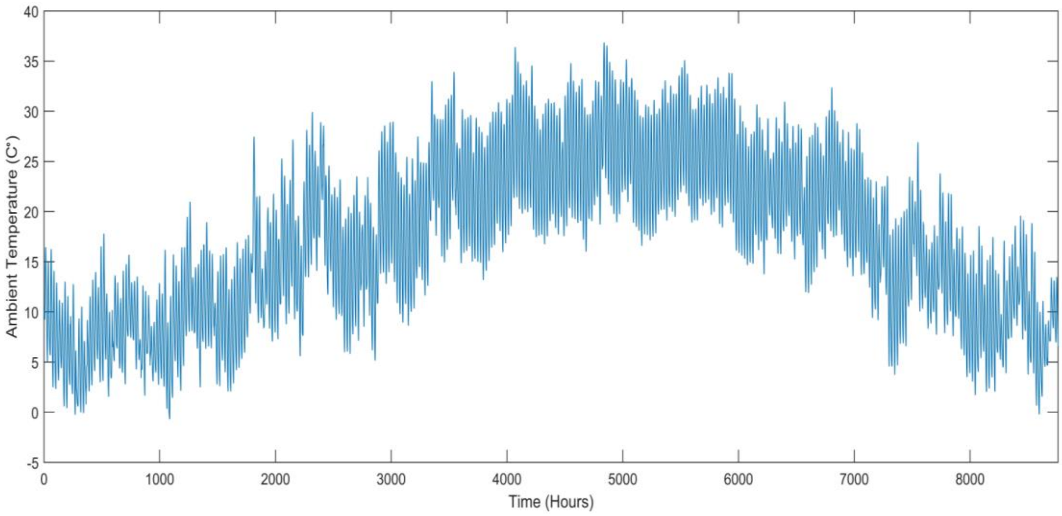

Figure 3.4: Hourly Ambient Temperature in Palestine

3.3 Hot water consumption profile (HWC)

The mean load volume of 180 liters per day was chosen for a single family house that has five persons. A short sequence of hot water consumption profile is shown in Figure 3.5. This figure is obtained from System Advisor Model (SAM) simulation software; SAM is developed by the National Renewable Energy Laboratory (NREL). According to NREL, SAM has both a performance and financial model planned to make decision making[1] for people involved in the renewable energy industry easy.

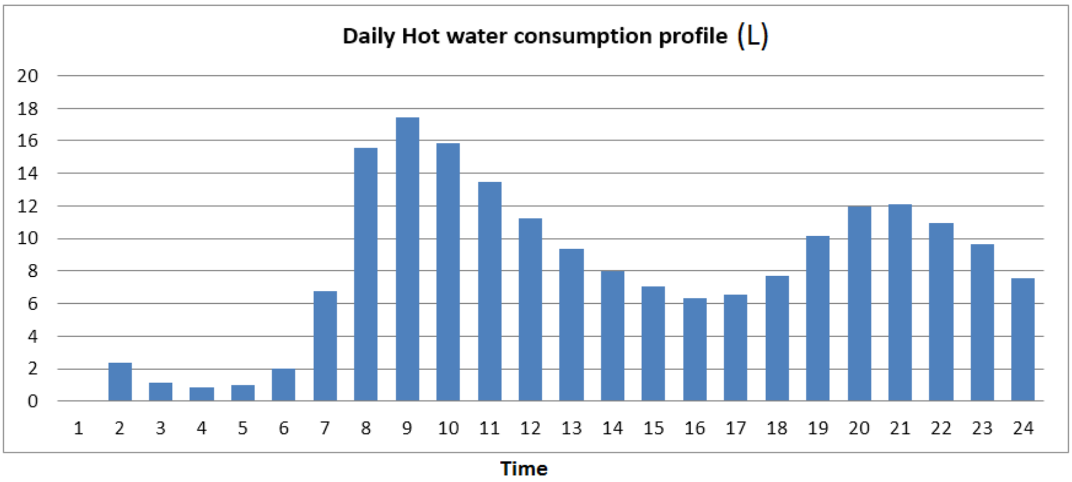

Figure 3-5: Daily hot water consumption profile were obtained from SAM software

As shown from the figure, the real consumption of hot water starts at 7 am and finishes at 12 am. There is no consumption during midnight, from 1_6 am.

It is necessary to know the daily hot water consumption profile for the system, which has an effect on the storage tank temperature, as it contributes to changing the solar collector performance.

[1]sam.nrel.gov

The average daily consumption from domestic hot water is 180 L. To compute the daily energy consumed by this 180 L of hot water, we assume that the water temperature is equal to ambient temperature and the solar collector will increase it to 55 C^{o}, then energy needed could be calculated by using the following equation:

$$Q = m \, . \, C_p \, . \, \Delta T$$

Where, Q is heating energy needed (kWh), m is the mass of hot water needed per day, Cp is the specific heat of water (4.18 kJ/kg.^{o}C), and ΔT is the temperature difference between water before entering the solar collector and after.

The average energy needed to raise the daily consumption of water temperature from the ambient temperature to 55 C^{o} in Palestine equals 7.8 kWh. Annual total consumption is 2847 kWh. Figure 3.6 shows the daily energy needed to heat the water in Palestine.

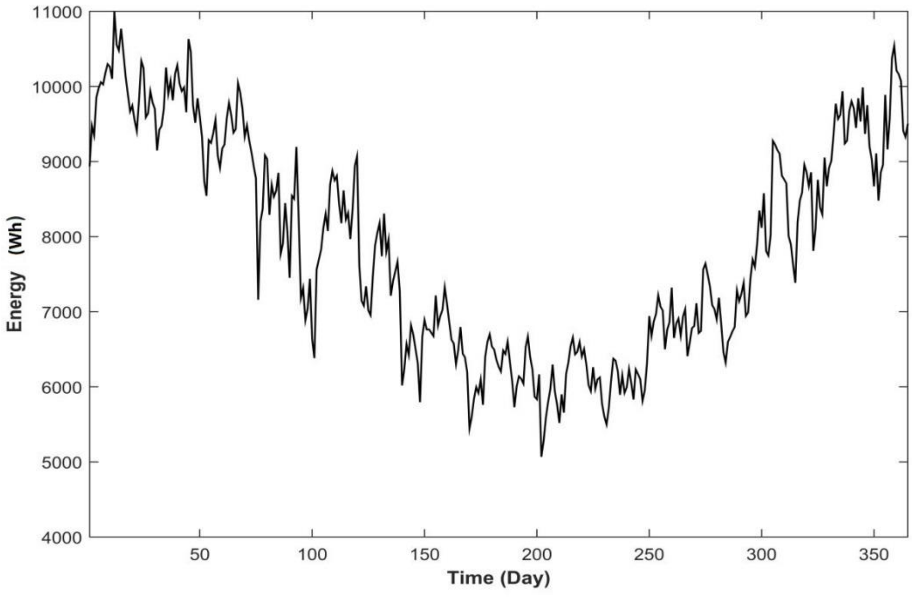

Figure 3.6: Energy needed to raise the water temperature from ambient temperature to 55 ^{o}C

Chapter Four

Mathematical Modeling of Photovoltaic Array

4 Mathematical Modeling of Photovoltaic Array

4.1 Photovoltaic module

Photovoltaic means conversion the sun light to direct current (DC) electricity. History of photovoltaic started at 1839, when Becquerel discovered the photovoltaic effect.

The nominal range of PV efficiency is 8-16% with the highest laboratory record of 32.6%[1]. Photovoltaic is one of the best types of renewable energy technologies because of modularity as one of the advantages. There are many applications for photovoltaic modules represented in the following fields:

- Water pumping.
- Communication station.
- Water desalination.
- Street lighting.
- Hybrid power system.

4.2 PV operating principle

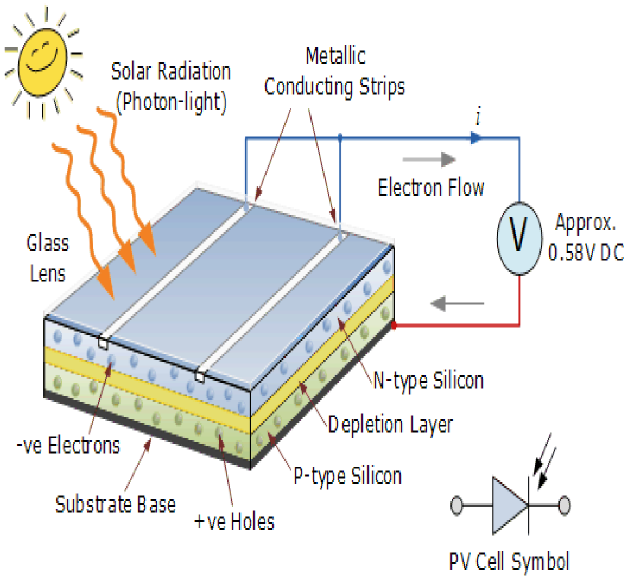

Figure 4.1: Construction of photovoltaic cell [17]

Photovoltaic cell consists of a high-purity silicon. It is made of two layers of semiconductor material at least. The first is positive charge; the second is negative charge. When photons fall on the PN junction, the electron freely moved from the negative layer; it takes the path through an external circuit and flows back into the positive layers. The electric current is generated by a flow of electrons. Figure (4.1) shows the construction of photovoltaic cell.

The majority of photovoltaic solar cells available for commercial purposes are with maximum solar power ratings; P max (W) equals the product of the cell voltage (V) and current (A) at the maximum power point at standard condition:

$$P_{max} = V_{mpp} \cdot I_{mpp} \tag{4.1}$$

Figure (4.2) represents the PV cell through a simple equivalent circuit.

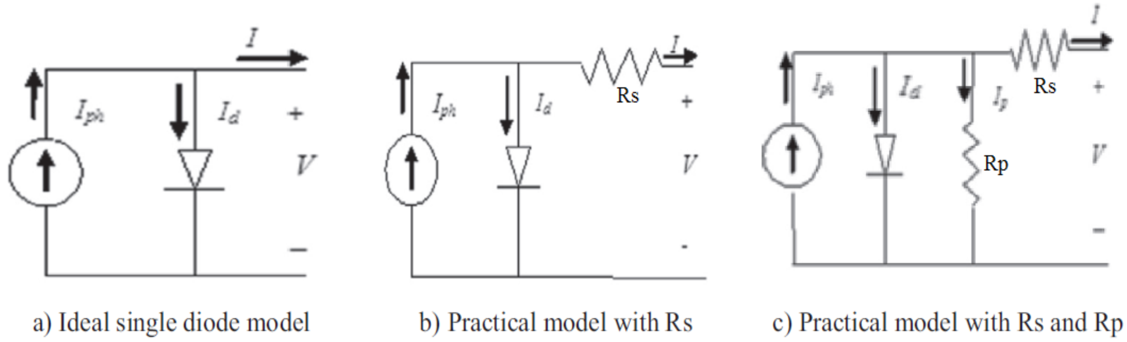

Figure 4.2: Equivalent circuit of a solar cell [18]

The model has a current source (I_{ph}). It also has one diode and a series resistance (R_s). It represents the resistance inside every cell and the connection that exist between the cells. The parallel leakage resistance or shunt resistance (R_p or R_{sh}) represents any parallel high conductivity paths across the solar cell p-n junction and lead to rise the shunt current. These shunt paths lead current away from output current (I) and their effects are harmful to the module performance. These resistances are normally ignored. For an ideal P-V cell there are no leakage current and series loss current ($R_s = 0$ and $R_{sh} = \infty$). The maximum power efficiency is produced if

R_p is at the minimum [20]. The current (I) is the difference between the diode current (I_d) and the photocurrent (I_{ph}).

$$I = I_{ph} - I_D = I_{ph} - I_o(\exp\frac{e(V+IR_S)}{mkT_c} - 1) \quad (4.2)$$

Where:

m is the idealizing factor (1_2-for Si-monocrystalline silicon cell, 1_3-for Si-polycrystalline cell)

k is the Boltzmann's constant ($1.38*10^{-23}$ J/K)

T_c is the absolute temperature of the cell

e is the electron charge ($1.6*10^{-19}$ Cb)

V is the voltage imposed across the cell

I_o is the dark saturation current (dependent on temperature)

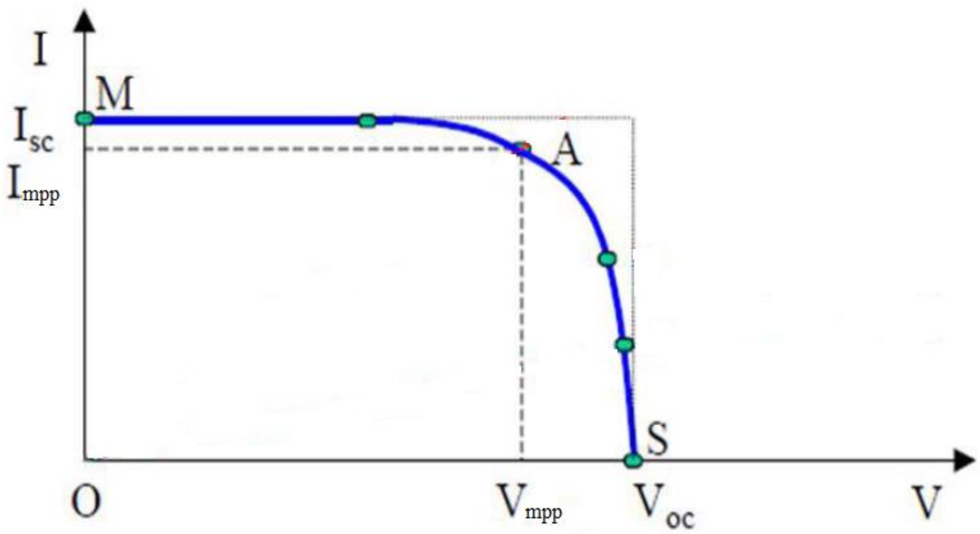

Figure 4.3: Atypical I-V characteristic of a Solar Cell [19]

A real solar cell characterized by the following parameters:

- **Short circuit current (I_{sc}):** It is the largest value of the current obtained from a cell. It is produced when the V=0, Figure (4.3).
- **Open circuit voltage (V_{oc}):** Corresponds to the voltage drop through the diode (p-n junction), when the generated current is I=0. It reflects

the voltage of the cell at no load and it can be mathematically expressed in equation (4.3):

$$V_{oc} = \frac{mkT_c}{e} \ln \frac{I_{ph}}{I_o} \tag{4.3}$$

- **Maximum power point:** it is the operating point A (V_{mpp}*I_{mpp}) at which the produced power is maximum.
- **Maximum efficiency:** it is the ratio between the maximum power and the input power.

$$\eta = \frac{P_{max}}{P_{in}} = \frac{I_{mpp}V_{mpp}}{A\,G_a} \tag{4.4}$$

Where G_a is the irradiation and A is the cell area.

- **Fill factor:** it is the ratio of the maximum power which is delivered to the load and the product of (I_{sc}) and (V_{oc}).

$$FF = \frac{P_{max}}{V_{oc}I_{sc}} = \frac{V_{mpp}I_{mpp}}{V_{oc}I_{sc}} \tag{4.5}$$

The value of fill factor is higher than 0.7 for a good cell. The fill factor is reduced if the cell temperature is increased.

The module (or another P-V device) performance becomes determined at certain conditions. The module features provided by the manufacturer are usually determined at special conditions, such a standard or nominal conditions. See Table (4.1).

Table 4.1: Standard and nominal conditions for P-V device [19]

Nominal conditions	Standard conditions
Irradiation: $G_{a,ref}=800\ W/m^2$	Irradiation: $G_{a,0}=1000\ W/m^2$
Ambient temperature: $T_{a,ref} = 20^\circ C$	Cell temperature: $T_0^C = 25^\circ C$
Wind speed: 1 m/s	

Figure 4.3 shows the I-V characteristics for P-V cells connected in series and parallel, in series connection the V_{oc} is redouble while the short circuit

current remains constant, and vice versa for parallel connections. Solar cells behave much like batteries by sunlight instead of chemical reactions.

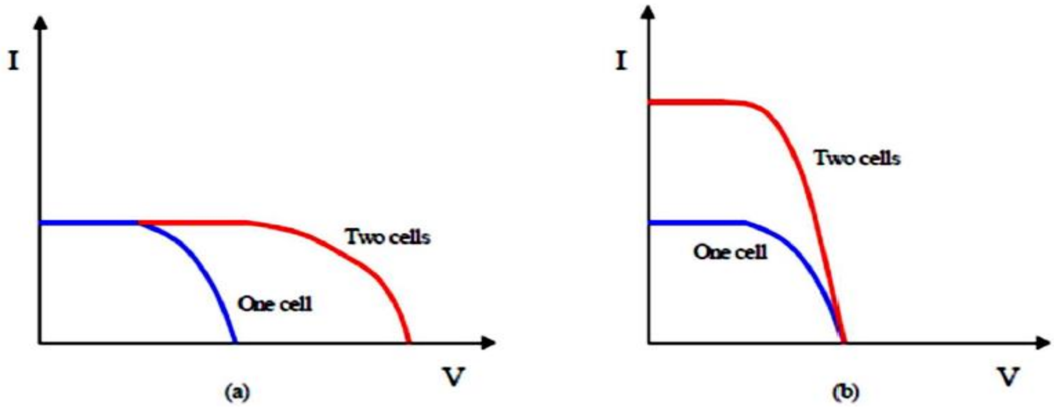

Figure 4.4: Parallel (a) and seriese (b) connection of identical cells [19]

The equivalent circuit of a P-V module, which consists of combination of parallel and series connected, is illustrated in Figure 4.5.

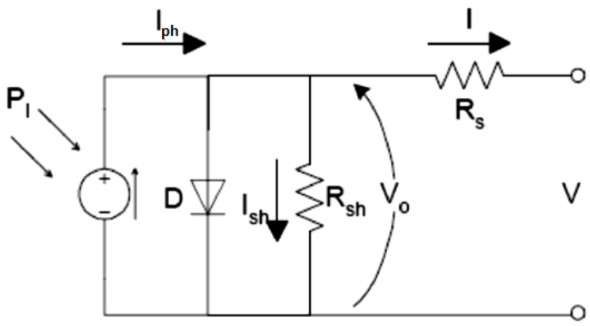

Figure 4.5: PV module eqivalent circuit [19]

The equations governing the equivalent circuit are:

$$V = V_0 - R_s I \tag{4.6}$$

$$\mathrm{I} = I_{ph} - I_D\left(\exp\frac{(qV_0)}{AkT} - 1\right) - I_{sh} \tag{4.7}$$

$$I_{sh} = \frac{V_0}{R_{sh}} \tag{4.8}$$

$$I_{ph} = I_{sc1}\,(\frac{G}{1000}) \tag{4.9}$$

Where (V) is the output voltage, (I) is the current, (q) is electron charge ($1.6*10^{-19}$ Cb), (K)is Boltzmann constant ($1.38*10^{-23}$ J/K), (T) is cell temperature in K, (A) is a quality factor (constant), (I_D)is a reverse or dark saturation current of the diode, (I_{ph})is a photocurrent which is dependent on temperature and solar radiation, and (G)is the insolation level in W/m^2 solar radiation. I_{sc1} is the short circuit current at 1000 W/m^2 solar radiation.

The PV cells characteristics are also dependent on other factors including the temperature of the cell and solar irradiation level. Output current varies with solar radiation and temperature through:

$$I = (I_n + K_I \Delta T)\frac{G}{G_n} \tag{4.10}$$

Where:

I_n presents the nominal PV cell output current at STC (25^{o}C and 1000 W/m^2)

K_I presents the current temperature variation coefficient (A/^{o}C)

ΔT presents the variation from the nominal temperature (25^{o}C)

G_n presents the nominal solar radiation (1000 W/m^2)

K_I value is very small so the effect of solar radiation on output current is linearly, and temperature effect on output current is roughly ignored. However, the temperature variation has strongly affected the reverse saturation current, Io in equation:

$$I_0 = \frac{I_{sc,n} + K_I \Delta T}{\exp(q(V_{oc,n} + K_v \Delta T)AKT) - 1} \tag{4.11}$$

Where:

$I_{sc,\,n}$ presents the nominal short circuit current of the PV cell

$V_{oc,\,n}$ presents the nominal open circuit voltage

K_I and K_v respectively present both the voltage and current temperature variation coefficients (in A/^{0}C and V/^{0}C).

A PV module is the result of connecting several PV cells in series in order to increase the voltage. The PV array consists of several interconnected modules. The PV modules have series and parallel connections. The numbers of such modules have to be calculated. As such, they modify the value of resistance in parallel and series. The values of equivalent resistance in series and parallels of the PV array are:

$$R_{s,array} = \frac{R_{s,modules}\, N_{ss}}{N_{pp}} \quad (4.12)$$

$$R_{p,array} = \frac{R_{p,module} \cdot N_{ss}}{N_{pp}} \quad (4.13)$$

Where:

N_{ss} represents the total number of modules within the series.

N_{pp} represents the number of modules in parallel.

Subsequently to extending the relation current voltage of the PV modules to a PV array, the following equation represents the calculation of the new relation of current voltage of the PV array:

$$I = I_{ph}N_{pp} - I_o N_{pp}\left[exp\left(\frac{V+R_s\left(\frac{N_{ss}}{N_{pp}}\right)I}{V_t A N_{ss}}\right) - 1\right] - \frac{V+R_s\left(\frac{N_{ss}}{N_{pp}}\right)I}{R_p\left(\frac{N_{ss}}{N_{pp}}\right)} \quad (4.14)$$

Where I_o, I_{ph} are the same parameters used for a PV module.

4.3 Validation of PV mathematical model on PV module

In order to validate the PV model, the PV model parameters were substituted with a real PV module (ARCO, M55). Then the PV module is simulated by PVsys design tool software under different temperatures and radiations. Table (4.2) shows the electrical characteristic for the chosen PV module.

Table 4.2: Electrical characteristics data of the PV module type (ARCO M55 siemens) at 25^{o}C and 1000W/m^2.

Electrical characteristics	**Value**
Maximum Power (P_{max})	53.1 W
Voltage at P_{max} (V_{mpp})	17.4 V
Current at P_{max} (I_{mpp})	3.05 A
Open circuit voltage (V_{oc})	21.8 V
Short circuit current (I_{sc})	3.27 A
(K_I) Temperature coefficient of I_{sc}	0.04 % /^{o}C
Number of cells connected in series (N)	36
NOCT	45±2 ^{o}C

4.4 Effect of solar intensity on PV performance

The open circuit voltage V_{oc} of a PV cell increases logarithmically as the incident solar radiation increases. The rate of irradiance change can be calculated unlike the effect on short circuit current, which is directly proportional to solar radiation. The manufacturer's standard will provide a short circuit current in data sheet for PV-cell. Figure 4.6 shows the effect of solar intensity on I-V characteristic at PV module consisting of 36 mono crystalline silicon cells (ARCO, M55).

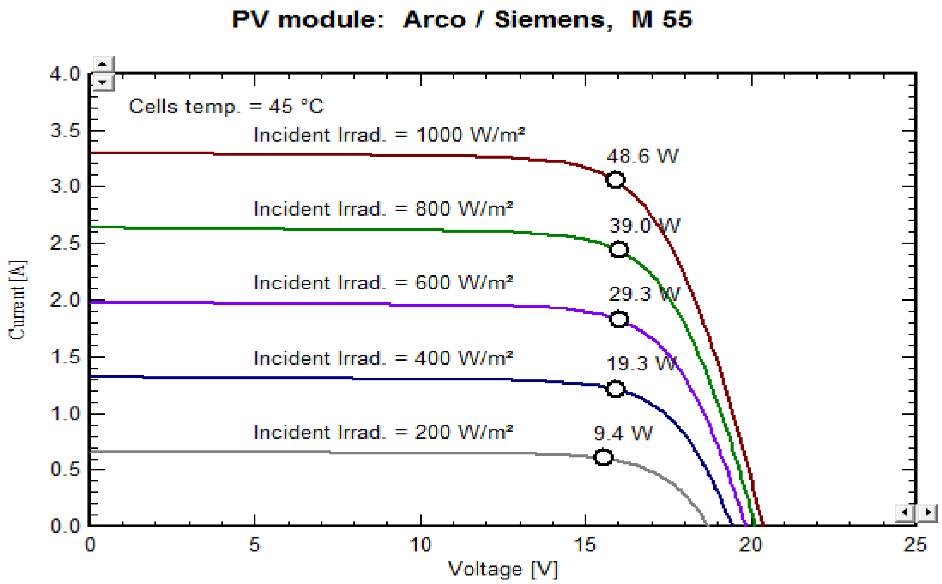

Figure 4.6: I-V characteristic curve at variation in solar radiation and constant temperature (obtained through simulation using PVsys software package)

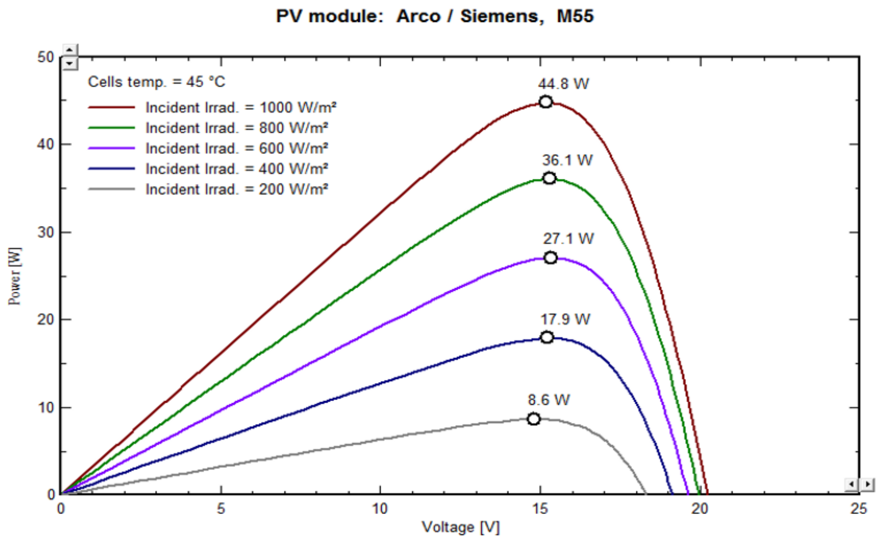

Figure 4.7: P-V characteristic curve at variation in solar radiation, and constant temperature (obtained through PVsys software package)

4.5 Effect of temperature on PV performance

The effect of irradiance and ambient temperature on cell performance will be take in careful consideration. The module open circuit voltage decreases by (2.3*N mV/C°), where N is the number of cells connected in series in the module. The cell temperature is calculated by this equation:

$$T_c = T_a + \left\{\frac{NOCT-20}{800\ W/m^2}\right\} G \tag{4.15}$$

Where:

T_c = cell temperature (C°).

T_a = Ambient temperature (C°).

G = Actual radiation.

$NOCT$ = (Nominal Operating Cell Temperature) is the temperature the cells will reach when operated at open circuit in an irradiance amounting to 800 W/m^2 and an ambient temperature of 20C°.

The next figures show the I-V and P-V characteristics respectively for (ARCO, M55) mono crystalline silicon cells with cell temperature variation and constant radiation.

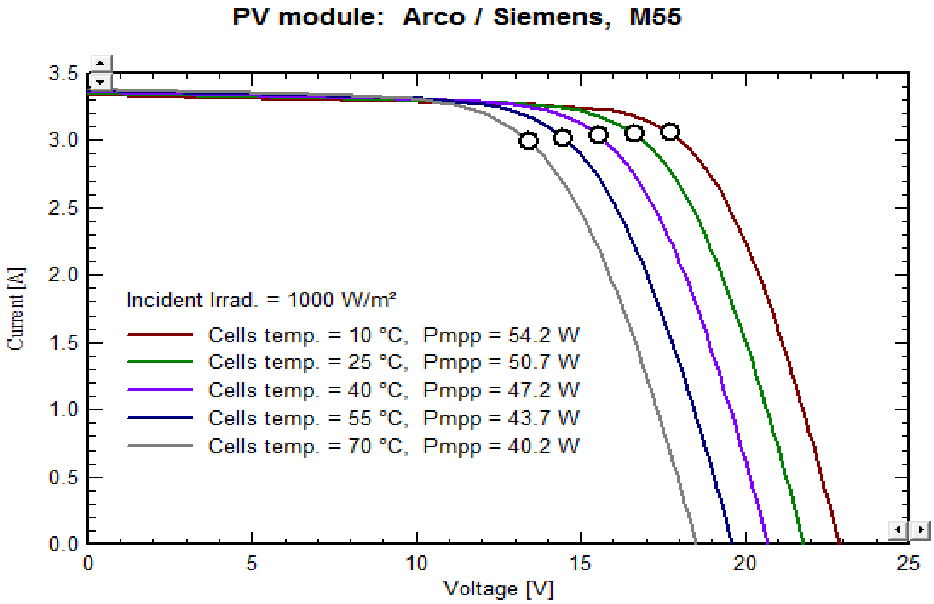

Figure 4.8: I-V curve with temperature variation and constant radiation (obtained through PVsys software package)

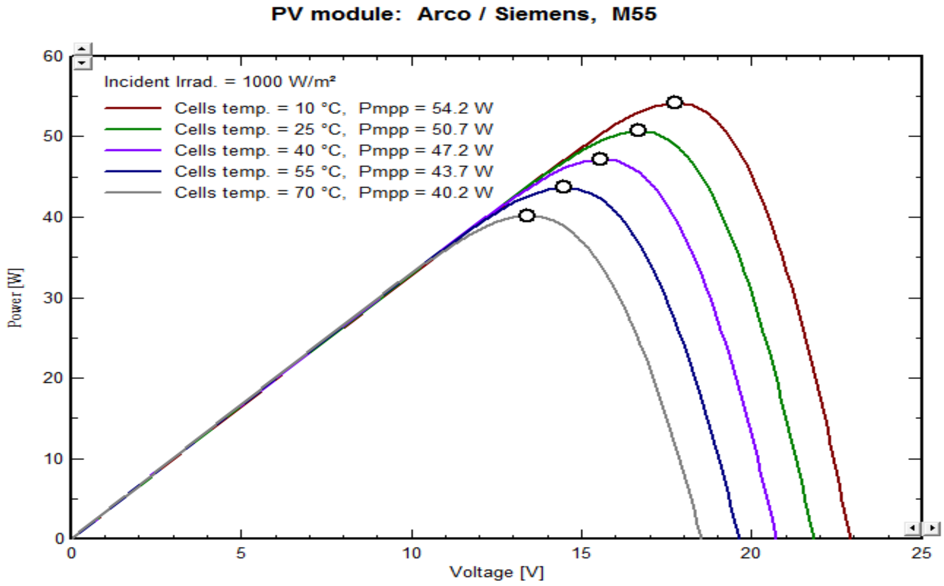

Figure 4.9: P-V curve with temperature variation and constant radiation (obtained through PVsys software package)

4.6 PV cell types

There are different solar cell types, such as poly-crystalline, mono-crystalline, compound thin film, amorphous silicon, etc…

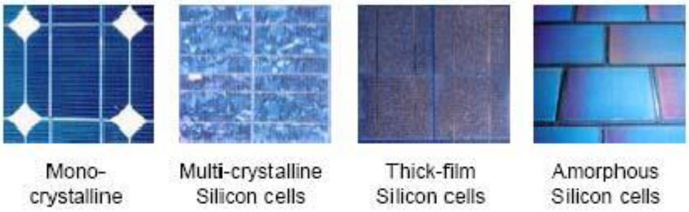

Figure 4.10: PV-cell types

Main characteristic of different PV module types:

- Single-crystal silicon module:

  It is made of mono crystalline silicon cells which are connected in series. Every cell has the parameters about Voc = 0.61 V, Isc = 3.4A/100cm^2 at STC, and has the best efficiency of about 15% [2].

- Poly-crystalline silicon module: It consists of polycrystalline cells connected in series. One cell has approximately V_{oc} = 0.58 V, I_{sc} = 2.8A/100cm^2, and it has a peak efficiency of about 12% [14].
- Thin film or Amorphous silicon(non-crystalline): This type has a high absorption coefficient, therefore about 10μm thickness is enough for one cell.

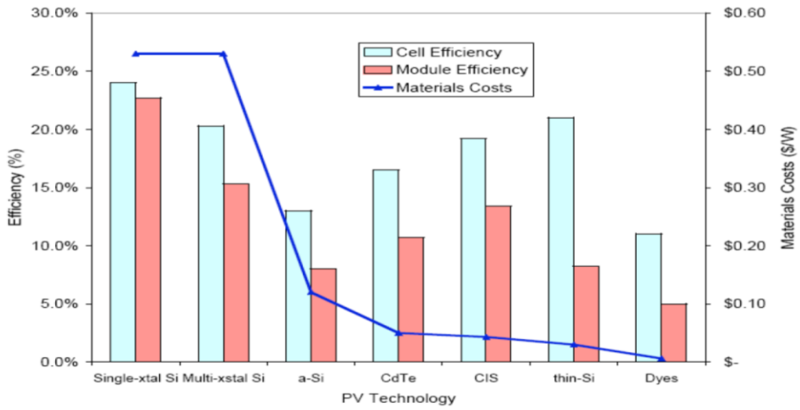

Figure 4.11: Comparison between PV technologies [15]

Chapter Five

Modeling of Flat Plate Solar Collector

5 Modeling of Flat Plate Solar Collector

Heat transfer through forced convection is formed on the front surface of the flat plate solar collector. Besides, heat losses induced by wind have an important impact on the efficiency of solar collectors. Thermal losses influence the performance of flat plate collector, beginning with the absorber to the ambient through the glass covers [21]. To investigate the thermal performance of a solar collector, the equation of heat transfer, fluid flow, and radiation need to be considered.

5.1 Solar fraction (SF)

It is known as the ratio of the solar contribution to the load divided by the total load required to heat the water. It estimates how much the home owner can offer to pay for the solar equipment if the auxiliary energy is natural gas or electricity [8]. It’s used to easily evaluation the performance of a system.

$$SF = 1 - \frac{Q_{Auxiliary}}{Q_{load}} \text{ [8]} \tag{5.1}$$

$$Q_{load} = Q_{Auxiliary} + Q_u \tag{5.2}$$

Where:

$Q_{Auxiliary:}$ is heat requirement to meet the load which is usually electrical heaters (Wh)

$Q_{Load:}$ is the total load needed to heat the water (Wh)

Q_u: is output solar energy produced from the collectors (Wh)

There are many factors effecting solar fraction [8]:

a) The amount of solar radiation

b) Collector inlet water temperature.

c) Sizing of solar system.

d) Actual water consumption.

e) Ambient air temperature around tank.

f) Tank insulation.

g) Necessary energy needed to circulate the water in the collector.

Figure 5.1 shows the schematic diagram of a typical solar water heating system include a flat plate solar collector, circulating pump and a storage tank.

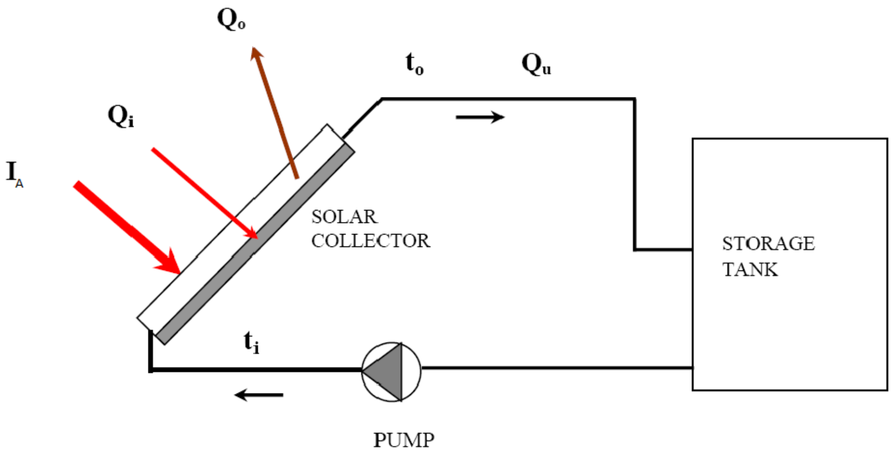

Figure 5.1: Typical solar energy systems

If (I) is the intensity of solar radiation (W/m^2) the surface of the collector having area A (m^2), then the amount of solar radiation absorbed by the collector is:

$$Q_i = I \,.\, A \quad [22] \tag{5.3}$$

However, as it is shown in Figure 5.2, some of this power is reflected to the sky. Another part of this power is absorbed by the glazing. The rest of the power is transmitted through the glazing and reaches the absorber plate as short wavelength. Consequently, the conversion factor represents the percentage of the solar rays which penetrate the transparent cover of the collector (transmission) and the percentage being absorbed (absorptivity) [22]. Qi is mainly the product as shown through the rate of transmission of the cover and the absorption rate of the absorber.

Thus,

$$Q_i = I(\tau\alpha)\,.A \qquad [22] \qquad (5.4)$$

As the collector heats, its temperature is become higher than that of the surrounding and heat is lost to the atmosphere by convection. The rate of heat loss (Q_o) depends on the collector temperature and the collector overall heat transfer coefficient (U_L).

$$Q_o = U_L A(T_c - T_a) \quad [22] \qquad (5.5)$$

Therefore, the rate of useful energy absorbed by the collector (Q_u) (knows as the rate of absorption under steady state conditions) is proportional to the rate of useful energy absorbed by the collector. This is expressed as follows:

$$Q_u = Q_i - Q_o = I\tau\alpha\,.A - U_L A(T_c - T_a) \qquad [8] \qquad (5.6)$$

It is also known that the rate of extraction of heat from the collector may be measured as the rate of heat carried away in the fluid passes through the collector.

$$Q_u = mc_p(T_o - T_i) \qquad (5.7)$$

Where, (m) is the mass of heated fluid (kg), c_p is the specific heat of fluid (J/kg. K), T_o and T_i is the outlet and inlet fluid temperature respectively.

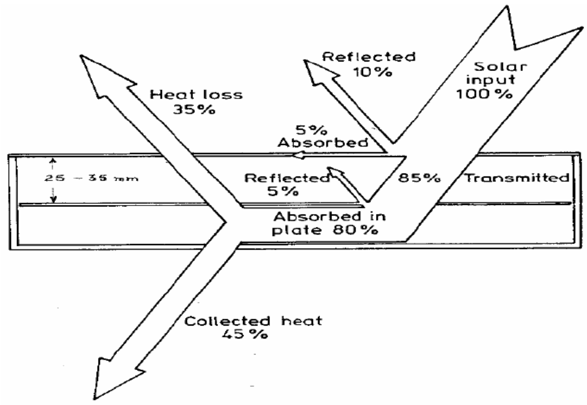

Figure 5.2: Heat flow through a flat plate collector [22]

5.2 Collector overall heat loss coefficient (U_L)

It is useful to develop the concept of overall loss coefficient (U_L) for solar collector to simplify the mathematical equation, Figure 5.3.a shows the thermal network for two-glass cover flat plate solar system. The thermal losses in the system are expressed as thermal resistance R for two glass cover, Plate, and back insulation. Where, I is equal to the incident solar radiation, the absorbed I is distributed to thermal losses through the bottom and the top of the collector and to useful energy gain. (T_p) is the temperature of plate; (Ta) is the ambient temperature. The main purpose is to convert the network in Figure 5.3.a to the vector diagram in Figure 5.3.b. The energy through the top losses is caused by radiation and convection between parallel plates. The steady state energy transfers between the plate at T_p and the first cover at T_{c1} is the same energy as between any other two adjacent covers and is also equal to the energy lost to surrounding from the top cover [8].

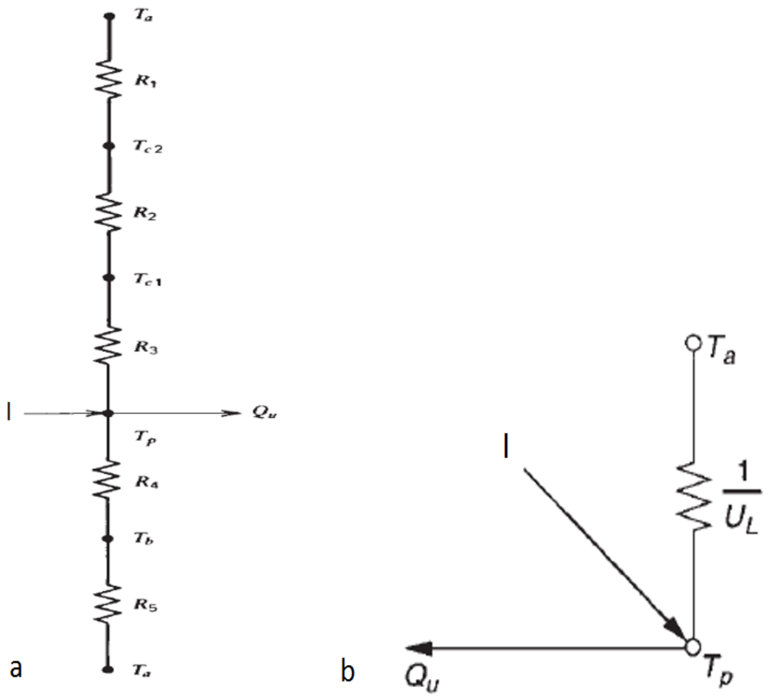

Figure 5.3: (a-Thermal network for a two-cover flat-plate collector in terms of resistance between plates. b-Equivalent thermal network for flat-plate solar collector) [8]

The overall heat loss coefficient can consist of two terms, the first is top loss coefficient (U_t), it deals with cover and plate losses, and the second is bottom loss coefficient (U_b) which deals with back and edge losses.

Top loss coefficient(U_t)

The overall top heat loss coefficient is a function of various parameters. They include the temperature of the plate, emissivity of absorber glass cover, glass cover and ambient, and the number of glass covers, etc. Duffie and Beckman also provide an equation of top loss coefficient for estimation of upward heat losses of solar water heater collector [8].

$$U_t = \frac{1}{R_1+R_2+R_3} \tag{5.8}$$

$$U_t = \left[\frac{N}{\frac{C}{T_{pm}}\left(\frac{T_{pm}-T_a}{N+F}\right)^e} + \frac{1}{h_w}\right]^{-1} + \left[\frac{\sigma(T_{pm}+T_a)(T_{pm}^2+T_a^2)}{\frac{1}{\varepsilon_p+.00591\,N\,h_w}+\frac{2N+f-1+.133\varepsilon_p}{\varepsilon_g}-N}\right] \text{[8]} \tag{5.9}$$

Where [8]:

$F = (1 + .089\, h_w - .1166 h_w \varepsilon_p)(1 + .07866\, N)$

$C = 520(1 - 0.000051\, \beta^2)$, For $0 < \beta < 70^o$

$e = 0.430 \left(1 - \frac{100}{T_{pm}}\right)$

N is the number of glass covers.

$F = (1 + .089\, h_w - .1166 h_w \varepsilon_p)(1 + .07866\, N)$.

$C = 520(1 - 0.000051\, \beta^2)$ For $0 <\beta< 70^o$

β is the collector tilt angle (deg)

ε_g is the emittance of glass (0.88)

ε_p is the emittance of plate (0.1-0.95)

Ta is the ambient temperature (K)

T_{pm} is the mean plate temperature (K)

h_w is the wind heat transfer coefficient (W/m^2 C^o)

Wind heat transfer coefficient (h_w)

Wind heat transfer from the upper surface of a flat plate solar collector greatly influences top heat losses. The convective heat transfer induced by wind has great impact on upward heat losses in case of single glazed collectors more than double glazed collectors. Its impact is the greatest in case of unglazed collectors [23]. In Palestine, however, single glazed collectors are most widely used specially for residential applications. Hence, it is important that we select appropriate values of wind heat transfer coefficient so that we can reduce error in computed values of top loss coefficient. There is more than one equation used to calculate the heat transfer coefficient:

McAdams (1954):

$h_w = 5.7 + 3.8\ V_{w},\ V_w \leq 5 m/s$ [23]

Wattmuff et al. (1977):

$h_w = 2.8 + 3\ V_{w},\ V_w \leq 5 m/s.$ [23]

Sharples and Charlesworth (1998):

$h_w = 6.5 + 3.3\ V_{w},\ V_w \leq 6 m/s.$ [23]

where, V_w: Wind velocity (m/s^2)

All above equations give approximate value for heat transfer coefficient, where Wattmuff equation is more widely used [8]. The next table shows the heat transfer coefficient for Palestine depending on wind speed measurements in 2013.

Table 5.1: Average wind velocity measurment in Palestine [3], and wind heat transfer coefficients for these velocities

Month	Jan	Feb	Mar	Apr	May	Jun	Jul	Aug	Sep	Oct	Nov	Dec	**AVG**
V_w (m/s^2)	4.74	3.66	4.16	3.83	4.42	5.26	5.48	4.94	4.57	3.82	2.86	3.76	4.29
h_w (W/m^2C)	17	13.8	15.3	14.3	16.1	18.6	19.2	17.6	16.5	14.3	11.4	14.1	15.67

Figure 5.4 shows the effect of wind speed on the top loss coefficient for flat plate solar collector, based on Wattmuff equation.

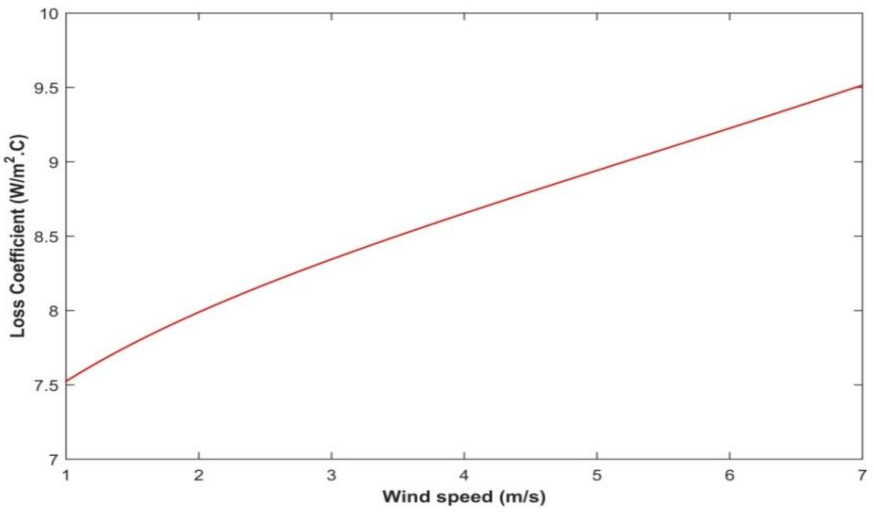

Figure 5.4: Effect of wind speed on top loss coefficient

From previous figures, we see that if the speed of wind increases, the loss coefficient also increases. Therefore, the overall efficiency of the system is decreased.

Bottom loss coefficient (U_b)

The energy loss through the bottom of the collector is represented by two resistors in series R4 and R5. In Figure 5.3.a**,** R4 represents the resistance to heat flow through the insulation and R5 represents the radiation and convection resistance to the environment. Thus the back loss coefficient U_b is given by:

$$U_b = \frac{1}{R_4} = \frac{K}{L} \tag{5.10}$$

Where K and L are the insulation thermal conductivity and thickness (mm) respectively. Tabor (1958) suggests edge insulation of approximately the same thickness for bottom insulation. The edge losses should be small; it represents less than 1% of the total losses. So, it is not necessary to consider it in mathematical calculations [8].

The collector overall heat loss coefficient U_L is the sum of the Top and bottom loss coefficients:

$$U_L = U_t + U_b \tag{5.11}$$

5.3 Fin efficiency factor (*f*)

The fin efficiency factor indicates the ratio of the heat transfer rate from a fin to the heat transfer rate that we obtained if the entire fin surface area were to be maintained at the same temperature as the primary surface [8].

In figure 5.5, W (m) represents tube spacing, the outer and inner diameter of tube is D and D_i respectively. The sheet is thin with a thickness δ. We will assume the sheet above the tube is at some local base temperature T_b. Figure 5.5shows the sheet and tube dimensions of Header/riser flat plate collector.

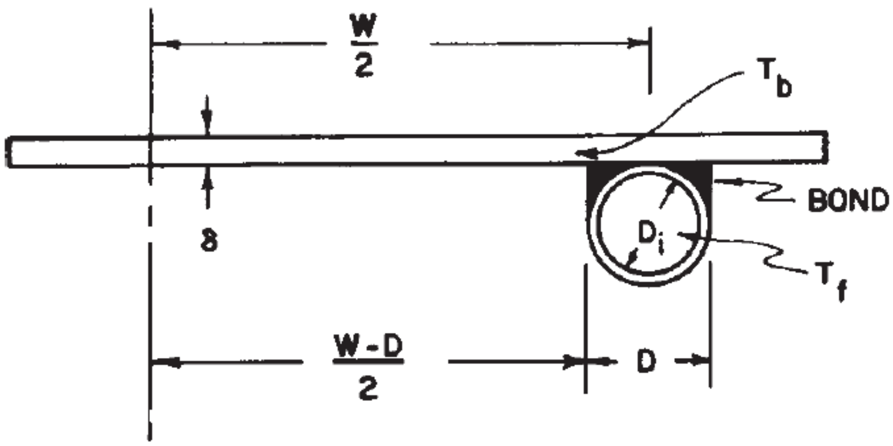

Figure 5.5: Sheet and tube dimension of header/riser flat plate collector [8]

The mathematical equation of fin efficiency factor can be given by

$$f = \frac{\tanh\left(\frac{\sqrt{\frac{U_L}{K\delta}}\,(W-D)}{2}\right)}{\frac{\sqrt{\frac{U_L}{K\delta}}\,(W-D)}{2}} \quad [8] \tag{5.12}$$

Where f is fin efficiency factor, U_L is overall heat loss coefficient in ($W/m^2.^oC$), K is plate thermal conductivity ($W/m.^oC$) and δ is sheet thickness (mm).

5.4 Collector efficiency factor (F′)

Collector efficiency factor is the proportion of the actual useful energy gain to the useful gain obtained if the collector absorbing surface was at the local fluid temperature [8]. The collector efficiency factor is given as F′:

$$F' = \frac{1/U_L}{W\left[\frac{1}{U_L\,[D+(W-D)F]}+\frac{1}{C_b}+\frac{1}{\pi\, D_i h_{fi}}\right]} \qquad [8] \qquad (5.13)$$

Where C_b, ($W/m.^oC$)is the bond conductance between the pipe and the sheet plate for the collector. The bond conductance is significant when it specifically describes the collector performance. It is concluding that it is necessary to have good metal to metal contact. Figure 5.6 shows the effect of increasing the C_b on the collector efficiency factor which shows that if the bond conductance is larger than 30 $W/m.^oC$, the collector efficiency factor become steady state, which means that the performance of the collector in high efficiency at this value and any increasing in bond conductance becomes unnecessary [8].

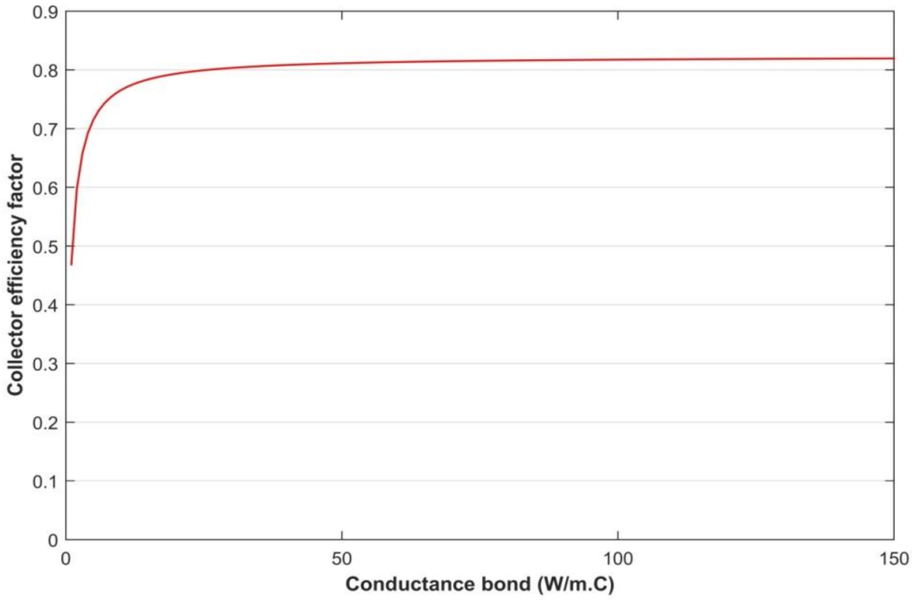

Figure 5.6: Effect of bond conductance on collector efficiency factor

Internal fluid heat transfer coefficient (h_{fi}) inside the tube indicates the state of fluid flow, laminar flow or turbulent flow. Figure 5.7 shows the effect of increasing the heat transfer coefficient on the collector efficiency factor.

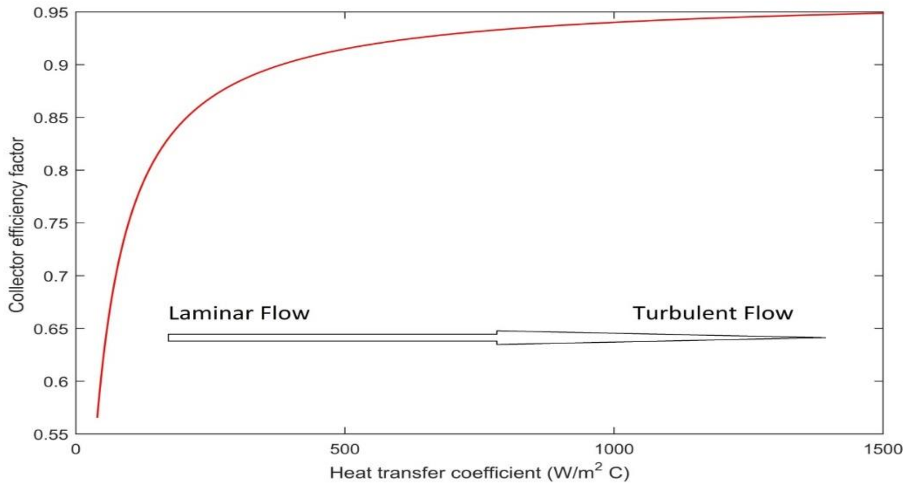

Figure 5.7: Relation of heat transfer coefficient with collector efficiency factor

5.5 Heat removal factor and flow factor (F_R, F'')

It is a quantity that relates the actual useful energy gain of a collector to the useful gain. The collector heat removal factor (F_R) can be expressed as follows:

$$F_R = \frac{\dot{m} C_p}{A_c U_L}\left[1 - \exp\left(-\frac{A_c U_L F'}{\dot{m} C_p}\right)\right] \quad [8] \qquad (5.14)$$

Where,

$\dot{m}$ is the flow rate for fluid (kg/s).

A_c is the area collector (m^2).

The quantity F_R is defined as the ratio of the actual heat transfer to the maximum possible heat transfer [8]. The maximum heat transfer occurs in the collector when the temperature of the whole collector is at the inlet fluid temperature and the heat losses to the surrounding are minimum. As the mass flow rate increases through the collector, the fluid temperature through the collector decreases. This causes lower losses since the average collector temperature is lower and there is a corresponding increase the useful energy gain [1]. The next Figure Shows the relation of increasing the flow rate on heat removal factor principle.

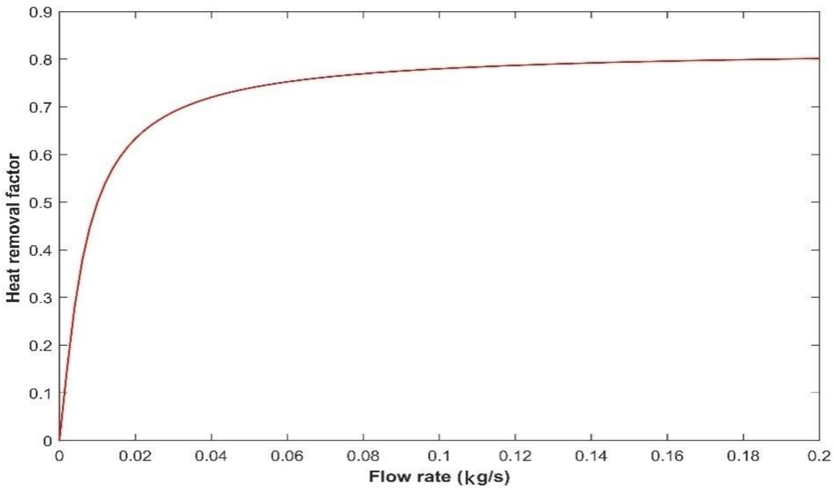

Figure 5.8: Flow rate versus heat removal factor

It is convenient to define the collector flow factor (F") as the ratio of F_R to F'.

$$F'' = \frac{F_R}{F'} = \frac{\dot{m}\, C_p}{A_c U_L F'}\left[1 - \exp\left(-\frac{A_c U_L F'}{\dot{m}\, C_p}\right)\right] \quad [8] \qquad (5.15)$$

5.6 Mean plate temperature and mean fluid temperature

It is necessary to evaluate the mean plate temperature (T_{pm}) and mean fluid temperature (T_{fm}) in the collector to define the total performance of the collector. When a collector producing a useful energy, the mean plate temperature must be bigger than the mean fluid temperature. The mean plate temperature can be used to calculate the useful gain of the collector,

$$T_{pm} = T_{fi} + \frac{Q_u/A_c}{F_R U_L}(1 - F_R) \quad [8] \qquad (5.16)$$

Where, T_{fi}: mean fluid temperature in the collector (°C)

The mean fluid temperature was given by this equation [8]:

$$T_{fm} = T_{fi} + \frac{Q_u/A_c}{F_R U_L}(1 - F'') \quad [8] \qquad (5.17)$$

This is proper temperature for evaluating the fluid properties.

Mean plate temperature equation can be solved iteratively with top loss coefficient equation. First, an estimate of mean plate temperature is made from which U_L is calculated. A new mean plate temperature is defined from equation 5.16and used to find the new value of overall loss coefficient. The new value of overall heat loss coefficient (U_L) is used to refine F_R and F'', and the process is repeated, the initial guess for mean plate temperature for liquid heating collector at typical flow rates from 0.01 to 0.02 Kg/m^{2}s is T_{fi} +10 C^o[8].

5.7 Collector performance

The main method used to measure the collector performance is by exposing the operating collector to solar radiation and measuring the fluid inlet temperature, outlet temperature (T_i ,T_o respectively), and of the flow rate for fluid. The useful gain, therefore, is:

$$Q_u = \dot{m}\, C_p\, (T_o - T_i) \quad [22] \qquad (5.18)$$

Where C_p is the specific heat for fluid, C_p for water at 20 C^o equal 4.186 (kJ/(kg K))

The next equation describes the thermal performance of a collector operating under steady state condition.

$$Q_u = A_c F_R [I_t(\tau\alpha) - U_L\,(T_i - T_a)] \quad [22] \qquad (5.19)$$

Where, I_t is Solar intensity on a tilted surface plane of the collector (usually angle of tilted collector in Palestine is 45^o), $\tau\alpha$ is the product of the rate of transmission of the cover and the absorption rate of the absorber.

Then the instantaneous efficiency of the collector is:

$$\eta = \frac{Q_u}{A_c I_t} = F_R(\tau\alpha) - \frac{F_R U_L\,(T_i - T_a)}{I_t} \quad [8] \qquad (5.20)$$

$$\eta = \frac{\dot{m} C_p (T_o - T_i)}{A_c I_t} \qquad [8] \qquad (5.21)$$

ASHRAE sets standard test procedures for solar water heaters (Figure 5.9). The essential feature of all of procedures can be summarized as follows:

1. Provide the collector with a fluid at controlled inlet temperature.
2. Measure the solar radiation by a pyranometer on the surface of the collector.
3. Measure the flow rate, outlet and inlet fluid temperature, ambient temperature and wind velocity.
4. Equipment are provided for measurement of pressure drop across the collector.

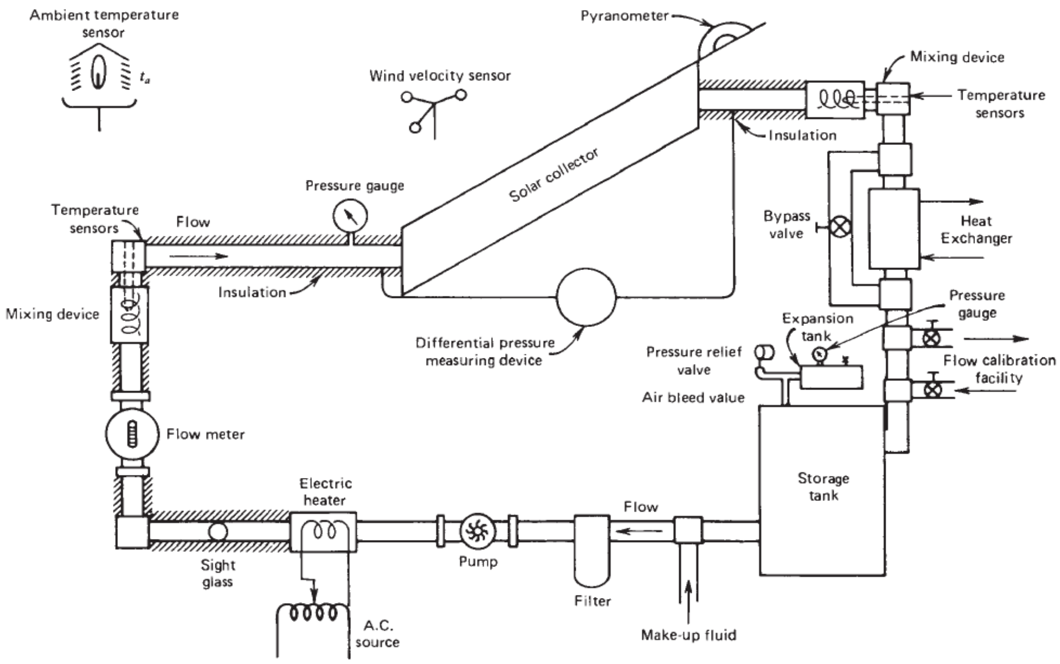

Figure 5.9: Closed-loop test setup for liquid heating flat-plate collector. [8]

5.8 Water storage

For many solar systems, water forms the best material to store useful heat. Energy is added to and removed from a storage tank by transport of the storage medium itself, thus eliminating the temperature drop between transport fluid and storage medium. Figure 5.10 shows a typical system in which water tank is used.

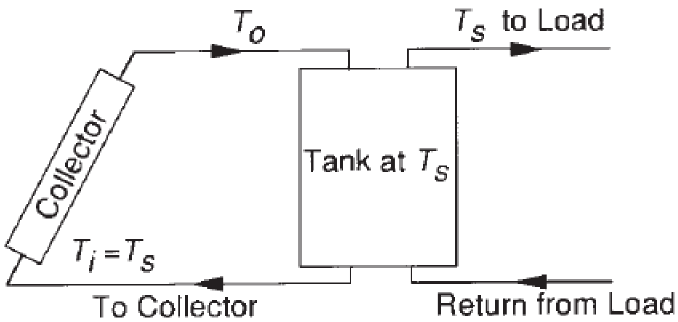

Figure 5.10: A typical diagram for system using water tank storage,with water circulation through collector

The energy storage capacity of water (or other liquid) in fully mixed tank is:

$$Q_L = (mC_p)\Delta T \qquad [22] \qquad (5.22)$$

Where Q_s is the total heat energy for a cycle operating through the temperature range (ΔT) and m is the mass of water in the unit. Equation 5.23 is used to find the tank temperature at the end of time increment (one hour).

$$T_s{}^{+} = T_s + \frac{1}{mC_p}\,[Q_u - L_s - (3600\,UA)(T_s - T_a{}')] \qquad [8] \qquad (5.23)$$

$$L_s = m_h C_p \Delta \mathrm{T} \qquad [22] \qquad (5.24)$$

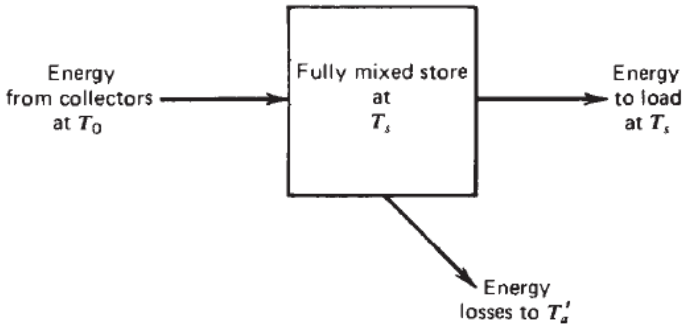

Figure 5.11: Fully mixed storage tank of mass (m) operating at temperature Ts in ambient temperature Ta' [8]

Where Ts^+ is the tank temperature at the end of the time increment which is usually one hour, Ts is the fluid temperature before time increment, and Q_u is the energy added to the tank from a solar collector. L_s is the energy removed from the tank and delivered to a load, UA is loss coefficient – area product (W/C^o) for a storage tank, m_h is the mass of heated water consumed in one hour.

Chapter Six

Design, Optimization and Performance Analysis of SWH

6 Design, Optimization and Performance Analysis of SWH

Many design parameters need to be optimized, the design for flat plate collector parameters is calculated by MATLAB software. Figure 6.1 represents the overall system flow chart of calculations of the mathematical model for SWH systems in 24h.

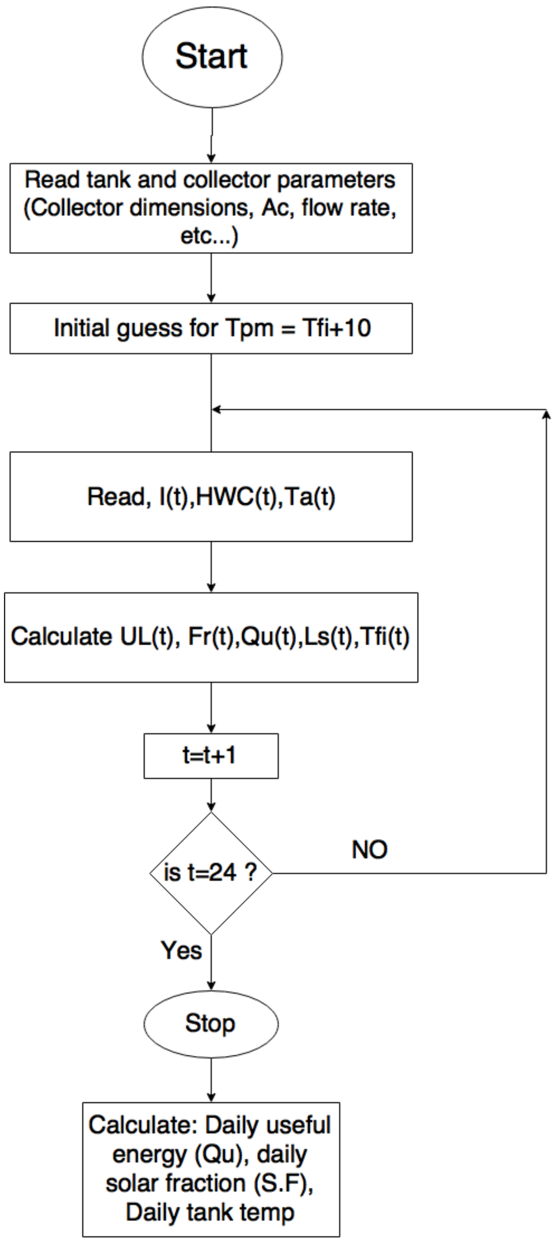

Figure 6.1: Calculation flow chart for the Solar Thermal System simulation

6.1 Tank size

Tank storage size is an important factor that highly effects on performance of the system. An undersized tank will not achieve the load hot water profile, whereas an increased tank size will cause an additional material costs and increase the convection losses to the environment through the increased surface area. Increasing the height of storage tank than 1.0 m has no significant effect on solar fraction [24]. Figure 6.2 shows the effect of increasing the tank volume and height (H_t) on annual solar fraction of the system when the fluid set point temperature is 60 ^oC .

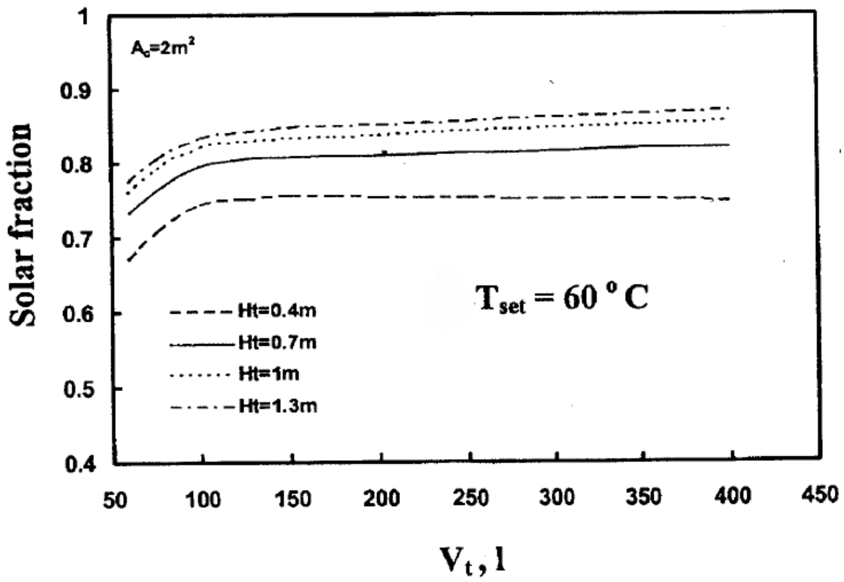

Figure 6.2: Variation of tank volume (Collector area, 2 m^2) on solar fraction for different tank heights [24]

From Figure 6.2 (V_t) from 60 liters to 400 liters results in an increase in solar fraction (SF) for all storage tank height (H_t), but when set point temperature is 60^{o}C there is no effect in in increasing V_t more than 150 liters any extra volume for storage tank will not give any significant increasing in solar fraction. Increasing H_t from 0.4 m to 1.3 m will result in increase in annual SF.

A tank volume of about 180 liters is the optimal size for a family consisting of 5 persons, (36 L hot water for one person). Further increasing in the tank volume has a little increasing in solar fraction. Table 6.1 show the storage tank dimensions and volumes used in Palestine.

Table 6.1: Dimensions of storage tanks usually used in Palestine [25]

Tank size	**Dimensions**	
Tank size(L)	Length (cm)	Width (cm)
200	120	56
150	100	56
120	90	56
80	85	47

Zahedi *et al*, studied different sizes of storage tank (V_t) when the collector area (A_c =1m^2) for different set point temperatures (T_{set}) of the tank (Figure 6.3). They found that changing the ratio of V_t /A_c does not affect too much on S.F for higher set point (Tset = 70°C and 80°C), increasing ratio caused decrease in S.F. In Palestine the set point temperature for storage tank mostly equal 60 °C. From Figure 6.3 when Tset =60 °C the maximum solar fraction happened when the ratio of V_t/A_c is 45-50 l/m^2. This means that 1m^2 of area collector required a volume of 45-50 L for storage tank.

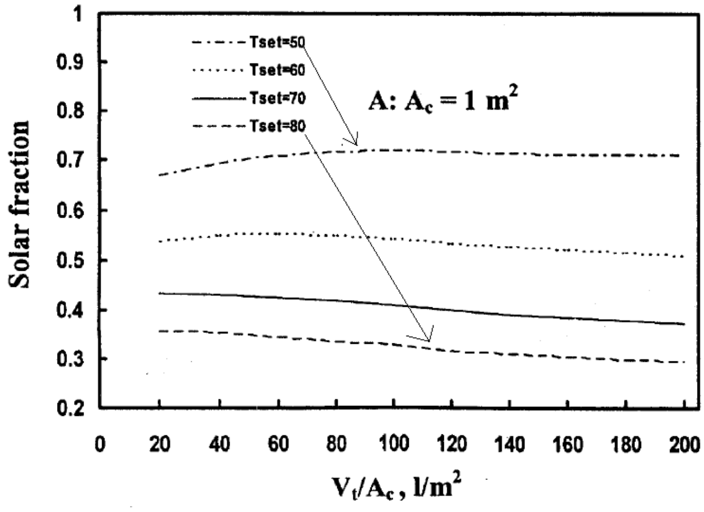

Figure 6.3: The effect of V_t / A_c on solar fraction for different T_{set} values and collector area A_c =1m^2 [24]

6.2 Tube spacing and pipe diameter

Tube spacing (W) represents the distance between two pipe (riser) in flat plate collector. It has a significant effect on fin efficiency factor (*f*). A general rule of thumb is that the fin efficiency should be about 90-95 % [26]. Figure 6.4 represents the relation of W(mm) with fin efficiency factor (*f*) based on equation 5.12 , and it shows the design range for tube spacing.

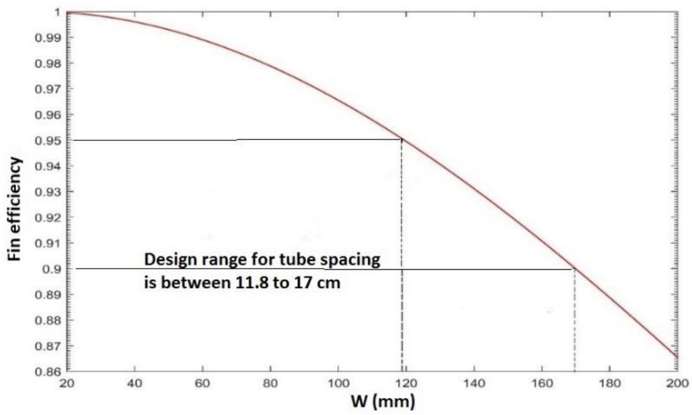

Figure 6.4: Design range for Tube spacing (W) when Fin efficiency is located between 90-95 % (U_L is 8.4 (W/m^2.^{o}C), K is 300 (W/m.^{o}C), δ is 0.5 (mm) and D is12.7(mm)).

Actually, the spacing between risers in the local collectors in Palestine falls within the design range area (Figure 6.4).

Figure 6.5 represents the effect of pipe diameter on heat removal factor. The diameter as it can be seen plays a little role on the heat removal factor, which leads to little change in the performance of the system. The riser pipe diameter used in Palestine is about 12.7mm (1/2").

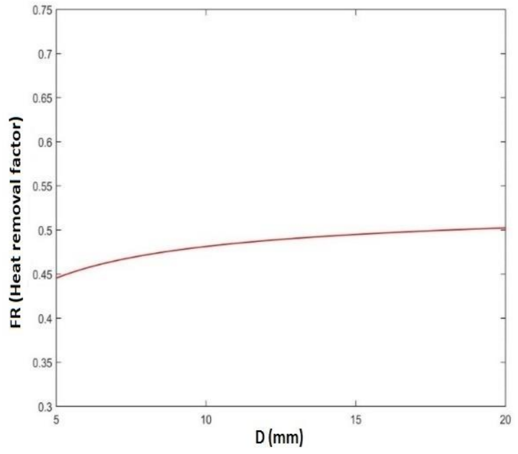

Figure 6.5: Effect of riser diameter (D) on

Using larger diameter will reduce the friction losses in the pipes, which leads to reducing the power needed to operate the P-V pump. However, using large pipe diameter will increase the initial cost, thus making the system to be infeasible.

6.3 Collector area

The performance of a solar collector is normally specified for a given area. European standards for collector considers the opening area (the area through which the incident radiation crosses) as well as the absorber area as a reference. As mentioned previously, the average energy needed to raise the daily consumption of water temperature from the ambient temperature to 55 C^o in Palestine equals 7.8 kWh. The annual average of solar radiation

(I_A) is 5.4 kWh/m^2.day. The daily load from hot water is about 180 L, and the average solar collector efficiency (μ_c) is about 35% [2].

To calculate the area needed for solar collector need to use this equations:

$$A_c = \frac{Q_u}{\mu_c . I_A} \quad (6.1)$$

As mentioned, the area for one collector used in Palestine is (190 cm x90 cm), so from the result in equation 6.1, this will require three collectors to cover our need from domestic hot water.

6.4 Module design

Most commercial and industrial systems require a large number of collectors to satisfy the heating demand. A module is a group of collectors that can be grouped into parallel flow and combined series-parallel flow. Parallel flow is more frequently used because it is inherently balanced, and has a low pressure drop [27]. Figure 6.7 illustrates the two most popular collector header designs: external and internal manifolds.

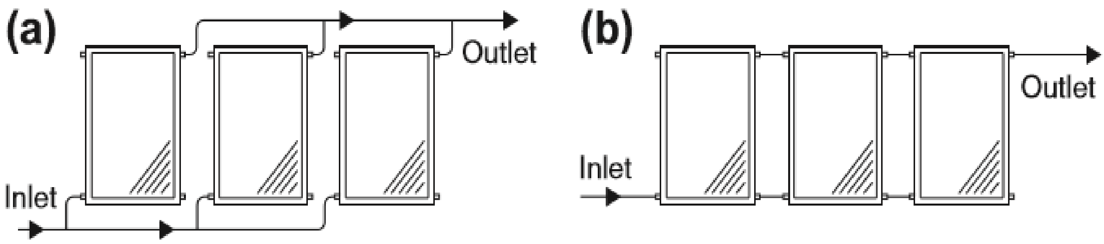

Figure 6.6: Collector manifolding arrangements for parallel flow modules. a) External manifolding. b) Internal manifolding.

Generally, flat plate collectors are made to connect to the main pipes of the installation in one of the two methods in Figure 6.7. The external manifold collector has a small diameter connection because it is used to carry the flow for only one collector. The internal manifold collector incorporates several collectors with large headers. The number of collectors that can be connected depends on the side of header. Internal manifolding is preferred for most places in Palestine because it offers a number of advantages. These are cost saving because the system avoids the use of extra pipes (and fittings), which need to be insulated and properly supported [27].

The choice of series or parallel arrangement depends on the temperature required from the system. Connecting collectors in parallel means that all collectors have as input the same temperature, whereas when a series connection is used, the outlet temperature from one collector is the input to the next collector.

It should be noted that the collector efficiency decreasing if the inlet fluid temperature to the collector is increased. Figure 6.8 shows the effect of increasing flow rate on the collector efficiency at different values of fluid inlet temperatures (T_{fi}). The reduction in the system performance from 73% (at T_{in} = 10C$^{o)}$ to 54% (at T_{in} = 40C^{o}) when the flow rate is 0.2 L/s.

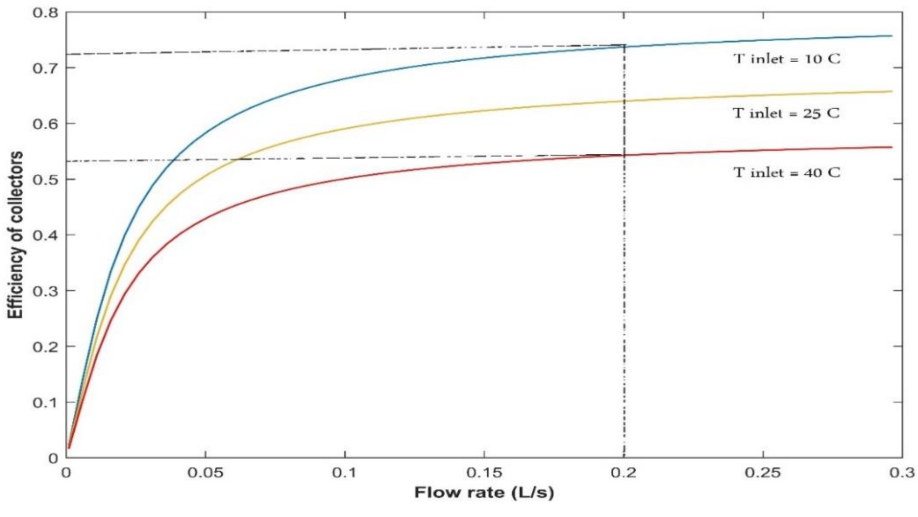

Figure 6.7: The effect of increasing the flow rate on collector efficiency at different values of fluid inlet temperature and collector area is $4m^2$

6.5 Flow rate

Flow rate is the most important factor affecting the performance of the system. The main goal is to have a flow rate that efficiently removes the heat that the sun deposits in the collector. Basically, flow rates too low as in Thermosyphon system (usually is 0.015 $L/s.m^2$ [2]) will not remove the heat efficiently from the collector, and the efficiency of the system will be low. Flow rates too high require a larger pumps and piping systems that increase both operating and initial costs. Therefore, exactly appropriate flow rate is important.

If the flow rate is quite low, then the temperature difference between the inlet fluid and the outlet fluid temperatures of the collector must be high in order to remove the solar heat. This means that the average temperature of the absorber is high, which is not good because the hot absorber loses more heat through the collector glazing and this reduces the efficiency of the collector. Although for further increasing in flow rate, the gain in efficiency become small.

The effect of flow rate on the main component of SDHW systems are summarized here:

- **Thermal collector**: its performance is characterized through a heat removal factor (F_R). The high collector flow rate leads to high efficiency of the collector. From the thermal collector viewpoint, it is preferred that the flow rate be at its maximum level.

- **Circulating pump:** Auxiliary power required to circulate the fluid is a quadratic function of flow rate. From the pump viewpoint, it is preferred that the flow rate be at minimum level.

6.5.1 Best flow rate

Table 6.2 shows the collector efficiency, the heating absorbed, solar fraction and fluid rise temperature when flow rate increased. The values in the table are based on these conditions:

- The collector is equivalent to a typical commercial flat plate collector with black painted absorber used in Palestine. The specifications for this collector are shown in Table 6-3.
- The initially inlet water temperature is 25 C^o, and the ambient air temperature is 25 C^o.
- The flow distribution inside the collector is uniform (all risers get the same flow rate).
- The heat transfer fluid is water.
- Solar intensity on the collector surface is 700 W/m^2.

Based on the table 6.2, we can note the following:

- At highly flow rate, flat plate collector is efficient, but may require a larger pump and larger pipes to circulate the fluids.
- Lower flow rate may be attainable with a smaller pump and lower diameter pipe, but will be less thermally efficient.

Table 6.2: Effect of flow rate on collector plate characteristics (I = 700W/m^2, T_a = 25^{o}C)

Flow Rate (L/s.m^2)	Heat Absorbed (W/m^2)	Efficiency	S.F	Fluid Rise Temperature
0.015	297.89	0.426	0.790	32.50
0.02	314.95	0.450	0.833	25.58
0.025	325.83	0.465	0.841	21.08
0.03	333.37	0.476	0.850	17.92
0.035	338.91	0.484	0.861	15.58
0.04	343.14	0.490	0.873	13.78
0.045	346.48	0.495	0.896	12.35
0.05	349.18	0.499	0.901	11.19
0.055	351.42	0.502	0.910	10.23
0.06	353.30	0.505	0.914	9.42
0.065	354.89	0.507	0.919	8.73
0.07	356.27	0.509	0.920	8.13
0.075	357.47	0.511	0.921	7.61

As shown in the above table the efficiency of the system increases from 42% to 49.9% when the flow rate increases from 0.015 L/s.m^2 to be 0.05 L/s.m^2. After that the system efficiency increases slowly. Moreover, increasing the flow rate leads to reduction in fluid temperature, which represents the difference between the outlet and inlet fluid temperatures of the collector. This indicates that the absorbed energy is high from the solar collector.

Table 6.3: Specifications for Flat Plate collector and Hot water Storage Tank used in Palestine [28]

Collectors	**Specification**
Number of collectors	3 Collector per system
Box	0.5 mm galvanized steel 190 x 90 x10 cm
Absorber plate	0.5 mm black steel
Risers	0.5" outer diameter steel pipes, 7, 9, 13 risers
Headers	1.0" outer diameter steel pipes
Insulation	3 cm polyurethane
Cover	0.4 mm ordinary glass
glass emissivity (εg)	.95
plate emissivity (εp)	0.8
transmittance absorptance product ($\tau\alpha$)	0.9
Hot Water Storage Tank	
Size	180 L
Shell	4-5 mm steel
Insulation	6 cm polyurethane
Outside Cylinder	0.4 mm galvanized steel
Pressure	12 bar

Flow rate from 0.047 to 0.055 L/s.m^2 is recommended for mostly active solar water heaters systems. The technical data for the Alta Energy Liquid Flat-Plate Collector Model ATL 100-1 recommends flow rates of 0.046 to 0.07 L/s to meet the maximum performance for the system [26]. For confirmation, the ASHRAE is recommended that the flow rate should be chosen between 0.048 to 0.055 L/s.m^2 [29].

6.6 Performance analysis and results of SWH

Table 6.4 shows the results of solar fraction through the year for two sizes of area collectors at low flow rate of 0.02 L/s.m^2 (typically used in Thermosyphon system in Palestine) and high flow rate of 0.05 L/s.m^2

which represents the developed SWH with circulation pump. Table 6.4 shows that the annual solar fraction increases with about 4 % for each size of the area collector when flow rate increases from 0.02 to 0.05 L/s.m^2. In January when area collector is 3.4 m^2, the solar fraction increases from 53 % to 61%. In June the solar fraction is constant through each size of area collector, because there is a high solar intensity and ambient temperature in this month, so any increasing in area collector or flow rate will not give any significant value in solar fraction. If we note when area collector is 3.4 m^2 (two collector) and flow rate is 0.05 L/s.m^2, the solar fraction value is equal 90%. However, when area collector is 5.1 m^2 (three collector) with flow rate 0.02 L/s.m^2, the solar fraction value is equal 90.9%. The two values of solar fraction is approximately equal; that is using SWH with two collectors and circulating pump to increase the flow rate gives approximately the same result of solar fraction when using SWH with three collector and without circulating pump.

Table 6.4: Monthly and annual solar fraction for SWH system with and without circulation pump for two sizes of area collectors (3.4 m^2 and 5.1 m^2) in Palestine

Area collector	Month	Jan	Feb	Mar	Apr	May	Jun	Jul	Aug	Sep	Oct	Nov	Dec	Annual solar fraction
3.4 m^2 (Two collector)	Solar fraction **without pump** (flow rate = **0.02** L/s.m^2)	53	63	87	96	100	100	100	98	97	96	80	67	**86.3**
	Solar fraction **with pump** (flow rate = **0.05** L/s.m^2)	61	68	92	98	100	100	100	100	99	98	87	77	**90.0**
5.1 m^2 (Three collector)	Solar fraction **without pump** (flow rate = **0.02** L/s.m^2)	64	70	92	98	100	100	100	100	100	99	90	78	**90.9**
	Solar fraction **with pump** (flow rate = **0.05** L/s.m^2)	78	83	94	99	100	100	100	100	100	100	93	87	**94.4**

From Figure 6.8 it can be seen that the incident solar radiation increases from morning hours to reach 970 w/m^2 as a maximum at about 13:00 pm and then start to decline until sunset. The outlet water temperature from the collector increases during the morning hours to reach 77^{o}C as a maximum at 3:00 pm and then starts to decline until sunset.

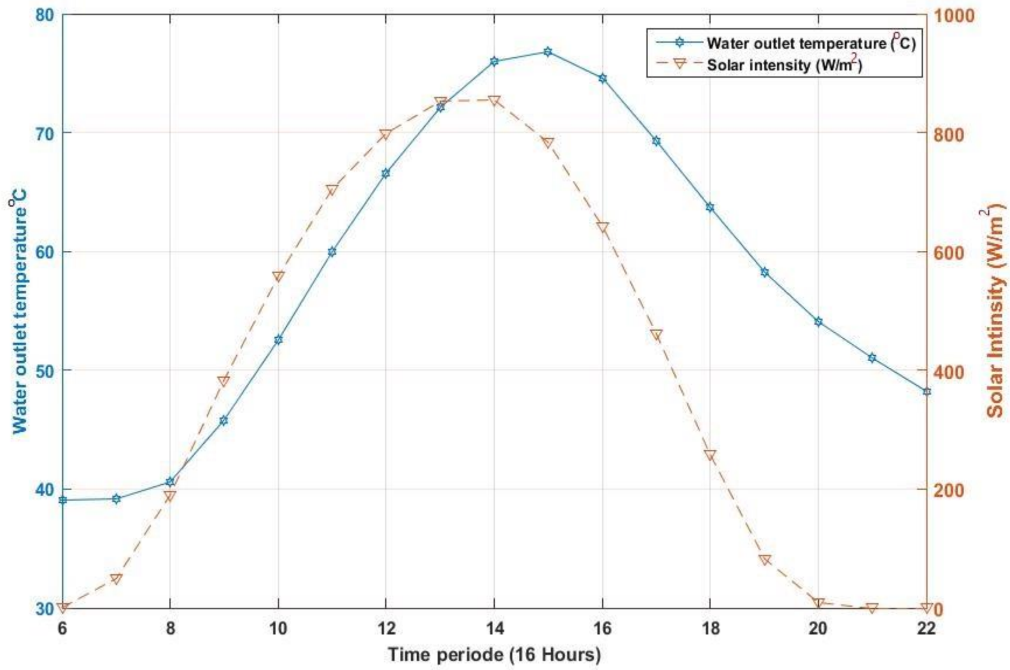

Figure 6.8: Variation of incident solar radiation and outlet water temperature with time (flow rate =0.05 l/s.m^2, Ac = 5.1m^2) on first day of June in Palestine

The monthly solar fraction, ambient temperature and solar intensity is shown in Figure 6.9. In this figure solar fraction values are fluctuating from 73% in January to reach 100% in June. The annual solar fraction is found to be 94%. Actually in the mid of year the solar fraction is higher than 100 %, which means that the SWH covers the needed energy to heat the water and there is extra energy not utilized in the collector. The solar fraction equals 93% in November while 83 % in February. Despite that, the two values have approximately the same solar radiation. This difference in solar fraction refers to the difference in ambient temperature. The average ambient temperature equals 15°C in November and could reach 10°C in February.

Figure 6.10 shows the auxiliary energy needed per month. It is important to note that heating is much required in winter than the other seasons of the year. The auxiliary energy needed during midyear is approximately neglected. The maximum auxiliary energy is needed during January (84 kWh) and February (68 kWh).

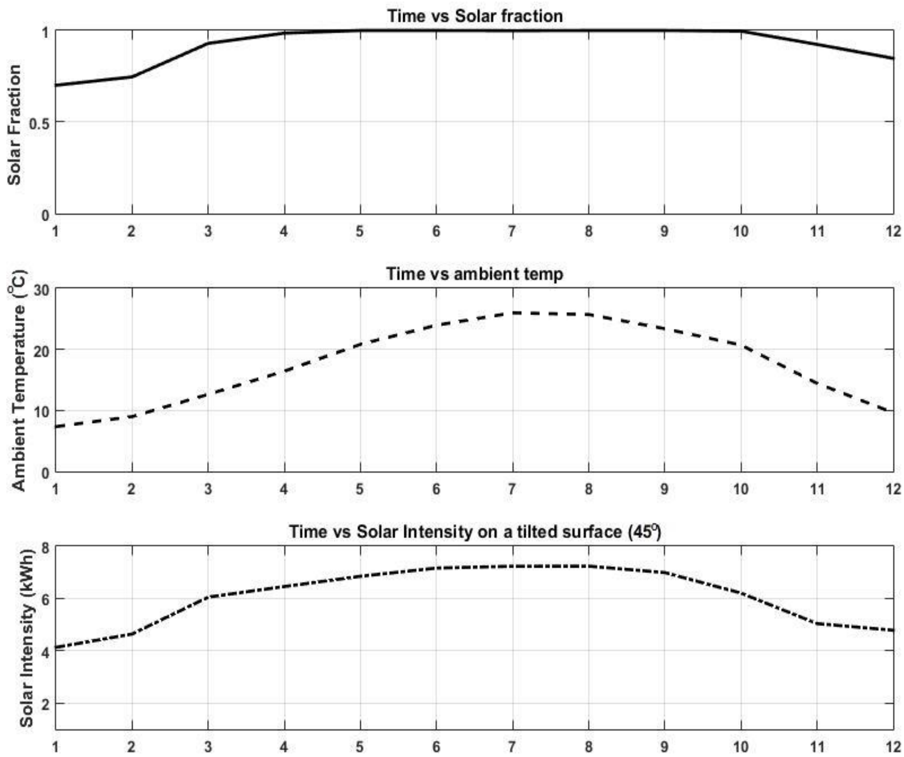

Figure 6.9: Predicted monthly solar fraction, ambient temperature, solar intensity of the solar water heater in Palestine

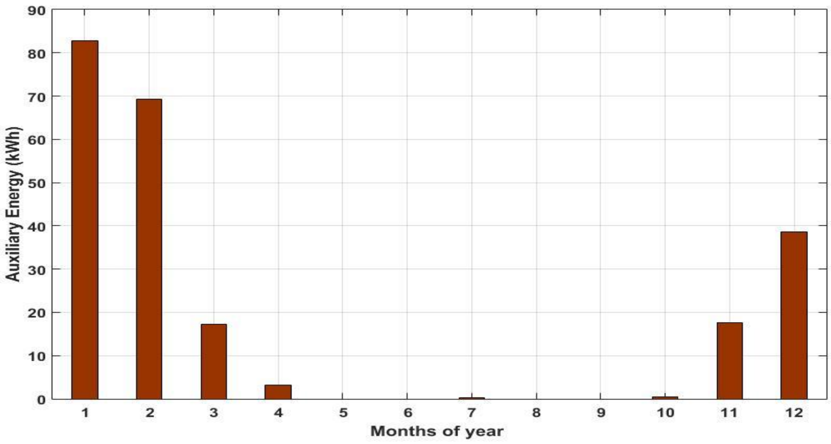

Figure 6.10: Predicted monthly auxiliary energy needed by the system

Figure 6.11 shows the effect of the flat plate collector area on solar fraction. Solar fraction increases from 54% to 96% as collector area increases from 1 to 14 m^2 respectively. As the collector area increases from 12 to 14 m^2, the solar fraction shows maximum value of about 96 %.

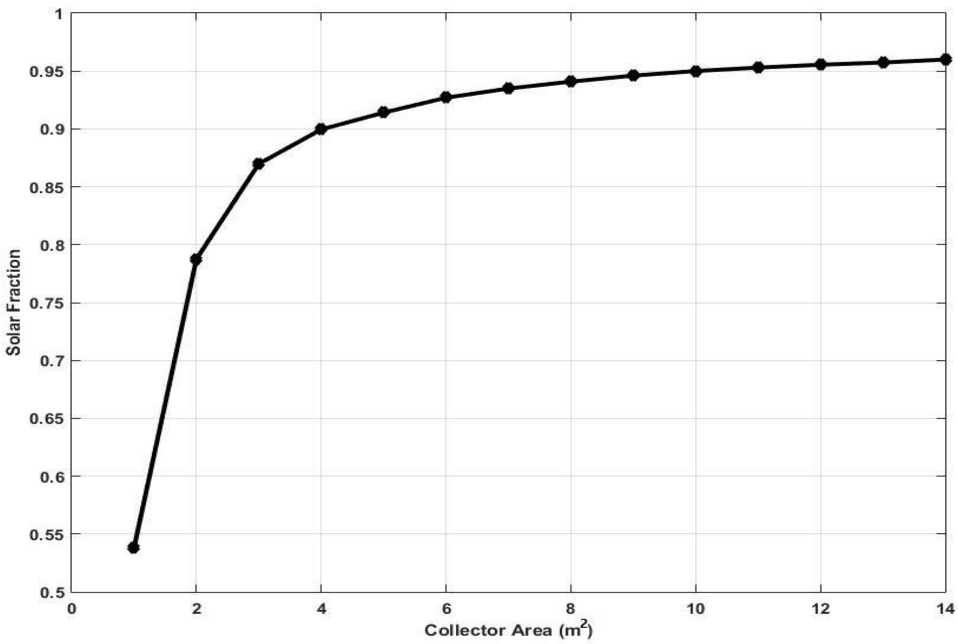

Figure 6.11: Annual Solar Fraction as a function of collector area, when flow rate is 0.05 $L/s.m^2$

Figure 6.12 shows the variation in temperature of water in a storage tank at different values of flow rates. The maximum water temperature in a storage tank variates between 60 to 63.5 ^{o}C when the flow rate increases from 0.015 to 0.055 L/s.m^2.

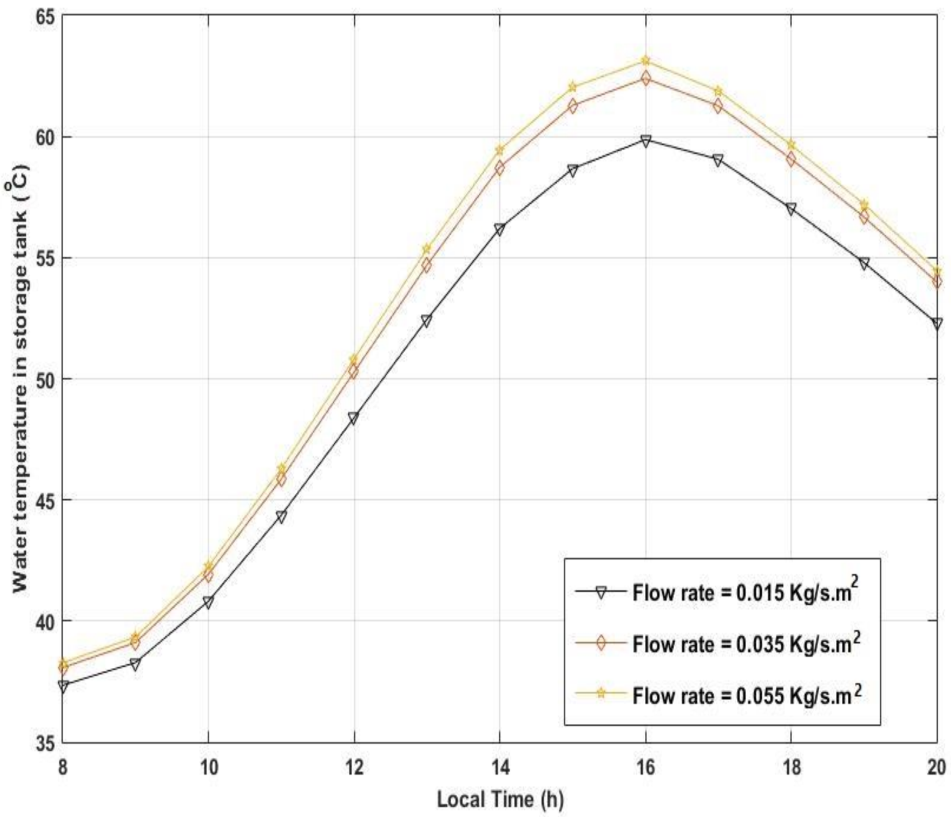

Figure 6.12: Variation of water temperature in a storage tank at different values of flow rate

Figure 6.13 shows the effect of flow rate on the collector efficiency at different values of solar intensity. At 500 W/m^2, the collector efficiency increases from 0% to 40% as the flow rate increases from 0 to 0.04 L/s. After that any increase in the flow rate will not give any significant value for the collector efficiency. Increasing the solar intensity increases the collector efficiency.

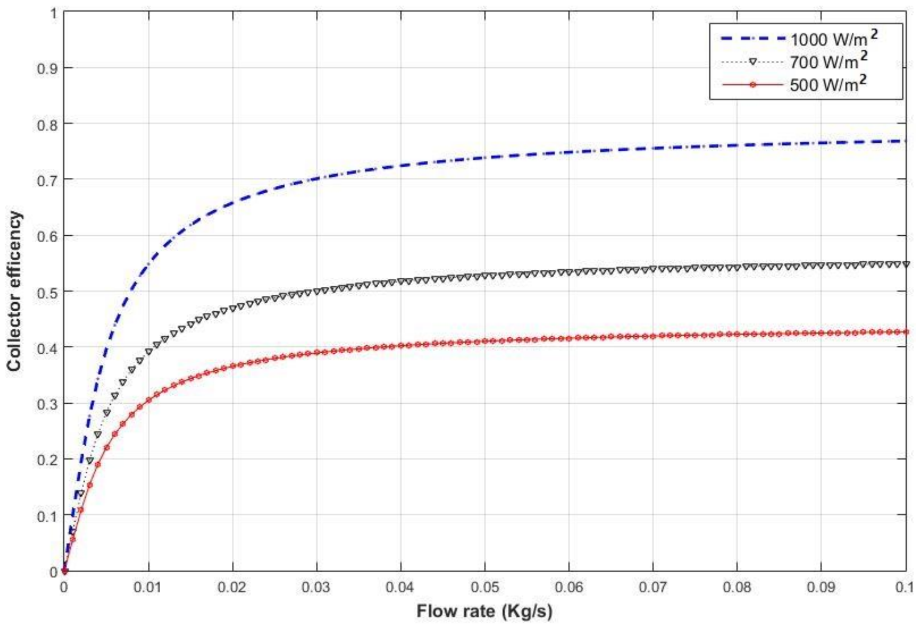

Figure 6.13: Variation of collector efficiency with flow rate at different values of solar intensity (Ac=5.1 m^2) [Matlab simulation]

The performance of a Flat-Plate collector can be approximated by measuring these three parameters: Solar irradiance (I), Fluid inlet temperature (T_i) and Ambient air temperature (T_a). The result is a single line (ΔT/I-curve) shown in Figure 9.7. The collector efficiency η is plotted against (T_i-T_a)/Intensity. The slope of this line (- F_RU_L) represents the rate of heat loss from the collector. For example, collectors with cover sheets will have less of a slope than those without cover sheets. There are two interesting operating points on Figure 6.14.

1. The first is the maximum collection efficiency, called the optical efficiency [20]. Thus occurs when the fluid inlet temperature equals ambient temperature ($T_i = T_a$). For this condition, the ΔT/I value is zero and the intercept is $F_R(\tau\alpha)$.

2. The other point of interest is the intercept with the ΔT/I axis. This point of operating can be reached when useful energy is no longer removed from the collector; a condition that can happen if fluid flows through the collector stops (power failure). In this case the energy coming from the collector is zero [22].

As shown in Figure 6.14, the intercept point increases when the system flow rate increases.

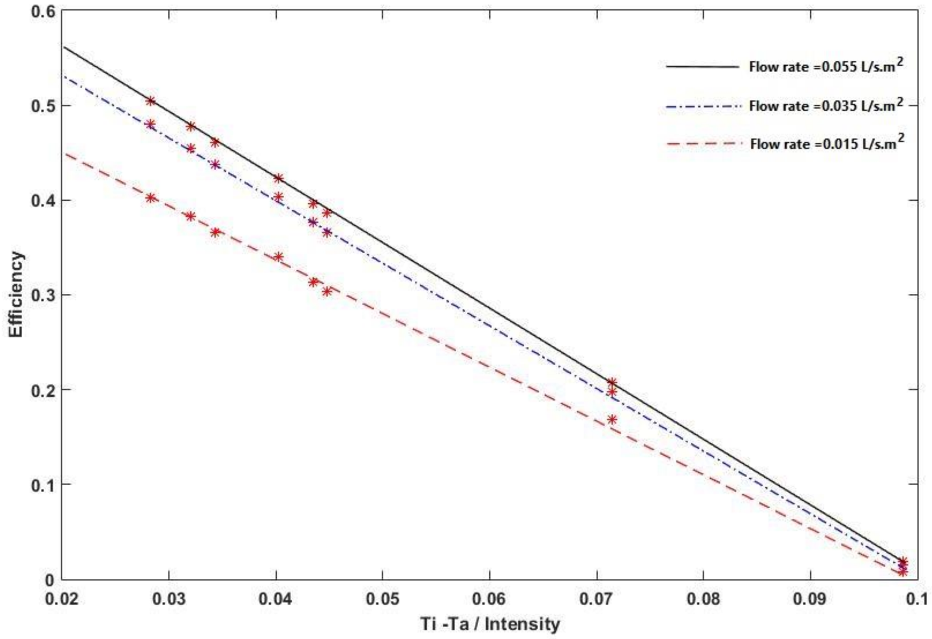

Figure 6.14: Performance curve of atypical flat plate collector with different flow rates, 7 point for each curve represents the result values from simulation

Table 6.5 shows the difference in SWH efficiency before using PV pump (when flow rate is 0.02 L/s.m^2) and after insert the PV pump (when flow rate is 0.05 L/s.m^2). The annual collector efficiency for thermosyphon system is approximately equal 33%, while after adding the circulation pump the annual collector efficiency increases to become 37%.

Table 6.5: Monthy and annual collector efficiency for SWH before and after adding the circulation pump (Ac=5.1 m^2)

Flow rate (L/s.m^2)	Jan	Feb	Mar	Apr	May	Jun	Jul	Aug	Sep	Oct	Nov	Dec	Avg
0.02 (Without pump)	30	30	32	35	35	33	30	30	34	37	37	33	**32.89 %**
0.05 (with pump)	35	35	36	38	39	35	34	34	38	41	41	38	**37.03 %**

Figure 6.15 shows the hourly result data from simulation of the solar water heater used in Palestine. Figure 6.15-A shows the hourly solar radiation in Palestine. It shows the sinusoidal curve for the solar intensity through the year. In the mid of the year the solar radiation will be at maximum, while during January and December the solar radiation is the lowest. Figure 6.15-B shows the relation between the inlet water temperature and the collector according to the lapse of hours through the year. The inlet water temperature therefore is higher during the mid-year and lower during the beginning and last months of the year following the degree of solar radiation. Figure 6.15-C shows the efficiency of flat plate collector in Palestine through the year. The efficiency of the collector is sinusoidal; it is increasing to the mid of year where the efficiency of the collector becomes lower as the inlet water temperature is higher (Figure 6.15-B). Figure 6.15-D shows the solar fraction of the solar water heater in Palestine. Beginning and last months of the year, the solar fraction is lower while in the mid of the year the solar fraction could reach to 100 % in some of days.

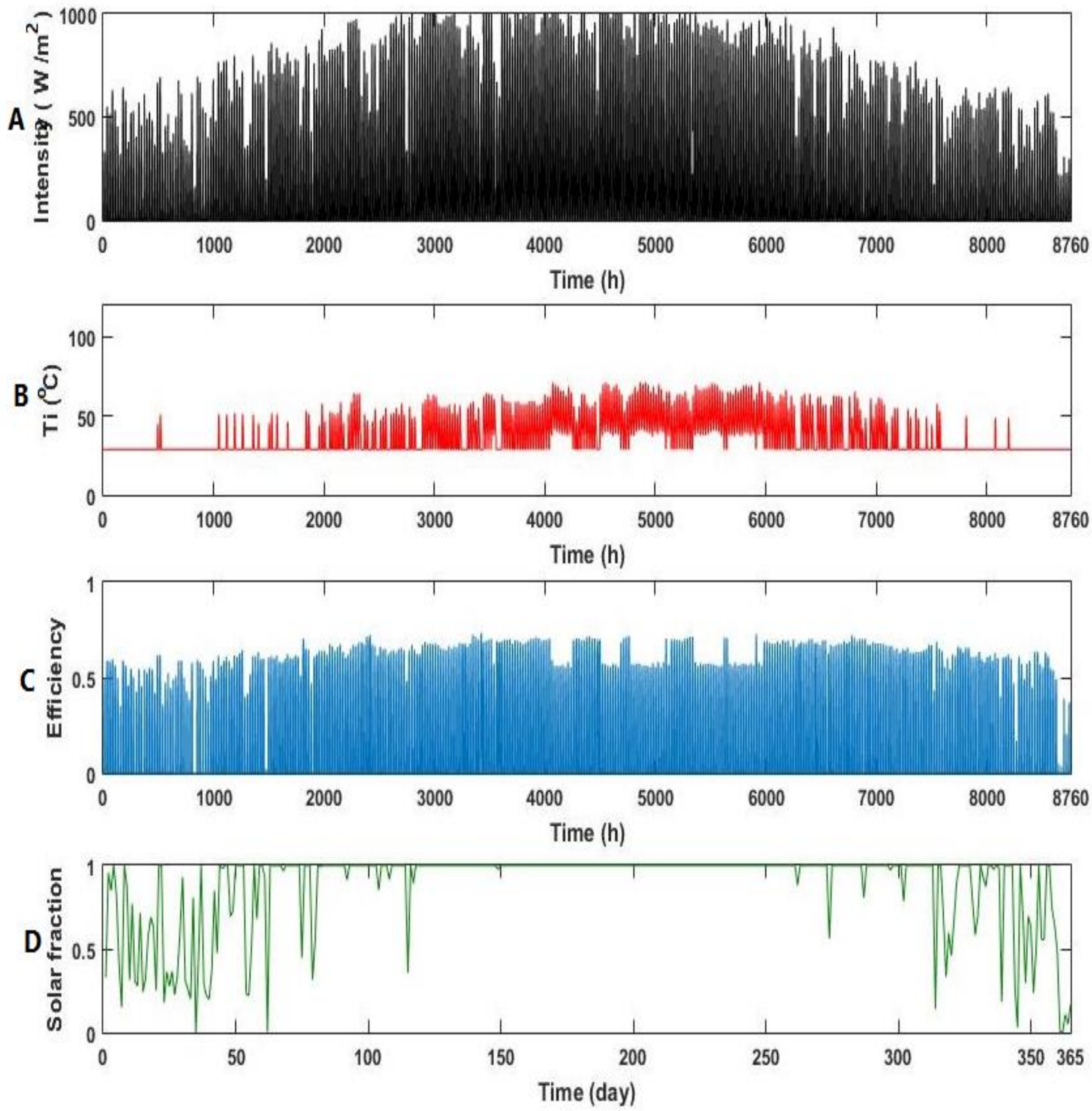

Figure 6.15: Hourly result data from the simulation of the SWHS in Palestine (flow rate =0.05 l/s.m^2, Ac = 5.1m^2) A) Time vs Intensity, B) Time vs Inlet water temperature, C)Time vs efficiency, D) Time vs solar fraction

Chapter Seven

PV Pumping System for SWH

7 PV Pumping System for SWH

7.1 Piping system

A piping system is the sum of pipes, valves and other elements which imposes a pressure drop or head that has to be counter forced by the pump. Pumping head consists of two parts, static head and dynamic head.

$$H = H_{stat} + H_{dyn} \quad (7.1)$$

Where:

H_{stat} : static head component.

H_{dyn} : dynamic head component.

H_{stat} represents the pressure drop through vertical elevation and H_{dyn} represents the flow-associated with pressure drops (T-joint, elbow, valves…etc.). In case of circulation fluid, static head component will be neglected. H_{dyn} could be related to the flow rate and the piping system configuration as follows:

$$H_{dyn} = f\left(\frac{L}{D}\right)\frac{v^2}{2g} \quad (7.2)$$

The head losses can also be expressed as pressure drop or pressure losses as follows:

$$P_{Loss} = \; H.g.\rho \quad (7.3)$$

Where $\boldsymbol{f}$ is the Darcy friction coefficient from moody chart, the coefficient of friction depends on the nature of the water flow expressed by Reynolds number (Re), and the roughness of the inner pipe surface. Normally the flow in heating pipes is turbulent (Re > 2300). (L/D) (m/m) is the length to diameter ratio of the piping system, v (m/s) is the fluid velocity inside the tube, (ρ) is fluid density, and (g) is the gravitational acceleration (9.8 m/s^2) The following Equations shows the Darcy friction coefficient $\boldsymbol{f}$ for pipes for each laminar and turbulent flow.

$$f = \frac{64}{Re}$$ For Laminar flow [1] (7.4)

$$f = \left(\frac{1}{-1.8\log\left[\left(\frac{\varepsilon/D}{3.7}\right)^{1.11} + \frac{6.9}{Re}\right]}\right)^2$$ For Turbulent flow [30] (7.5)

$$Re = \frac{\rho . v . D}{\mu} \quad (7.6)$$

$$v = \frac{\dot{m}}{\rho\, A} \quad (7.7)$$

Where,

ρ = is the density of the fluid (kg/m^3)

$v =$ is the maximum velocity of the object relative to the fluid (m/s)

$\dot{m}$ = is the mass flow rate of the fluid through the pipe

D = pipe diameter (m)

ε = 0.1 mm for Steel pipe, from moody chart

A = is the pipe cross sectional area (m^2)

μ = is the dynamic viscosity of the fluid (N s/m^2); for water at 20°C the dynamic viscosity is 1.002 $x10^{-3}$ N s/m^2

Equation 7.8 is used to calculate the electric power consumption P_{el} for circulating pump [31]:

$$P_{el} = \frac{\Delta P . Q}{\eta_p . \eta_{mo}} \quad (7.8)$$

Where Q is the flow rate (m^3/s), and η_p and η_{mo} are the pump efficiency and the electric motor efficiency respectively where the combined motor-pump efficiencies ranged from 5-30 % [31] based on pump and system characteristic, ΔP is the pressure drop (Pa).

Figure 7.1 shows the schematic diagram for solar collector commonly used in Palestine with circulating pump, PV module and auxiliary heater. It shows three collectors; each collector area is 1.71 m^2 facing south direction at 45^o tilt angle. PV-module is a power source to drive the pump. Steel pipes have a total length of 4m. Auxiliary electric heaters cover the reduction in hot water specially in winter season. The size of storage tank is 180 L.

According to chapter 6, the flow rate for SWH system with circulation pump is 0.05 $L/m^2.s$ (50 $cm^3/m^2.s$). From pipe length, flow rate and diameter we can define the required pump to circulate the fluid in the collector. We have four steps to determine the power of circulation pump [32]:

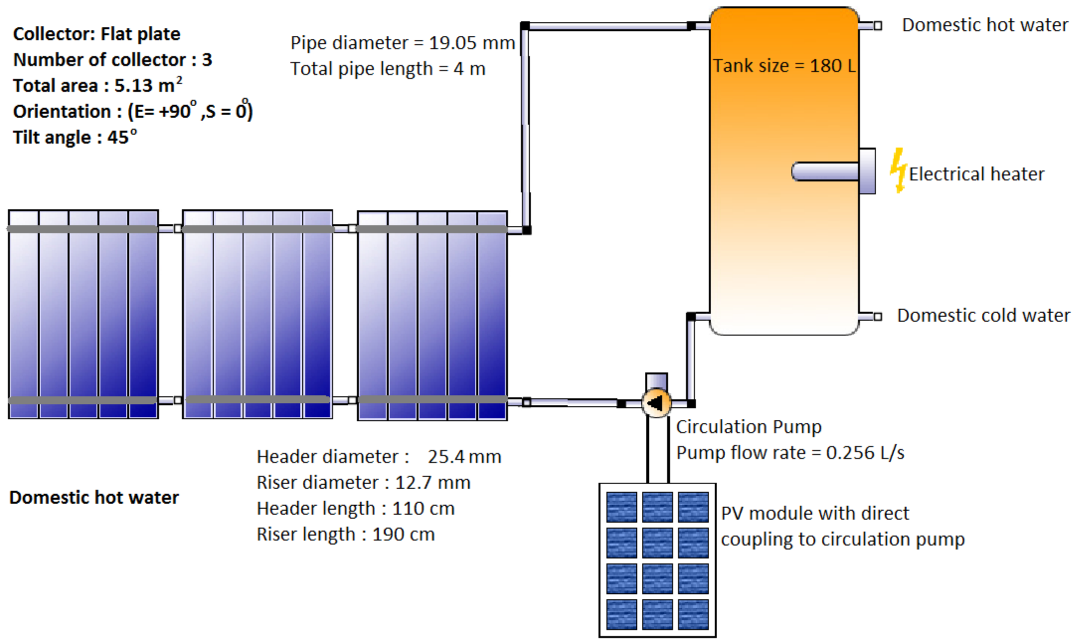

Figure 7.1: Schematic diagram for solar water heater system

Step 1: Calculate the flow to the collectors

The collectors need to have sufficient flow to remove the heat from the collectors. From Figure 7.1 we have three flat plate collectors; each collector area is 1.71 m^2, so the total area is 5.13 m^2.

The recommended flow rate per square meter for SWH with circulation pump is 0.05 L/s instead of 0.02 L/s for thermosiphon system, so the target flow rate is:

(5.13 m^2) x (0.05 L/s m^2) = 0.256 L/s

Step 2: Calculate the pressure drop in the pipe, header, and risers

In this step, we will calculate the total pressure drop through the system for the collectors and supply and return pipes of the collectors. To get the pressure drop for the pipe, we should know the length, diameter, flow rate and velocity. Table 7.1 shows this parameter for each tube in SDWH system.

Table 7.1: Diameter, lengh, flow rate, and velocity of water inside the tube for each tube in SDWH system

	Diameter (mm)	**Length (m)**	**Mass flow rate (kg/s)**	**Velocity (m/s)**
Supply and return pipes	19.05	4	0.256	0.892
Headers	25.4	6.6	0.256	0.505
Risers	12.7	1.9	0.01	0.08

As shown in Table 7.1, the velocity of fluid inside the tube is calculated based on Equation 7.7. The mass flow rate in the risers is small. Suppose that each collector has 7 risers, we have three collectors in the system, so the total number of risers is 21, the mass flow rate ($\dot{m}_r$) in each risers is:

$\dot{m}_r$=0.256 / 21 = 0.01 kg/s

From Equation 7.2 we can define the dynamic head loss for each tube in the system, the head loss through supply and return pipes (H_{psr}) is:

$$H_{psr} = f\left(\frac{L}{D}\right)\frac{v^2}{2g}$$

From Table 7.1 the total length of pipe(L) is 4 m, pipe diameter (D) is 0.01905 m, fluid velocity (V) is 0.898 m/s. The Darcy friction coefficient is calculated based on Reynolds number. The Reynolds number is calculated by Equation 7.6:

$$Re = \frac{\rho\,.v.D}{\mu}$$

Where the density of water (ρ) is equal (1000 kg/m^3), the dynamic viscosity (μ) for water at 30^{o}C is 0.798x10^{-3} N s/m^2.

$$Re = \frac{1000 \text{ x } 0.898 \text{ x } 0.01905}{0.798\ x\ 10^{-3}} = 21437$$

The value of Reynold number is greater than 2300, so the fluid flow is turbulent, from Equation 7.5, the Darcy friction coefficient (f) is:

$$f = \left(\frac{1}{-1.8\log\left[\left(\frac{\varepsilon/D}{3.7}\right)^{1.11}+\frac{6.9}{Re}\right]}\right)^2 = \left(\frac{1}{-1.8\log\left[\left(\frac{0.1/19.05}{3.7}\right)^{1.11}+\frac{6.9}{21437}\right]}\right)^2 = 0.034$$

The dynamic head loss (H_{psr}) for supply and return pipe is:

$$H_{psr} = f\left(\frac{L}{D}\right)\frac{v^2}{2g} = 0.034\left(\frac{4}{0.01905}\right)\frac{0.898^2}{2\ x\ 9.8} = 0.293 \text{ m}$$

Converting the head losses to pressure losses can be by using Equation 7.3 as follows:

$$P_{psr} = H.g.\rho = 0.293\ x\ 9.8\ x\ 1000 = 2871 \text{ Pa}$$

Table 7.2 shows the result of Reynold number, Darcy friction coefficient, pressure losses through the supply and return pipes (P_{psr}), headers (P_h), and risers tube (P_r).

Table 7.2: Reynold number, Darcy friction, pressure loss for each tube in SWH

	Re	Darcy friction coefficient (f)	Head loss (m)	Pressure loss (Pa)
Supply and return pipes	21437	0.034	0.293	2871
Headers	16073	0.033	0.111	1093
Risers	1286	0.049	0.0023	22.5
Total	**-**	**-**	**0.4063 m**	**3986 Pa**

As shown in Table 7.2, the pressure drop through the collector's riser tubes themselves is small. It can probably be ignored because each riser only sees about 0.01 (L/s) and has a length of 1.9 m with (0.5 inch) diameter, so the pressure drop is 22.5 Pa. Since all the risers are in parallel, this is the total pressure drop over the risers.

Step 3: Fitting pressure drops

Fluid head loss through a fitting (elbows, Tees, etc.) in the system can be calculated by the following equation [33]:

$$H_{Fitting} = NK\frac{v^2}{2g} \tag{7.9}$$

Where,

N = quantity of fitting part

H = fluid head loss (m)

K= manufacturers published "K" factor for the fitting

v = velocity of fluid (m/s)

g = acceleration due to gravity (m/s^2)

Table 7.3 shows fittings type, quantity, mass flow rate, velocity of fluid in each type, (K) factor for each fitting and pressure losses due to fittings friction.

Table 7.3: Pressure loss due to fitting friction

	T-Joint	**Steel elbow (90^o)**	**Entrance + Exit**	**Total**
(K) Factor	1.5	0.3	1	-
Quantity	2	4	2	-
Mass flow rate (kg/s)	0.256	0.256	0.256	-
Fluid velocity (m/s)	0.505	0.898	0.892	-
Head loss (m)	0.04	0.05	0.08	**0.17 m**
Pressure loss (Pa)	392	500	784	**1676 Pa**

Step 4: Selecting a pump

Table 7.2 and Table 7.3 show that the total head losses for each tube and pipe fitting is 0.5763 m (0.4063 m + 0.17 m). It can be expressed as pressure losses, which is equal 5662 Pa (3986 Pa + 1676 Pa). Now, we need to pick a pump that provides a flow rate of around 0.256 L/s or 0.92 m^3/h with piping friction loss of 5662 Pa. We will use the pump curve family for the ECO CIRC circulator pump. This series of pumps has been used for lots of solar applications [34]. Figure 7.2 shows some of pump curves for the ECO CIRC series circulators. For each pump, the curves show the combination of flow rates, pressure drop, and power consumption.

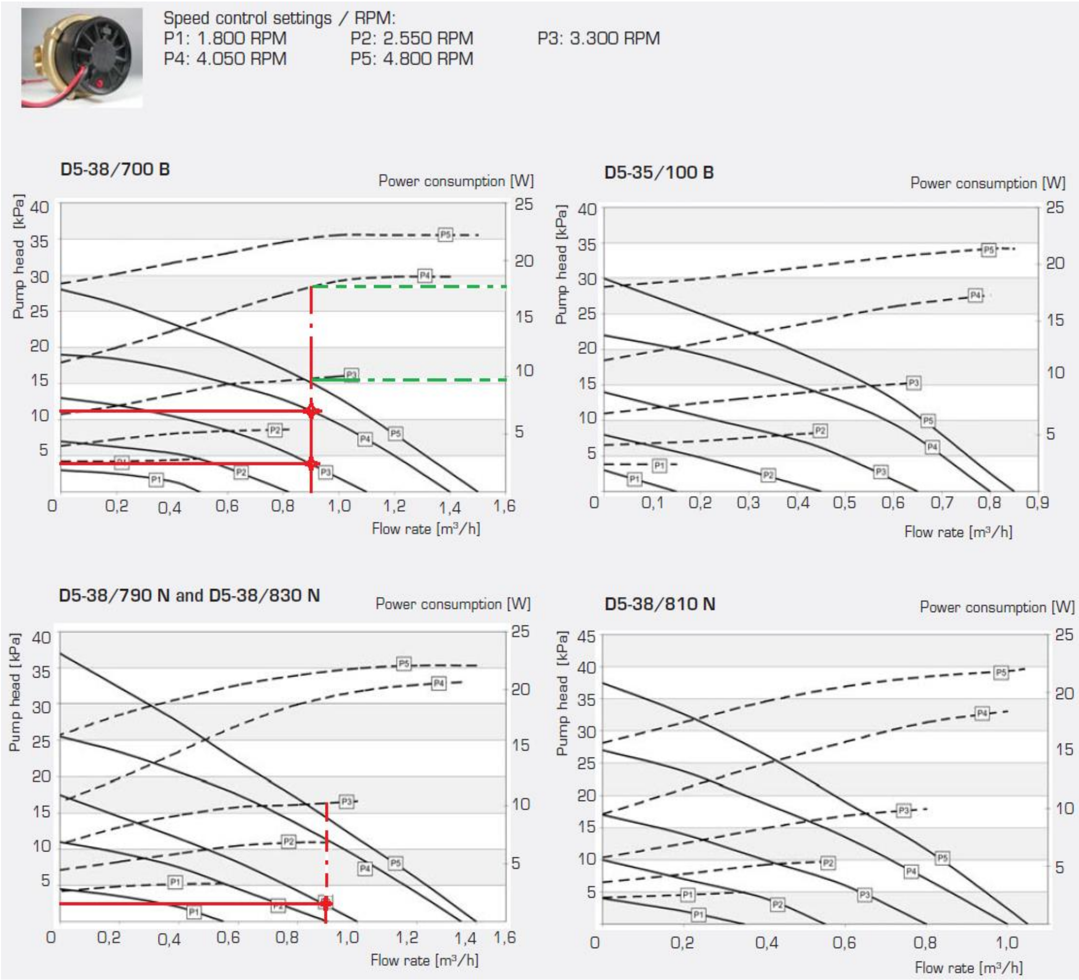

Figure 7.2: Pump curves for the ECO CIRC pump series circulators [32]

We need a pump that produces 0.92 m^3/h with 5.6 kPa of pressure drop. To see how each pump works in meeting this requirement, go vertically up the 0.92 m^3/h line, and read to the left of the pressure head that each pump can produce. For example, (D5-38/790 N) pump when the speed control setting at (P3), the pressure drop reads about 2.5 kPa. There is a low pressure drop which is not meeting our pump requirement. If we look at (D5-38/700 B) when the speed control at (P3), the pressure drop is about 4.8 kPa and the power consumption is about 8 W. This pump also cannot achieve the design requirement.

If we look at (D5-38/700 B) pump when speed control at (P4), this pump can achieve the requirement pressure where the pressure head at 0.92 m^3/h is about 11 kPa. The power consumption is about 17 W. This pump meets the required flow rate and pressure drop of the pump design. Combined motor pump efficiency for this pump is calculated as follows:

$$\eta_p \ . \eta_{mo} = \frac{\Delta P \ . Q}{P_{el}} = \frac{(11000 \ Pa) \ x \ (0.92 \frac{m^3}{3600 \ s})}{(17 \ W)} = 16.5 \ \%$$

Choosing (D5-38/700 B) at speed control P4 guarantees the fluid flow in the pipes as its pressure head is higher than the result value (5.6 kPa). Table 7.4 shows the technical data for this pump.

Table 7.4: Technical data for ECO CIRC pump circulators [33]

Technical Data	
Motor design	Electronically commutated spherical motor with permanent magnet
Voltage	12 V
Power consumption	start-up power consumption less than 1 W , Max power consumption 22 Watts
Current	0.25 - 1.46 A
Acceptable media	domestic hot water, heating water, water/glycol mixtures
Insulation class	IP42 / Class F
Pump housing material	Brass
Max system temperature	-10C^o to 95C^o
Weight	0.7 kg

7.2 Direct coupled PV pumping systems

7.2.1 Overview

A direct coupled PV pumping system is a group of interactive pieces of equipment designed to collect and convert the solar radiation into electrical energy and to convert the electrical energy into mechanical energy to provide enough mechanical torque to spin a pump to circulate a fluid [1].

Direct coupled PV systems consist of PV module, a DC-motor, a pump and hydraulic piping system. The direct coupled PV pumping system has no electric storage device, such as batteries, and no power conditioning units such as inverters or converters. Figure 7.3 shows the schematic drawing of a direct-coupled PV pumping system.

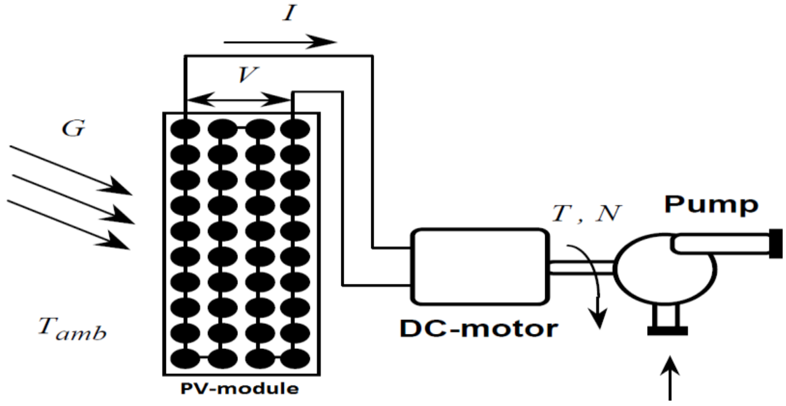

Figure 7.3: Schematic diagram for Direct-Coupled PV Pumping System

PV-module is the power generator of the system. The PV module, Dc-motor, and a pump are characterized by their current voltage relation (I-V curve). The power output (P) is the product of current (I) and voltage (V). Figure 7.4 shows the I-V and P-V characteristic of module made of 40 cells connected in series with the I-V curve of a load comprising of a DC-motor coupled to a centrifugal pump.

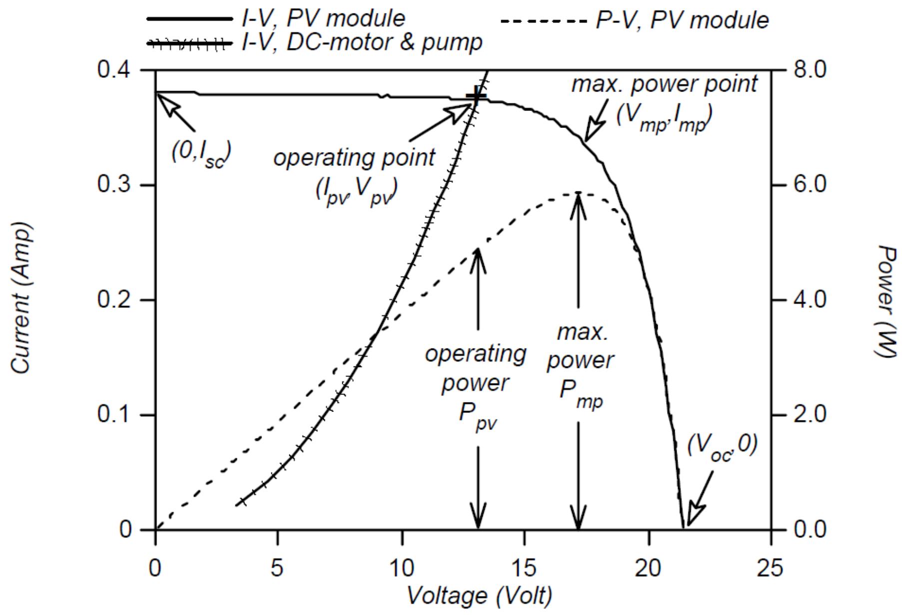

Figure 7.4: The I-V and P-V curves of a PV module and the I-V curve of a load comprising of a DC-motor coupled to a centrifugal pump [1]

From Figure 7.4, the operating point of a PV system when the DC-motor is ON is the point at which the characteristics of both the PV module and the load match (I and V of the PV cells match I and V of the load). Figure (7.5) depicts also the system operating points if the PV module was directly coupled to the separately excited DC-motor and the centrifugal pump mentioned above. The system operating points fall along the I-V curve of the DC motor and pump [1].

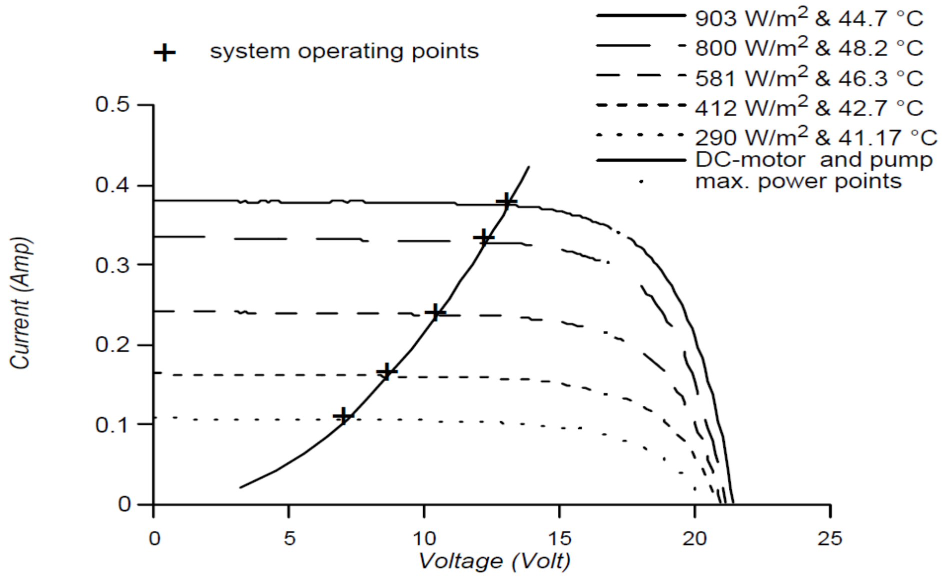

Figure 7.5: The effect of solar radiation intensity on PV I-V curves and PV system operating points [1]

A PV module is a nonlinear power source. The output current and voltage depend on the level of radiation and temperature. When the solar radiation and ambient temperature is changed, the operating point of the PV module couple to a pump-motor will change. PV pumping system requires a threshold radiation level (G_{th}), to start pumping. In this study the PV-SWHS is designed to start at solar radiation of about 150 W/m^2 .

Using the direct coupled PV pumping system can act as a fast-response sensor to solar energy and therefore pumping will only be working at the times when the thermal collector is also receiving solar radiation.

7.2.2 PV module selected

The design of PV module depends on the I-V characteristics of DC pump motor. Table 7.5 shows the technical data for the selected pump motor.

Table 7.5: Technical data for DC pump motor [35]

Technical Data

Motor design	Electronically commutated spherical motor with permanent magnet rotor/impeller
Voltage	8 - 24 Volt
Power consumption*	min. start-up power consumption less than 1 Watt, max. power consumption 22 Watts
Current draw	0,25 - 1,46 A
Acceptable media	domestic hot water, heating water, water/glycol mixtures, other media on request**.
Insulation class	IP 42 / Class F

From table 7.5, the motor start-up power consumption is 2W (8 V X 0.25 A). To choose the appropriate PV module, we need to take into account that the motor will be start-up when threshold solar radiation (G_{th}) is more than 150 W/m^2. The rationale for choosing this value is to warrant that the pump works non-stop all day long as the solar radiation in Palestine is above 150 W/m^2. If we use a module of 10 W peak power as shown in Figure 7.6, note that the motor start rotating when the solar radiation is more than 420 W/m^2. This is not appropriate because the motor will turn off when the solar radiation is less than this value. While using a PV module of 20 W peak power, the motor started when solar radiation is more than 250 W/m^2.

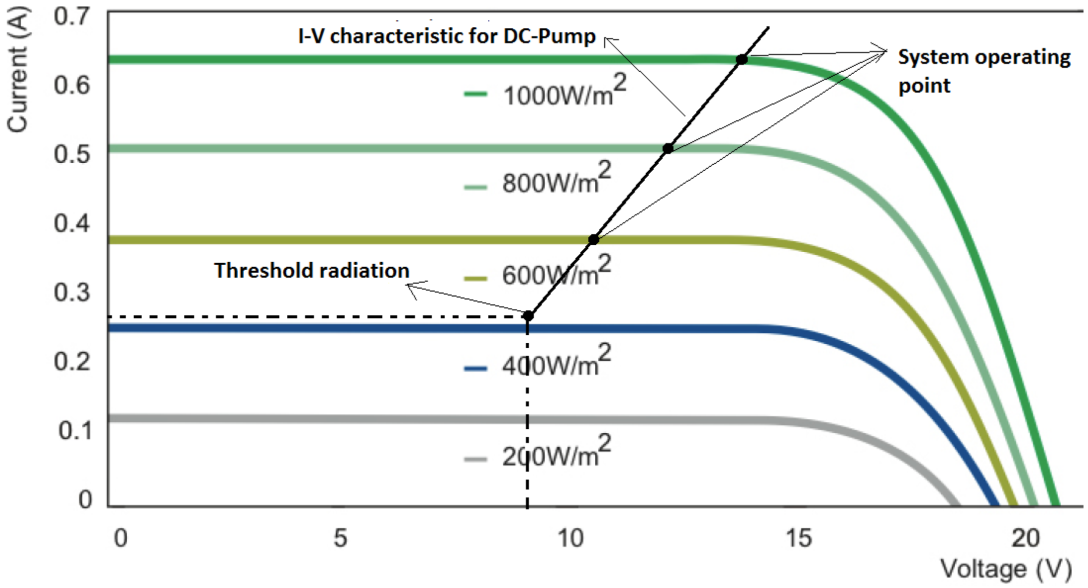

Figure 7.6: The I-V curve of a PV module and the I-V characteristics of a DC-pump from data sheet of PV module [Appendix 5]

Table 7-6 shows three types of modules with different peak power (10W, 20W, 30W) and the electrical characteristics for each type.

Table 7.6: Threshold radiation and electrical characteristics for three types of PV modules

Type	Module Name	Maximum Power at STC (W)	V_{mpp} (V)	I_{mpp} (A)	V_{oc} (V)	I_{sc} (A)	Module Efficiency	Threshold Radiation (W/m^2)
1	SE-410J	10	16.8	0.59	21	0.65	8.80%	420
2	SE-420J	20	16.8	1.19	21	1.29	9.40%	250
3	SE-330J	30	16.8	1.78	21	1.94	10.50%	150

From table 7.6, the threshold radiation for PV module type 3 is 150 W/m^2.This means that the DC-pump is starting pump when solar radiation is above this value. Type 3 will be chosen because it achieves the required power to start the pump.

Chapter Eight

Economic and Environmental Impact for Using SWH

8 Economic and Environmental Impact for Using SWH

8.1 Economical study

The initial investment for an average Palestinian SWHS is about 1950 NIS [14]. Every 3.8 NIS is about 1 US$. The SWHS is expected to last at maximum 30 years after all maintenance. One major advantage of SWHS is that the cost of 1 unit of useful energy is not dependent on price increases in other fuel. In addition, solar heater is nonpolluting. Many families are starting to buy gas geyser system or electrical geyser because the initial investment for this system is low. There are advantages of prompt heating of water; however, it may cause gas explosion. Moreover, the running costs for this type of heater is high, which obviously has a negative economic impact. In addition, the life cycle for these heaters is low; they have relatively thin pipes, pipe corrosion caused by salt content of the utility water used. The expected life cycle is 15 years after all repeated maintenance. The solar water heaters with electrical coils are a viable option for providing the Palestinian family.

The objective of this chapter is to study the economics of gas boilers and SWHS (with and without a PV pump) compared with electrical heaters.

By using present worth analysis (PW) we will compare between three alternatives, gas boiler, electrical boiler, and solar heater with electric coil.

8.1.1 Economic study of gas boiler

For economic analysis for gas boiler we need to know the life cycle for this alternative, interest rate (8%), initial cost, annual costs or running costs, and salvage value.

From the result in chapter 3, the average daily energy load for heating the 180 L of water from ambient temperature to 55C^{o} is 7.8 kWh in Palestine, 2847 kWh annually. The initial cost of gas boiler is 650 NIS from market.

The calorific value for using gas is 12.87 kWh /kg of gas [36]. Every tank of gas contains 12 Kg of fuel, and the average price for this tank is 60 NIS.

The total average efficiency is 82% [37], now to find the annual cost:

Input energy needed = 2847 / 0.82 = 3472 kWh

Total energy in fuel tank = 12 Kg x 12.87 kWh/Kg = 154.44 kWh.

Annual number of tanks needed = 3472 kWh / 154.44 Kwh = 22.4 Tank.

Annual cost for tanks = 22.4 Tanks x 60 NIS = 1344 NIS.

Annual maintenance = 40 NIS.

Salvage value = 100 NIS.

The Life cycle for gas boiler is 15 years, but in cash flow the time period used is 30 years because the time period for solar heaters is 30 years. The least common multiple (LCM) is 30 years. Figure 8.1 shows the cash flow analysis for gas boiler.

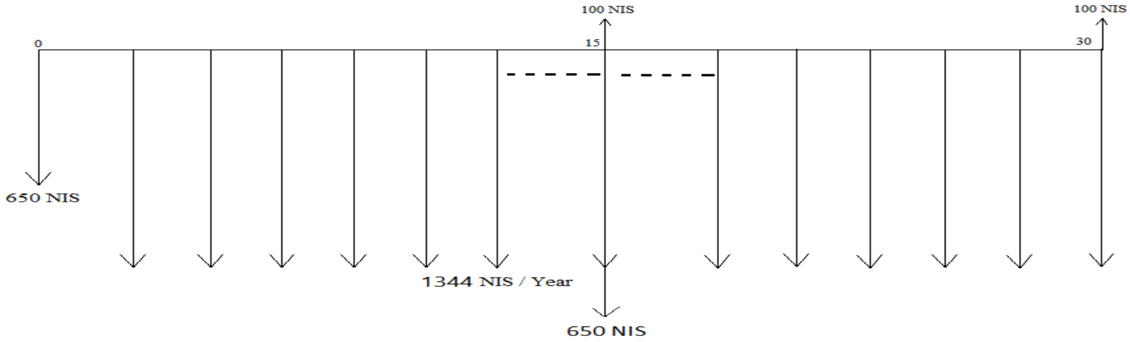

Figure 8.1: Cash flow diagram for Gas boiler

P.W $_G$ = - 650 - 550 (P/F, 8%, 15) + 100 (P/F, 8%, 30) – 1344 (P/A, 8%, 30)

P.W $_G$ = -650 - 550 x 0.3152 + 100 x 0.0994 – 1344 x 11.257 = -15941 NIS

Where,

P.W = is the present worth analysis for gas boiler

To find the best alternative, we should find the present worth analysis for all alternatives.

8.1.2 Economic study of electrical boiler

Electrical boiler is the same as gas boiler but the used type of fuel is different. The initial cost of electrical boiler is 450 NIS; the salvage value is 70 NIS; the annual maintenance is 30 NIS. The life cycle is the same as gas boiler; the interest rate is 8%, the annual load following the result of simulation from Chapter 3 is 2847 kWh, the efficiency of the system is 92% [36]. Now to find the annual running cost:

The price of 1 kWh = 0.6 NIS.

Input energy needed = 2847 / 0.92 = 3094 kWh

Annual cost = 3094 kWh x 0.6 NIS = 1856 NIS.

Figure 8.2 shows the cash flow diagram for electrical boiler at time period is 30 years.

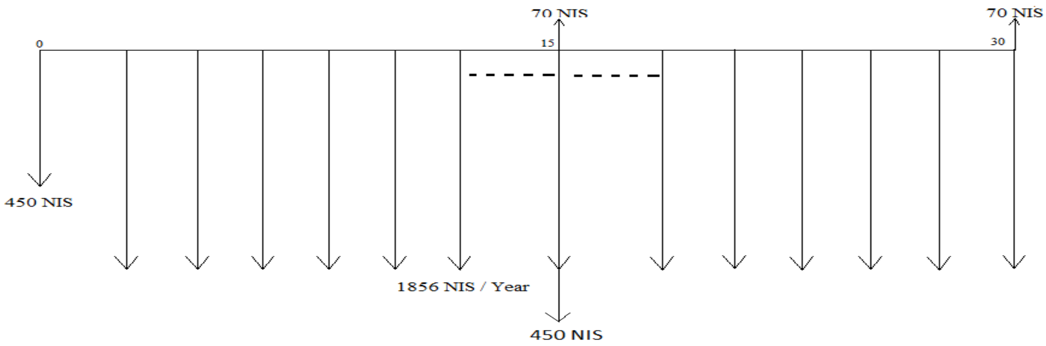

Figure 8.2: Cash flow diagram for electrical boiler

$P.W_E$ = - 450 - 380 (P/F, 8%, 15) + 70 (P/F, 8%, 30) – 1856 (P/A, 8%, 30)

$P.W_E$ = -450 - 380 x 0.3152 + 70 x 0.0994 – 1856 x 11.257 = - 21454 NIS.

The value of present worth for electrical boiler is less than present worth for gas boiler, so the gas boiler until now is the best alternative.

8.1.3 Economic study of solar heaters with electric coil

Thermosyphon Solar heaters with electric coil are the most commonly used systems. The solar heating is competitive with other means of heating. The unit price of SWH with electric coil is about 2400 NIS. The unit price for electric coil is about 200 NIS. It needs to be replaced every 15 years in the system. So it is necessary to know the annual solar fraction for solar collector, which is:

$$S.F = \frac{Q_u}{Q_L}$$

Where Q_S is a useful absorbed energy from the collector and Q_L is the annual energy needed to heat the water to 55°C. Table 8.1 shows the daily collector properties for solar heaters in three months (January, March and June) in Palestine. The results in this table are based on simulating the mathematical model of flat plate collector in MATLAB software.

Table 8.1: A Daily collector properties through January in Palestine, area collector = 5.1 m^2, volume of tank =180 Liters, flow rate =0.015 L/s.m^2 [Solar radiation and ambient temperature are obtained from PVSys software],

Day	Daily Solar Radiation ($kWh/m^2.day$) on a tilted surface (45°)	T_a (C°)	Q_u (kWh) [Equation 5.6]	Q_L (kWh) [$m.C_p.\Delta T$]	η (%) [$\frac{Q_u}{A_c . I}$]	S.F (%) [$\frac{Q_u}{Q_L}$]
1	2.51	12.3	3.7	8.95	29.0	42
2	5.59	9.7	10.1	9.48	35.4	100
3	4.96	10.3	9.9	9.35	39.2	100
4	6.50	7.9	11.2	9.85	33.9	100
5	5.44	7.3	10.3	9.98	37.2	100
6	3.48	7	5.2	10.06	29.3	52
7	2.13	7.1	1.9	10.03	17.5	19
8	6.55	6.4	11.0	10.18	32.9	100
9	5.91	5.8	11.1	10.3	37.0	100
10	3.06	6	4.1	10.26	26.0	40
11	5.17	6.7	9.7	10.1	36.6	96
12	3.03	2.5	4.2	11	27.1	38
13	3.17	4.6	3.7	10.55	22.8	35
14	5.26	4.9	9.3	10.48	34.8	89
15	3.11	3.6	3.3	10.77	20.8	31
16	2.56	5.1	4.2	10.45	32.0	40
17	4.41	6.6	7.3	10.14	32.6	72
18	4.76	7.7	8.5	9.9	35.1	86
19	4.29	8.8	7.6	9.67	34.7	79
20	2.57	8.4	3.1	9.75	23.6	32
21	6.62	9.4	10.9	9.55	32.4	100
22	6.87	10.1	11.5	9.4	32.8	100
23	2.27	8	2.2	9.83	19.1	22
24	3.61	5.6	4.7	10.34	25.6	46
25	2.39	6.1	3.6	10.24	29.4	35
26	3.13	9.2	4.4	9.59	27.6	46
27	2.30	8.9	2.7	9.64	23.3	28
28	2.98	7.5	4.2	9.94	27.6	42
29	3.98	8.2	5.8	9.79	28.4	59
30	5.77	8.7	9.9	9.7	33.5	100
31	2.59	11.3	3.6	9.15	27.1	39
Total average	**4 ($kWh/m^2.day$)**		**6.5 kWh**		**29.8 %**	**64.23 %**

Table 8.1: B Daily collector properties through March in Palestine.

Day	Daily Solar Radiation (kWh/m^2.day) on a tilted surface (45^o)	T_a (C^o)	Q_u (kWh)	Q_L (kWh)	η (%)	S.F (%)
1	6.25	12.4	11.1	8.9	34.8	100
2	5.89	11.2	12.2	9.2	40.6	100
3	5.37	10.9	8.9	9.2	32.5	96
4	1.21	9.3	4.0	9.6	64.8	41
5	7.36	8.3	11.8	9.8	31.4	100
6	7.66	9.0	12.5	9.6	32.0	100
7	6.03	10.2	10.1	9.4	32.8	100
8	7.47	9.9	12.4	9.4	32.5	100
9	7.05	7.0	11.7	10.0	32.5	100
10	6.13	7.6	10.7	9.9	34.2	100
11	6.79	8.7	11.6	9.7	33.5	100
12	7.22	10.4	12.0	9.3	32.6	100
13	6.69	9.7	11.3	9.5	33.1	100
14	6.03	10.7	10.6	9.3	34.5	100
15	6.56	11.4	11.3	9.1	33.8	100
16	5.48	12.3	8.8	8.9	31.5	98
17	3.16	13.1	4.9	8.8	30.4	56
18	5.08	20.8	10.4	7.2	40.1	100
19	7.39	15.8	13.0	8.2	34.5	100
20	6.94	15.0	12.1	8.4	34.2	100
21	2.74	11.6	3.6	9.1	25.8	40
22	3.51	11.8	5.6	9.0	31.3	62
23	4.95	15.4	10.6	8.3	42.0	100
24	5.91	13.5	9.4	8.7	31.2	100
25	7.87	14.2	12.9	8.5	32.1	100
26	6.92	13.9	11.8	8.6	33.4	100
27	5.71	12.7	8.7	8.8	29.9	98
28	6.82	17.9	12.4	7.8	35.7	100
29	6.92	17.2	12.4	7.9	35.1	100
30	6.77	14.6	11.5	8.4	33.3	100
31	6.94	16.5	12.3	8.1	34.8	100
Total average	**6.03 (kWh/m^2.day)**		**10.4 kWh**		**34.5 %**	**91.68 %**

Table 8.1: C Daily collector properties through June in Palestine.

Day	Daily Solar Radiation (kWh/m^2.day) on a tilted surface (45^o)	T_a (C^o)	Q_u (kWh)	Q_L (kWh)	η (%)	S.F (%)
1.0	7.7	22.7	14.1	6.8	35.9	100
2.0	7.4	22.7	13.2	6.8	35.0	100
3.0	7.4	22.9	13.3	6.7	35.2	100
4.0	7.2	23.1	13.1	6.7	35.7	100
5.0	6.5	20.5	12.0	7.2	36.2	100
6.0	7.4	22.4	13.3	6.8	35.2	100
7.0	7.5	21.8	13.4	6.9	35.0	100
8.0	7.2	21.4	12.7	7.0	34.6	100
9.0	7.5	20.0	12.9	7.3	33.7	100
10.0	7.3	21.0	12.7	7.1	34.1	100
11.0	7.5	22.2	13.4	6.9	35.0	100
12.0	7.3	23.3	13.3	6.6	35.7	100
13.0	7.3	23.6	13.1	6.6	35.2	100
14.0	6.5	24.9	11.8	6.3	35.6	100
15.0	6.8	24.0	12.1	6.5	34.9	100
16.0	7.2	22.5	12.9	6.8	35.1	100
17.0	7.6	24.2	13.9	6.4	35.9	100
18.0	7.3	24.5	10.7	6.4	28.7	100
19.0	7.2	25.4	10.6	6.2	28.9	100
20.0	7.6	29.0	11.6	5.4	29.9	100
21.0	7.5	28.2	10.8	5.6	28.2	100
22.0	7.4	27.1	10.8	5.8	28.6	100
23.0	7.2	26.4	10.4	6.0	28.3	100
24.0	7.1	26.7	10.4	5.9	28.7	100
25.0	6.6	25.9	9.6	6.1	28.5	100
26.0	7.4	27.5	11.2	5.8	29.7	100
27.0	7.2	24.4	10.3	6.4	28.1	100
28.0	6.6	23.5	9.6	6.6	28.5	100
29.0	6.0	23.0	11.5	6.7	37.6	100
30.0	6.6	23.8	12.0	6.5	35.7	100
Total average	**7.2 (kWh/m^2.day)**		**12.0 kWh**		**32.9 %**	**100 %**

As we have shown from Table 8-1, the average solar fraction through January is 64.2%, through March is 91.68 %, and through June is 100 %. Table 8-2 shows the average monthly solar fraction for all months through the year.

Table 8.2: Average monthly solar fraction for conventional SWHS in Paletine through the year

Month	Jan	Feb	Mar	Apr	May	Jun	Jul	Aug	Sep	Oct	Nov	Dec
S.F(%)	64.23	70.68	91.68	98.18	99.82	100	99.60	100	99	98.98	90.01	80.42

The average annual solar fraction in Palestine is about 90%. To compensate the reduction in solar fraction, the electric heaters should be used to raise the water temperature to the required heating point. The annual expenses for using the electric heaters is:

Annual cost = Q_L x (1 - S.F) x (0.6)

Annual cost = 2847 kWh x (1 - 0.9) x 0.6 = 171 NIS/Year.

Figure 8.3 shows the cash flow diagram for using the Thermosyphon solar heater. The salvage value for the system is 100 NIS and annul rate is 8%.

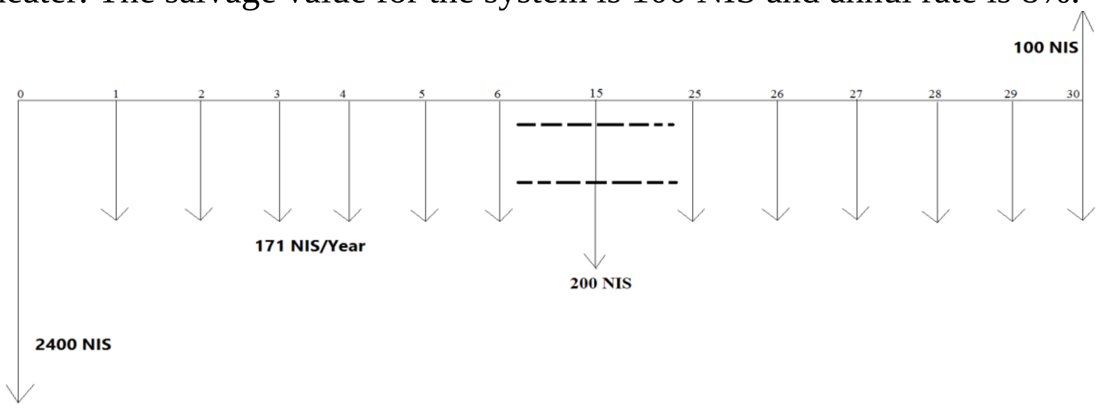

Figure 8.3: Cash flow diagram for conventional SWHS in Palestine

P.W $_s$ = - 2400 + 100 (P/F, 8%, 30) – 171 (P/A, 8%, 30) – 200(P/F, 8%, 15).

P.W $_s$ = -2400 + 100 x 0.0994 – 171 x 11.257– 200 x 0.3152 = - 4378 NIS

To find the simple payback period (S.P.B.P) compared with electrical boilers:

$$S.P.B.P = \frac{Investment}{Saving}$$

Saving= Annual cost for electrical heater — Annual cost for solar heater

Saving= 1856 NIS — 171 NIS =1658 NIS/year

Where investment represents the initial cost for the solar collector, saving is the difference between the annual cost for electrical and solar heaters.

$S.P.B.P = \frac{2400\ NIS}{1685\ NIS}$ = 1.42 Years.

From Ret screen software the result of payback period is equal 1.45 Years, which approximately equals the calculated value. Figure 8.4 shows the cash flow diagram for solar collector when the project life is 10 years. (For more details about the input parameters for Ret screen software See Appendix 3).

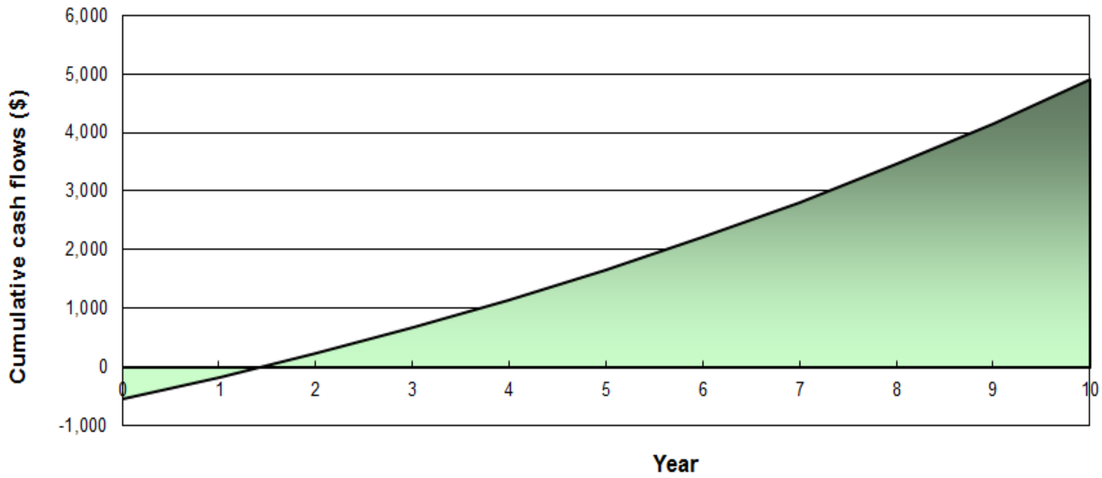

Figure 8.4: Cash flow diagram for solar thermal collector

8.1.4 Economic study of solar heaters with electric coil and PV pump

Using the PV powered pump to increase the flow rate in pipe collector increases the efficiency of the system. So the solar fraction for the system is increased and it has a big effect on annual cost of the system. Table 8.3 shows the monthly solar fraction in Palestine after adding the circulating pump (flow rate =0.05 l/s.m^2). The annual solar fraction in Palestine increases from 90% to become about 94 % after adding the circulation pump. Table 8-4 shows the initial cost for basic parameters used in solar system.

Table 8.3: Average monthly solar fraction after adding the circulating pump for SWHS in Paletine

Month	Jan	Feb	Mar	Apr	May	Jun	Jul	Aug	Sep	Oct	Nov	Dec
S.F (%)	78	83	94	99	100	100	100	100	100	100	93	87

Table 8.4: Initial cost for the basic parameters used in suggested SWHS in Palestine

Parameters	Initial cost (NIS)
Solar collectors with electric coil	2400
PV pump	250
Solar panel module	300
Total	**2950**

The power needed to running the PV-pump is 15-20W. The pump is running when the solar intensity exists. Suppose the pump is running 9 hours every day, the annual total power consumption is 55.85 kWh. The power needed to operate the pump is covered by the solar panel. The annual cost in water heating after improvement in SWHS:

$$Annual\ electrical\ heaters\ cost = Q_L\ x\ (1 - S.F)\ x\ 0.6$$

Annual cost = 2847 kWh x (1 – 0.94) x (0.6) NIS = 102 NIS/year

The initial cost for the system is 2950 NIS, system salvage value is 120 NIS. Figure 8.5 shows the cash flow diagram for the system after improvement.

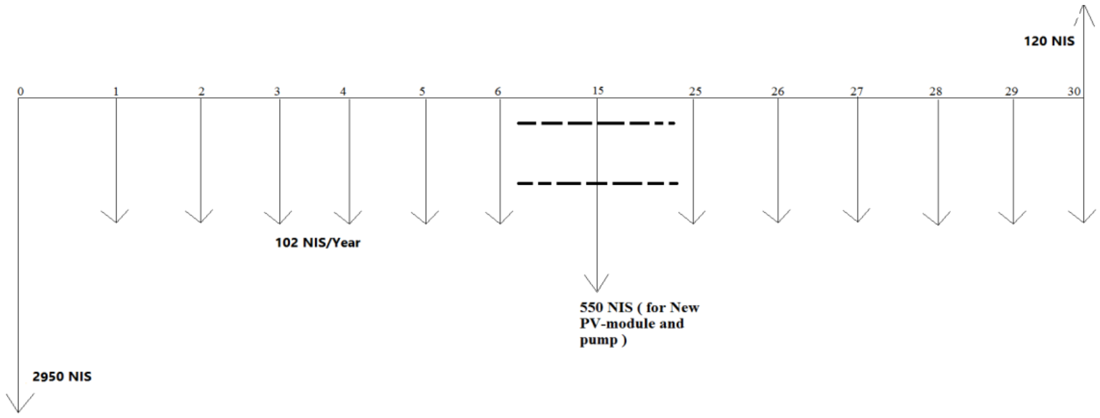

Figure 8.5: Cash flow diagram for SWHS with circulating pump and PV solar panel

$P.W_{s.p}$ = - 2950 + 120 (P/F, 8%, 30) – 102 (P/A, 8%, 30) – 550 (P/F, 8%, 15)

$P.W_{s.p}$ = -2950 + 120 x 0.0994– 102 x 11.257 – 550 x 0.3152 = - 4259 NIS

As we have shown from the result of P.W analysis that there is a little difference between the P.W of SWHS with circulating pump and P.W for SWHS without pump because the initial cost for SWHS with circulating pump is higher. Solar system with PV powered pump is indeed the best alternative for using in water heating.

8.2 Environmental effect of solar water heater

Solar thermal is one of the best ways to lower buildings carbon footprint and help protect the environment. Water heating can account for over 50% of greenhouse gas emissions which make the solar heater an ideal solution [38].

Here are a few reasons why solar hot water systems make good environment sense.

- Reducing the need to extract and transport fossil fuels.
- Increasing boiler and water heater efficiency and life expectancy especially in commercial and industrial buildings.
- Reducing greenhouse gas emissions

From previous section the result of solar fraction for SWHS with PV-pump in Palestine is 94 %, which means that the SWHS saves 94 % from annual electricity used to heat the water. Table 8-5 shows the greenhouse gases emissions from 1kWh of electricity.

Table 8.5: GHG emissions value used to express reduction achieved by 1 kWh produced from electric heaters [38]

GHG gases	Quantity (kg)
CO_2	0.7
CH_4	0.00001
CO	0.00015
SO_2	0.005
NOx	0.0025

The annual required load used to raise the water temperature in Palestine is 2847 kWh. SWHS covers 94 % from this value. Table 8-6 shows the quantity of GHG emissions reduction from using SWHS instead of electrical heaters.

Table 8.6: Annual GHG emissions reduction from using SWHS instead of electrical heater

GHG gases	Quantity (kg)
CO_2	1873.33
CH_4	0.03
CO	0.40
SO_2	13.38
NOx	6.69

Chapter Nine

Conclusions

9 Conclusions

In Palestine there are different kinds of solar water heaters like evacuated tube collector, active solar water heater (both used in commercial and industrial places) and thermosiphon SWH (used in residential places). In this thesis, the thermosiphon SWH was simulated under weather conditions in Palestine. The system has a capacity of 180 L hot water tank. The solar water heater has a total collector area of $5.1m^2$. The thermal performance of Thermosyphon flat plate solar water was investigated and optimized by MatLab software. Thermosiphon SWH in Palestine is usually used without circulation pump. In this thesis we could raise the solar fraction from 90 % to 94 % by using circulation pump with PV panel. It is expected that the system could provide most of the hot/warm water needed for residential places in Palestine. Adding the circulation pump to thermosyphon system helps to raise the annual collector efficiency for the collector from 33% to 37%. Using SWH in residential places as an alternative source from using the electrical boiler contributes to reduce the CO_2 emissions. The reduction in CO_2 emissions from using SWH instead of electrical heaters may reach to 1873 kg/year. Improvement in thermosyphon system saves 70 NIS every year. Using PV pump with two panel of flat plate collector gives the same energy by using three panels of flat plate collector. That means we can save the space needed for one panel flat plate collector by using the PV driven pump. Based on table 6.4 , when the collector area is 5.1 m^2, the solar fraction increases from 76 % to 86 %, particularly in November to

February after using the PV powered pump. This adds to the efficiency of SWHSs and lowers the electrical energy consumption.

References

1. Al-Ibrahim, M. A. (1997). **Optimum Selection of Direct-Coupled Photovoltaic Pumping System in Solar Domestic Hot Water Systems**. Doctoral Thesis. University of Wisconsin-Madison
2. Prof. Marwan Mahmoud. ***Lectures on Renewable Energy***. Department of Electrical Engineering, An-Najah national University.
3. Household Energy Survey (2013). **Palestine Central Bureau of Statistics** (2013).
4. Statistical Yearbook of Palestine (2011). **Palestine Central Bureau of Statistics** (2011).
5. Solar Water Heaters. Retrieved from: http://energy.gov/energysaver/solar-water-heaters
6. Patel. K. Patel. P & Patel, J. (2012). ***Review of Solar Water Heating Systems.*** **International Journal of Advanced Engineering Technology,** 3(4), pp. 146-149.

7 Solar Flat Plate Systems (2014). Retrieved from: http://www.solarpanelsplus.com/residential/water-heating-flat-plates/

8 Duff, J. A. & Beckman W. A. (2013). ***Solar Engineering of Thermal Processes*.** Wiley

9 Solar Thermal Water Heating (2004). Retrieved from: http://www.volker-quaschning.de/articles/fundamentals4/index.php

10 Ibrik I., Marwan M. M. (2005). ***Energy efficiency improvement procedures and audit results of electrical, thermal and solar applications in Palestine.*** **Energy Policy**, 33, pp. 651-658.

11 Solar Hot Water Collectors (2017). Retrieved from: http://www.greenspec.co.uk/building-design/solar-collectors/

12 Evacuated Tube Solar Collector (2013). Retrieved from: http://greenterrafirma.com/evacuated_tube_collector.html

13 Hasan, A. (1995). ***Optimization of Domestic Solar Water Heating.*** **International Journal of Solar Energy**, 17 (2-3), pp. 135-144.

14 Mubarak, G. (2008). **The Implementation of Renewable Energy Technologies in Historic Centers of Towns in Rural Palestine.** M.A Thesis. The University of Nottingham.

15 Omar, A. M. (2007). **Computer Aided Design and Performance Evaluation of PV-Diesel Hybrid System**. M.A Thesis. An-Najah national University.

16 ***Meteorological Conditions in the Palestinian Territory Annual Report 2007*** (2008). Palestine Central Bureau of Statistics

17 Sayed, A. O. (May 12th, 2014). Solar Cells. Retrieved from: http://www.slideshare.net/vasistatiruveedi/solar-cell-47447105

18 Bellia, H., Youcif, R & Fatima. M. (2014). ***A Detailed Modeling of Photovoltaic Module Using Matlab.*** **NRIAG Journal of Astronomy and Geophysics,** 3, pp. 53-61.

19 Kharouf. A. A. (2014). **The Techno-Economical Impact of PV on-Grid Systems on the Security of Palestinian Electrical Supply (Jericho PV System- case Study).** M.A Thesis. An-Najah National University.

20 Pan, L. (2013). ***Analysis of Photovoltaic Module Resistance Characteristics*. International Journal of Engineering**, 26(11), pp. 1369-1376.

21 Ekramian E. , Etemad S. & Haghshenasfard M. (2014). ***Numerical Analysis of Heat Transfer Performance of Flat Plate Solar Collectors.*** **Journal of Fluid Flow, Heat and Mass Transfer**, 1, pp. 38-42

22 Struckmann, F. (2008). ***Analysis of a Flat-plate Solar Collector***. Project Report, Heat and Mass Transport, Lund, Sweden.

23 Kumar, S. & Mullick, S.C (2010). ***Wind heat transfer coefficient in solar collectors in outdoor conditions.*** **Solar Energy,** 84, pp. 956-963.

24 Zahedi, H.R, Adam, N.M., Sapuan, S.M.& Ahmad, M. (2007). ***Effect of storage tank geometry on performance of solar water heater.*** **Journal of Scientific & Industrial Research,** 66, pp. 146-151.

25 ***Itemaad Solar Water Heaters***. Retrieved from: http://itemaad-solar.com/

26 Dayan, M. (1997). **High Performance in Low Solar Domestic Hot water Systems.** M.A Thesis, University of Wisconsin-Madison.

27 Kalogirou, S. A. (2014). **Solar Energy Engineering. Academic Press**

28 Yaseen, B. (2007). ***Renewable Energy Applications in Palestine.*** **Palestinian Energy and Environment Research Center** *(PEC)* – Energy Authority.

29 Khaled, Z, Guizani, A. Sebai, R. & Kerkeni, C. (2012). ***Solar Thermal Systems Performances versus Flat Plate Solar Collectors Connected in Series.*** **Engineering,** 4, pp. 881-893.

30 Benjamin, M. (2012). ***Hydraulics and Open Channel Flow***. Retrieved from http://faculty.washington.edu/markbenj/CEE345/

31 Tommerup, H. & Nørgård, J. (2007). ***Proper Sizing of Circulation Pumps***. Proceedings ECEEE Summer Study. Retrieved from: http://www.eceee.org/library/conference_proceedings/eceee_Summer_Studies/2007/Panel_6/6.346/paper

32 ***Pump and a pipe sizing for a solar water*** (June 25, 2010). http://www.builditsolar.com/Projects/SpaceHeating/PipeSizing/PipeSizing.htm

33 ***Pipe Fitting Loss Calculations***. Retrieved from: http://www.pipeflow.com/pipe-pressure-drop-calculations/pipe-fitting-loss-calculation

34 ***Ecocirc PRO High Efficiency Hot water Circulation Pumps***. Retrieved from: http://lowara.com/pumps-circulators/wet-rotor-circulators/ecocirc-pro-high-efficiency-hot-water-circultator/

35 ***Laing Circulation Pump.*** Retrieved from: http://www.sustainable.co.za/laing-ecocirc-d5-38-700b-circulation-pump.html

36 ***Liquefied Petroleum Gas.*** Retrieved from: https://en.wikipedia.org/wiki/Liquefied_petroleum_gas

37 ***Condensing Boilers Efficiency.*** Retrieved form http://www.usboiler.net/condensing-boilers-efficiency.html

38 ***Solar Thermal Environmental Benefits.*** Retrieved form: http://sunwatersolar.com/solar-thermal/environmental-benifits

Appendix

Appendix 1

Friction loss tables for steel pipes:

FRICTION LOSS CHARACTERISTICS
SCHEDULE 40 STANDARD STEEL PIPE C=100
PSI loss per 100 feet of pipe (PSI/100 FT)

Sizes 1/2" thru 6"
Flow GPM 1 thru 600

SIZE	1/2"		3/4"		1"		1 1/4"		1 1/2"		2"		2 1/2"		3"		4"		6"		SIZE
OD	0.840		1.050		1.315		1.660		1.900		2.375		2.875		3.500		4.500		6.625		OD
ID	0.622		0.824		1.049		1.380		1.610		2.067		2.469		3.068		4.026		6.065		ID
WALL THK	0.109		0.113		0.133		0.140		0.145		0.154		0.203		0.216		0.237		0.280		WALL THK
FLOW G.P.M.	VELOCITY F.P.S.	P.S.I. LOSS	VELOCITY F.P.S.	P.S.I. LOSS	VELOCITY F.P.S.	P.S.I. LOSS	VELOCITY F.P.S.	P.S.I. LOSS	VELOCITY F.P.S.	P.S.I. LOSS	VELOCITY F.P.S.	P.S.I. LOSS	VELOCITY F.P.S.	P.S.I. LOSS	VELOCITY F.P.S.	P.S.I. LOSS	VELOCITY F.P.S.	P.S.I. LOSS	VELOCITY F.P.S.	P.S.I. LOSS	FLOW G.P.M.
1	1.05	0.91	0.60	0.23	0.37	0.07	0.21	0.02	0.15	0.01	0.09	0.00									1
2	2.10	3.28	1.20	0.84	0.74	0.26	0.42	0.07	0.31	0.03	0.19	0.01	0.13	0.00							2
3	3.16	6.95	1.80	1.77	1.11	0.55	0.64	0.14	0.47	0.07	0.28	0.02	0.20	0.01	0.13	0.00					3
4	4.21	11.85	2.40	3.02	1.48	0.93	0.85	0.25	0.62	0.12	0.38	0.03	0.26	0.01	0.17	0.01					4
5	5.27	17.91	3.00	4.56	1.85	1.41	1.07	0.37	0.78	0.18	0.47	0.05	0.33	0.02	0.21	0.01					5
6	6.32	25.10	3.60	6.39	2.22	1.97	1.28	0.52	0.94	0.25	0.57	0.07	0.40	0.03	0.26	0.01					6
7	7.38	33.40	4.20	8.50	2.59	2.63	1.49	0.69	1.10	0.33	0.66	0.10	0.46	0.04	0.30	0.01					7
8	8.43	42.77	4.80	10.89	2.96	3.36	1.71	0.89	1.25	0.42	0.76	0.12	0.53	0.05	0.34	0.02	0.20	0.00			8
9	9.49	53.19	5.40	13.54	3.33	4.18	1.92	1.10	1.41	0.52	0.85	0.15	0.60	0.06	0.39	0.02	0.22	0.01			9
10	10.54	64.65	6.00	16.46	3.70	5.08	2.14	1.34	1.57	0.63	0.95	0.19	0.66	0.08	0.43	0.03	0.25	0.01			10
11	11.60	77.13	6.60	19.63	4.07	6.07	2.35	1.60	1.73	0.75	1.05	0.22	0.73	0.09	0.47	0.03	0.27	0.01			11
12	12.65	90.62	7.21	23.07	4.44	7.13	2.57	1.88	1.88	0.89	1.14	0.26	0.80	0.11	0.52	0.04	0.30	0.01			12
14	14.76	20.56	8.41	30.69	5.19	9.48	2.99	2.50	2.20	1.18	1.33	0.35	0.93	0.15	0.60	0.05	0.35	0.01			14
16	16.87	54.39	9.61	39.30	5.93	12.14	3.42	3.20	2.51	1.51	1.52	0.45	1.07	0.19	0.69	0.07	0.40	0.02			16
18	18.98	92.02	10.81	48.88	6.67	15.10	3.85	3.98	2.83	1.88	1.71	0.56	1.20	0.23	0.78	0.08	0.45	0.02			18
20			12.01	59.41	7.41	18.35	4.28	4.83	3.14	2.28	1.90	0.68	1.33	0.29	0.86	0.10	0.50	0.03			20
22			13.21	70.88	8.15	21.90	4.71	5.77	3.46	2.72	2.10	0.81	1.47	0.34	0.95	0.12	0.55	0.03	0.24	0.00	22
24			14.42	83.27	8.89	25.72	5.14	6.77	3.77	3.20	2.29	0.95	1.60	0.40	1.04	0.14	0.60	0.04	0.26	0.01	24
26			15.62	96.57	9.64	29.83	5.57	7.86	4.09	3.71	2.48	1.10	1.74	0.46	1.12	0.16	0.65	0.04	0.28	0.01	26
28			16.82	110.8	10.38	34.22	5.99	9.01	4.40	4.26	2.67	1.26	1.87	0.53	1.21	0.18	0.70	0.05	0.31	0.01	28
30			18.02	125.9	11.12	38.89	6.42	10.24	4.72	4.84	2.86	1.43	2.00	0.60	1.30	0.21	0.75	0.06	0.33	0.01	30
35					12.97	51.74	7.49	13.62	5.50	6.44	3.34	1.91	2.34	0.80	1.51	0.28	0.88	0.07	0.38	0.01	35
40					14.83	66.25	8.56	17.45	6.29	8.24	3.81	2.44	2.67	1.03	1.73	0.36	1.00	0.10	0.44	0.01	40
45					16.68	82.40	9.64	21.70	7.08	10.25	4.29	3.04	3.01	1.28	1.95	0.44	1.13	0.12	0.49	0.02	45
50					18.53	100.2	10.71	26.37	7.87	12.46	4.77	3.69	3.34	1.56	2.16	0.54	1.25	0.14	0.55	0.02	50
55							11.78	31.47	8.65	14.86	5.25	4.41	3.68	1.86	2.38	0.65	1.38	0.17	0.61	0.02	55
60							12.85	36.97	9.44	17.46	5.72	5.18	4.01	2.18	2.60	0.76	1.51	0.20	0.66	0.03	60
65							13.92	42.88	10.23	20.25	6.20	6.00	4.35	2.53	2.81	0.88	1.63	0.23	0.72	0.03	65
70							14.99	49.18	11.01	23.23	6.68	6.89	4.68	2.90	3.03	1.01	1.76	0.27	0.77	0.04	70
75							16.06	55.89	11.80	26.40	7.16	7.83	5.01	3.30	3.25	1.15	1.88	0.31	0.83	0.04	75
80							17.13	62.98	12.59	29.75	7.63	8.82	5.35	3.72	3.46	1.29	2.01	0.34	0.88	0.05	80
85							18.21	70.47	13.37	33.29	8.11	9.87	5.68	4.16	3.68	1.44	2.13	0.39	0.94	0.05	85
90							19.28	78.33	14.16	37.00	8.59	10.97	6.02	4.62	3.90	1.61	2.26	0.43	0.99	0.06	90
95									14.95	40.90	9.07	12.13	6.35	5.11	4.11	1.78	2.39	0.47	1.05	0.06	95
100									15.74	44.97	9.54	13.33	6.69	5.62	4.33	1.95	2.51	0.52	1.10	0.07	100
110									17.31	53.66	10.50	15.91	7.36	6.70	4.76	2.33	2.76	0.62	1.22	0.08	110
120									18.88	63.04	11.45	18.69	8.03	7.87	5.20	2.74	3.02	0.73	1.33	0.10	120
130											12.41	21.68	8.70	9.13	5.63	3.17	3.27	0.85	1.44	0.12	130
140											13.36	24.87	9.37	10.47	6.06	3.64	3.52	0.97	1.55	0.13	140
150											14.32	28.26	10.03	11.90	6.50	4.14	3.77	1.10	1.66	0.15	150
160											15.27	31.84	10.70	13.41	6.93	4.66	4.02	1.24	1.77	0.17	160
170											16.23	35.63	11.37	15.01	7.36	5.22	4.27	1.39	1.88	0.19	170
180											17.18	39.61	12.04	16.68	7.80	5.80	4.53	1.55	1.99	0.21	180
190											18.14	43.78	12.71	18.44	8.23	6.41	4.78	1.71	2.10	0.23	190
200											19.09	48.14	13.38	20.28	8.66	7.05	5.03	1.88	2.21	0.26	200
225													15.08	25.22	9.75	8.76	5.66	2.34	2.49	0.32	225
250													16.73	30.65	10.83	10.65	6.29	2.84	2.77	0.39	250
275													18.40	36.57	11.92	12.71	6.92	3.39	3.05	0.46	275
300															13.00	14.93	7.55	3.98	3.32	0.54	300
325															14.08	17.32	8.18	4.62	3.60	0.63	325
350															15.17	19.87	8.81	5.30	3.88	0.72	350
375															16.25	22.57	9.43	6.02	4.15	0.82	375
400															17.33	25.44	10.06	6.78	4.43	0.92	400
425															18.42	28.46	10.69	7.59	4.71	1.03	425
450															19.50	31.64	11.32	8.43	4.99	1.15	450
475																	11.95	9.32	5.26	1.27	475
500																	12.58	10.25	5.54	1.40	500
550																	13.84	12.23	6.10	1.67	550
600																	15.10	14.37	6.65	1.96	600

Note: Shaded areas of chart indicate velocities over 5' per second. Use with Caution.

Friction loss tables for Copper pipes:

Hunter®

FRICTION LOSS CHARACTERISTICS
TYPE K COPPER WATER TUBE C = 140
PSI loss per 100 feet of tube (PSI/100 FT)

Sizes 1/2" thru 3"
Flow GPM 1 thru 600

SIZE	1/2"		5/8"		3/4"		1"		1 1/4"		1 1/2"		2"		2 1/2"		3"		SIZE
OD	0.625		0.750		0.875		1.125		1.375		1.625		2.125		2.625		3.125		OD
ID	0.527		0.652		0.745		0.995		1.245		1.481		1.959		2.435		2.907		ID
WALL THK	0.049		0.049		0.065		0.065		0.065		0.072		0.083		0.095		0.109		WALL THK
FLOW G.P.M.	VELOCITY F.P.S.	P.S.I. LOSS	VELOCITY F.P.S.	P.S.I. LOSS	VELOCITY F.P.S.	P.S.I. LOSS	VELOCITY F.P.S.	P.S.I. LOSS	VELOCITY F.P.S.	P.S.I. LOSS	VELOCITY F.P.S.	P.S.I. LOSS	VELOCITY F.P.S.	P.S.I. LOSS	VELOCITY F.P.S.	P.S.I. LOSS	VELOCITY F.P.S.	P.S.I. LOSS	FLOW G.P.M.
1	1.46	1.09	0.95	0.39	0.73	0.20	0.41	0.05	0.26	0.02	0.18	0.01	0.10	0.00					1
2	2.93	3.94	1.91	1.40	1.47	0.73	0.82	0.18	0.52	0.06	0.37	0.03	0.21	0.01					2
3	4.40	8.35	2.87	2.97	2.20	1.55	1.23	0.38	0.78	0.13	0.55	0.05	0.31	0.01	0.20	0.00			3
4	5.87	14.23	3.83	5.05	2.94	2.64	1.64	0.65	1.05	0.22	0.74	0.09	0.42	0.02	0.27	0.01	0.19	0.00	4
5	7.34	21.51	4.79	7.64	3.67	3.99	2.06	0.98	1.31	0.33	0.93	0.14	0.53	0.04	0.34	0.01	0.24	0.01	5
6	8.81	30.15	5.75	10.70	4.41	5.60	2.47	1.37	1.57	0.46	1.11	0.20	0.63	0.05	0.41	0.02	0.28	0.01	6
7	10.28	40.11	6.71	14.24	5.14	7.44	2.88	1.82	1.84	0.61	1.30	0.26	0.74	0.07	0.48	0.02	0.33	0.01	7
8	11.75	51.37	7.67	18.24	5.88	9.53	3.29	2.33	2.10	0.78	1.48	0.34	0.85	0.09	0.55	0.03	0.38	0.01	8
9	13.22	63.89	8.63	22.68	6.61	11.86	3.70	2.90	2.36	0.97	1.67	0.42	0.95	0.11	0.61	0.04	0.43	0.02	9
10	14.69	77.66	9.59	27.57	7.35	14.41	4.12	3.53	2.63	1.18	1.86	0.51	1.06	0.13	0.68	0.05	0.48	0.02	10
11	16.15	92.65	10.55	32.89	8.08	17.19	4.53	4.21	2.89	1.41	2.04	0.61	1.16	0.16	0.75	0.05	0.53	0.02	11
12	17.62	108.85	11.51	38.64	8.82	20.20	4.94	4.94	3.15	1.66	2.23	0.71	1.27	0.18	0.82	0.06	0.57	0.03	12
14			13.43	51.41	10.29	26.87	5.76	6.57	3.68	2.21	2.60	0.95	1.48	0.24	0.95	0.08	0.67	0.04	14
16			15.35	65.83	11.76	34.41	6.59	8.42	4.21	2.83	2.97	1.22	1.70	0.31	1.10	0.11	0.77	0.05	16
18			17.27	81.88	13.23	42.80	7.41	10.47	4.73	3.52	3.34	1.51	1.91	0.39	1.23	0.13	0.86	0.06	18
20			19.19	99.53	14.70	52.02	8.24	12.73	5.26	4.28	3.72	1.84	1.12	0.47	1.37	0.16	0.96	0.07	20
22					16.17	62.06	9.06	15.18	5.79	5.10	4.09	2.19	2.33	0.56	1.51	0.20	1.06	0.08	22
24					17.64	72.92	9.89	17.84	6.31	5.99	4.46	2.58	2.55	0.66	1.65	0.23	1.15	0.10	24
26					19.11	84.57	10.71	20.69	6.84	6.95	4.83	2.99	2.76	0.77	1.78	0.27	1.25	0.11	26
28							11.53	23.73	7.37	7.98	5.20	3.43	2.97	0.88	1.92	0.30	1.35	0.13	28
30							12.36	26.97	7.89	9.06	5.58	3.89	3.18	1.00	2.06	0.35	1.44	0.15	30
35							14.42	35.88	9.21	12.06	6.51	5.18	3.72	1.33	2.40	0.46	1.68	0.19	35
40							16.48	45.95	10.52	15.44	7.44	6.63	4.25	1.70	2.75	0.59	1.93	0.25	40
45							18.54	57.15	11.84	19.20	8.37	8.25	4.78	2.12	3.00	0.73	2.17	0.31	45
50									13.16	23.34	9.30	10.03	5.31	2.57	3.44	0.89	2.41	0.38	50
55									14.47	27.85	10.23	11.97	5.84	3.07	3.78	1.06	2.65	0.45	55
60									15.79	32.71	11.16	14.06	6.37	3.60	4.12	1.25	2.89	0.53	60
65									17.10	37.94	12.09	16.31	6.91	4.18	4.47	1.45	3.13	0.61	65
70									18.42	43.52	13.02	18.70	7.44	4.80	4.81	1.66	3.37	0.70	70
75									19.74	49.46	13.95	21.25	7.97	5.45	5.16	1.89	3.62	0.80	75
80											14.88	23.95	8.50	6.14	5.50	2.13	3.86	0.90	80
85											15.81	26.80	9.03	6.87	5.84	2.38	4.10	1.01	85
90											16.74	29.79	9.56	7.64	6.19	2.65	4.34	1.12	90
95											17.67	32.93	10.09	8.44	6.53	2.93	4.58	1.24	95
100											18.60	36.21	10.63	9.28	6.88	3.22	4.82	1.36	100
110													11.69	11.08	7.56	3.84	5.31	1.62	110
120													12.75	13.01	8.25	4.52	5.79	1.91	120
130													13.82	15.09	8.94	5.24	6.27	2.21	130
140													14.88	17.31	9.63	6.01	6.75	2.54	140
150													15.94	19.67	10.32	6.83	7.24	2.88	150
160													17.01	22.17	11.00	7.69	7.72	3.25	160
170													18.07	24.81	11.69	8.61	8.20	3.64	170
180													19.13	27.58	12.38	9.57	8.69	4.04	180
190															13.07	10.58	9.17	4.47	190
200															13.76	11.63	9.65	4.91	200
225															15.48	14.47	10.86	6.11	225
250															17.20	17.58	12.07	7.43	250
275															18.92	20.98	13.27	8.86	275
300																	14.48	10.41	300
325																	15.69	12.07	325
350																	16.89	13.85	350
375																	18.10	15.73	375
400																	19.31	17.73	400
425																			425
450																			450
475																			475
500																			500
550																			550
600																			600

Note: Shaded areas of chart indicate velocities over 5' per second. Use with Caution.

Equivalent length of Feet for pipe Fittings:

PRESSURE LOSS IN VALVES AND FITTINGS
Equivalent Length in Feet of Standard Steel Pipe

Nominal Pipe Size	Globe Valve	Angle Valve	Sprinkler Angle Valve	Gate Valve	Side Outlet Std. Tee	Run of Std. Tee	Std. Elbow	45° Elbow
1/2	17	9	2	0.4	4	1	2	1
3/4	22	12	3	0.5	5	2	3	1
1	27	15	4	0.6	6	2	3	2
1-1/4	38	18	5	0.8	8	3	4	2
1-1/2	45	22	6	1.0	10	3	5	2
2	58	28	7	1.2	12	4	6	3
2-1/2	70	35	9	1.4	14	5	7	3
3	90	45	11	1.8	18	6	8	4
4	120	60	15	2.3	23	7	11	5
6	170	85	20	3.3	33	12	17	8

PRESSURE LOSS THROUGH COPPER AND BRONZE FITTINGS

	EQUIVALENT FEET OF STRAIGHT TUBING										
	WROUGHT COPPER					CAST BRONZE					
Nominal Tube Size	90° Elbow	45° Elbow	Tee Run	Tee Side Outlet	90° Bend	180° Bend	90 Elbow	45° Elbow	Tee Run	Tee Slide Output	Com-pression Stop
3/8	1/2	1/2	1/2	1	1/2	1/2	1	1/2	1/2	2	9
1/2	1/2	1/2	1/2	1	1/2	1	1	1	1/2	2	13
5/8	1/2	1/2	1/2	2	1	1	2	1	1/2	3	17
3/4	1	1/2	1/2	2	1	2	2	1	1/2	3	21
1	1	1	1/2	3	2	2	4	2	1/2	5	30
1-1/4	2	1	1/2	4	2	3	5	2	1	7	-
1-1/2	2	2	1	5	2	4	8	3	1	9	-
2	2	2	1	7	3	8	11	5	2	12	-
2-1/2	2	3	2	9	4	16	14	8	2	16	-
3	3	4	-	-	5	20	18	11	2	20	-
3-1/2	4	-	-	-	7	24	24	14	2	31	-
4	-	-	-	-	8	28	28	17	2	37	-
5	-	-	-	-	10	37	41	22	2	48	-
6	-	-	-	-	13	47	52	28	2	61	-

PRESSURE LOSS THROUGH SWING CHECK VALVES–PRESSURE LOSS (PSI)

FLOW G.P.M.	VALVE SIZE						FLOW G.P.M.	VALVE SIZE					
	1/2	3/4	1	1-1/4	1-1/2	2		1-1/4	1-1/2	2	2-1/2	3	4
2	0.2						46	2.1	1.1	0.4			
3	0.5						48	2.2	1.2	0.5			
6	1.0	0.3					50	2.4	1.3	0.5			
8	1.7	0.5					55	2.9	1.5	0.6			
10	2.6	0.8	0.3				60	3.4	1.8	0.7			
12	3.6	1.1	0.5				65	3.9	2.0	0.8			
14	4.8	1.5	0.6				70	4.5	2.4	0.9	0.4		
16		2.0	0.9				75		2.7	1.0	0.5		
18		2.4	1.0				80		3.0	1.2	0.6		
20		3.0	1.2	0.4			90		3.7	1.5	0.7		
22		3.5	1.4	0.5			100		4.6	1.8	0.9	0.4	
24		4.1	1.7	0.6			120			2.5	1.2	0.5	
26		4.8	2.0	0.7	0.4		140			3.3	1.6	0.7	
28			2.2	0.8	0.5		160			4.3	2.1	0.9	0.3
30			2.5	0.9	0.5		180			5.3	2.6	1.1	0.4
32			2.9	1.1	0.6		200			6.5	3.1	1.4	0.5
34			3.2	1.2	0.6		250				4.7	2.1	0.7
36			3.6	1.3	0.7		300				6.6	2.9	1.0
38			3.9	1.5	0.8		350					3.8	1.3
40			4.3	1.6	0.8	0.3	400					4.9	1.7
42			4.7	1.7	0.9	0.3	450						2.1
44				1.9	1.0	0.4	500						2.6

Appendix 2

Data sheet for circulating Pump

DC pumps
ecocirc® solar

Application

The Ecocirc solar pump can be used wherever a highly efficient circulation pump is needed without a direct connection to AC power. It can be connected directly to a photovoltaic panel and is characterized by its small size, high efficiency, very low power consumption and its MPP tracking. The shaftless spherical motor technology enables a long, maintenance free and quiet service life. Areas of application are thermal solar systems for single family homes.

Design

The principle of the spherical motor, which was invented by Laing, is fundamentally different from conventional canned motor pumps. The only moving part in a spherical motor is a hemispherical rotor/impeller unit, which sits on an ultra-hard, wear-resistant ceramic ball. There are no conventional shaft bearings or seals. This rules out, in effect, the possibility of play in the bearings and the increase in noise associated with it. These pumps are particularly robust and give exceptionally long service. The self-realigning bearing is lubricated and cooled by the media. Maintenance is not necessary under normal conditions and even after lengthy shutdown periods a reliable start-up is virtually guaranteed. The parts exposed to the fluid are completely corrosion resistant.

Soft start-up

The pump has been programmed for a soft start-up. When the photovoltaic panel provides sufficient power, the pump first goes through the alignment phase, turning the rotor into the position required for start-up. Then the processor waits until the built-in capacitor has recharged sufficiently. This enables a start-up with minimal power (less than one Watt). Cycling due to unsuccessful starting attempts is minimized. Even after prolonged shutdown, the pump will start reliably.

Integrated overtemperature protection

The pump comes with an integrated overtemperature safety device, which shuts the pump electronics off when reaching overtemperature. Normally the temperature of the pumped media during operation at the highest speed setting is 95° C at this point.

A complete shutdown after reaching overtemperature condition can result in adverse effects on the circulating system. Since the temperature of the electronic components is influenced by the temperature of the pumped media as well as by the speed setting, the pump will lower its speed automatically after reaching a critical temperature level in order to avoid a total shutdown. However, if the temperature continues to rise (caused e.g. by too hot pumped media), the pump will eventually shut down completely. After cooling down, the pump will restart automatically.

Automatic performance optimization – MPP tracking

The Ecocirc DC pumps are the first and only spherical motor pumps with self-optimizing software (see diagram). Every three seconds, the processor will modify its operating point on the voltage-current curve of the PV panel to find the point of maximum performance. This is called the "Maximum Power Point" (MPP).

At this point, the pump achieves the maximum rpm and therefore the maximum performance. There is no need for a separate performance adaptation, the pump will always find its best operating point under any given light and temperature conditions by itself.

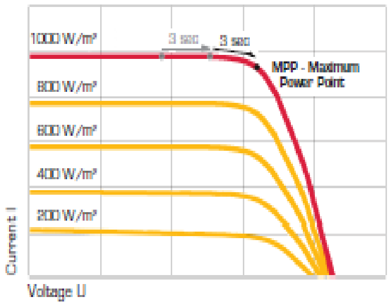

Typical Current-Voltage-curve of a photovoltaic panel. By employing MPP tracking every three seconds, the Ecocirc DC pumps always automatically achieve maximum performance at any given insolation.

Technical Data

Motor design	Electronically commutated spherical motor with permanent magnet rotor/impeller
Voltage	8 - 24 Volt
Power consumption*	min. start-up power consumption less than 1 Watt, max. power consumption 22 Watts
Current draw	0,25 - 1,46 A
Acceptable media	domestic hot water, heating water, water/glycol mixtures, other media on request**.
Insulation class	IP 42 / Class F

Pump housing material	Brass	Noryl
Max. system pressure	1 Mpa (10 bar)	0,15 MPa (1,5 bar)
Max. system temperature***	-10 to + 95°C	+/- 0 to + 60°C
Weight	0,7 kg	0,35 kg

* Power consumption and start may vary in different installations
**please check pump performance with more than 20 % glycol
*** non-freezing

Model names

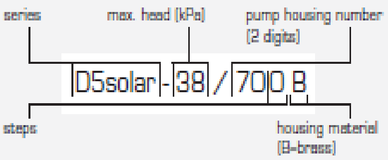

Design

DC pumps Ecocirc solar

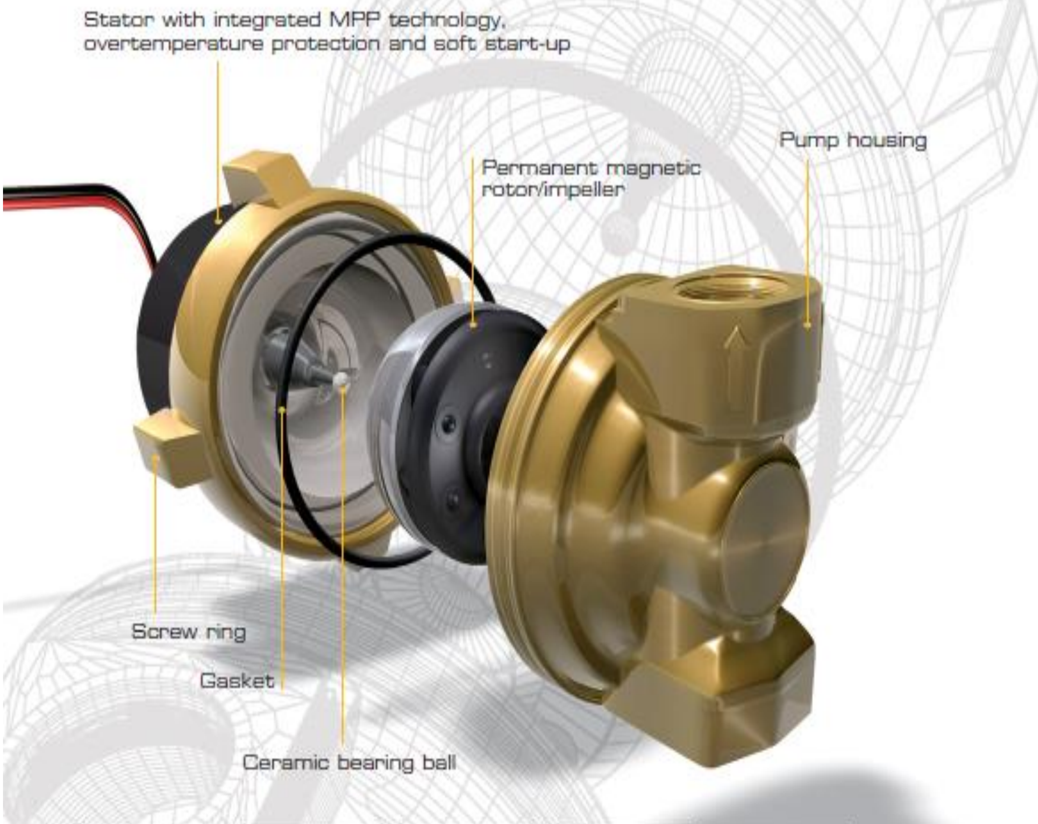


D5solar-38/700 B


D5solar-38/100 B


D5solar-38/830 N


D5solar-38/810 N


D5solar-38/790 N

ecocirc® solar DC pumps

Model	Part number	Pump housing material	Max. system temperature	Housing design / Length Others	Connection	Product category
D5solar-38/700 B	60 00 403	Brass	95° C	Inline / 65mm	1/2" female thread	H
D5solar-38/100 B	60 00 413			Inline / 110mm / RV+KV*	1 1/4" male thread**	
D5solar-38/830 N	60 00 423	Noryl	60° C	Angled housing	1/2" male thread	
D5solar-38/810 N	60 00 433			Angled housing	1/2" hosebarb thread	
D5solar-38/790 N	60 00 443			Angled housing	3/4" hosebarb thread	

* integrated check valve and ball valve
** for connection to 3/4" union components. Housing has additionally a 1/2" female connection

ecocirc® solar Accessories, components and spare parts

Model	Part number	Description	Product category
D5solar-38/000	60 00 490	Replacement motor for D5 solar incl. gasket	C
F 72	95 00 732	Rotor/Impeller incl. gasket for Ecocirc solar D5	
MW C	95 00 041	Mounting plate for Ecocirc solar D5 with Noryl pump housing	

Dimensional drawings for Ecocirc® solar DC pumps

All dimensions in mm unless rated

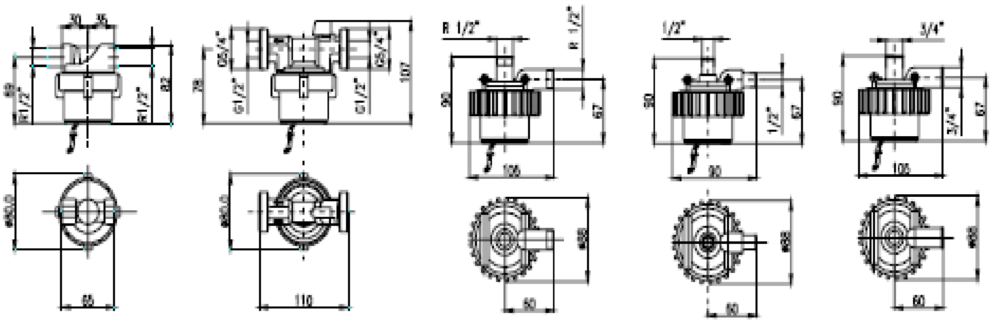

D5solar-38/700 B D5solar-38/100 B D5solar-38/830 N D5solar-38/810 N D5solar-38/790 N

Pump curves

At 12 Volt, min. start-up power consumption less than 1 Watt (12 Volt panel), max. power consumption approx. 22 Watt;

D5solar-38/700 B

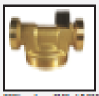

D5solar-38/100 B

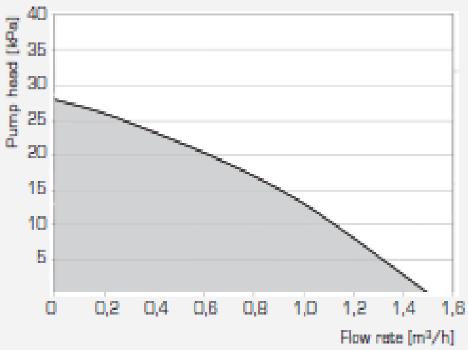

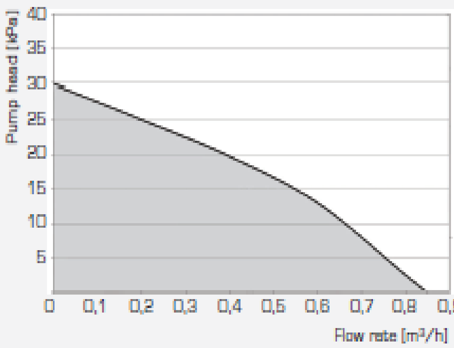

D5solar-38/830 N

D5solar-38/790 N

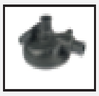

D5solar-38/810 N

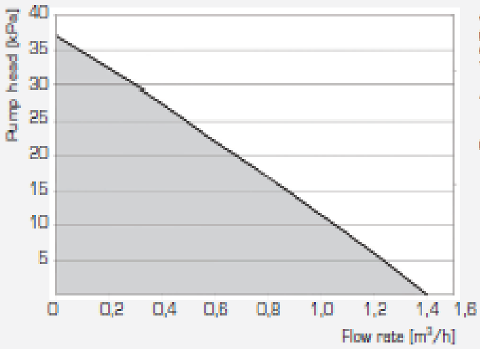

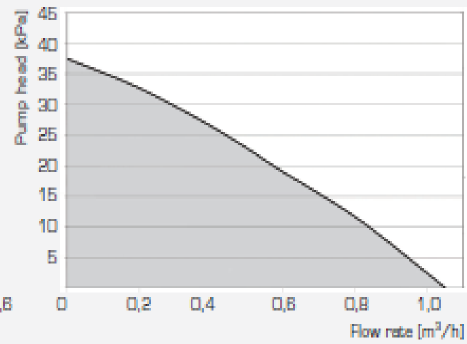

LAING

Appendix 3

Input SWHS Parameters in RetScreen software to draw the cash flow diagram for SWHS used in Palestine.

Technology	Solar water heater

Load characteristics

Application

- ○ Swimming pool
- ⦿ Hot water

	Unit	Base case	Proposed case
Load type		House	
Number of units	Occupant	5	
Occupancy rate	%	80%	
Daily hot water use - estimated	L/d	240	
Daily hot water use	L/d	180	180
Temperature	°C	55	55
Operating days per week	d	7	7

☐ **Percent of month used**

	Unit	Base case
Supply temperature method		Formula
Water temperature - minimum	°C	16.7
Water temperature - maximum	°C	21.4

	Unit	Base case	Proposed case	Energy saved	Incremental initial costs
Heating	MWh	2.8	2.8	0%	$ -

Resource assessment

	Unit	
Solar tracking mode		Fixed
Slope	°	32.0
Azimuth	°	0.0

☐ **Show data**

Solar water heater

	Unit	Value		Incremental initial costs
Type		Glazed		$ 550
Manufacturer		Green Sun Rising		
Model		K420-DH		
Gross area per solar collector	m²	2.00		
Aperture area per solar collector	m²	2.00		
Fr (tau alpha) coefficient		0.70		
Fr UL coefficient	(W/m²)/°C	4.90		
Temperature coefficient for Fr UL	(W/m²)/°C²			
Number of collectors		2	1	
Solar collector area	m²	4.00		
Capacity	kW	2.80		
Miscellaneous losses	%	5.0%		

Balance of system & miscellaneous		
Storage		Yes
Storage capacity / solar collector area	L/m²	46
Storage capacity	L	184.0
Heat exchanger	yes/no	No
Miscellaneous losses	%	5.0%
Pump power / solar collector area	W/m²	5.00
Electricity rate	$/kWh	0.150

Summary		
Electricity - pump	MWh	0.0
Heating delivered	MWh	2.2
Solar fraction	%	81%

Heating system				
☐ Project verification		Base case	Proposed case	
Fuel type		Electricity	Electricity	
Seasonal efficiency		95%	95%	
Fuel consumption - annual	MWh	2.9	0.5	MWh
Fuel rate	$/kWh	0.150	0.150	$/kWh
Fuel cost	$	434	81	

☑ Emission Analysis

Base case electricity system (Baseline) Country - region	Fuel type	GHG emission factor (excl. T&D) tCO2/MWh	T&D losses %	GHG emission factor tCO2/MWh
Israel	Coal	0.840	5.0%	0.884

GHG emission					
Base case	tCO2	2.6			
Proposed case	tCO2	0.5			
Gross annual GHG emission reduction	tCO2	2.1			
GHG credits transaction fee	%				
Net annual GHG emission reduction	tCO2	2.1	is equivalent to	0.4	Cars & light trucks not used

GHG reduction income		
GHG reduction credit rate	$/tCO2	

Financial Analysis

Financial parameters			
Inflation rate	%	8.0%	
Project life	yr	10	
Debt ratio	%		
Initial costs			
Heating system	$	550	100.0%
Other	$	0	0.0%
Total initial costs	$	550	100.0%
Incentives and grants	$		0.0%
Annual costs and debt payments			
O&M (savings) costs	$	0	
Fuel cost - proposed case	$	85	
Other	$		
Total annual costs	$	85	
Annual savings and income			
Fuel cost - base case	$	434	
Other	$		
Total annual savings and income	$	434	
Financial viability			
Pre-tax IRR - assets	%	76.1%	
Simple payback	yr	1.6	
Equity payback	yr	1.4	

Cumulative cash flows graph

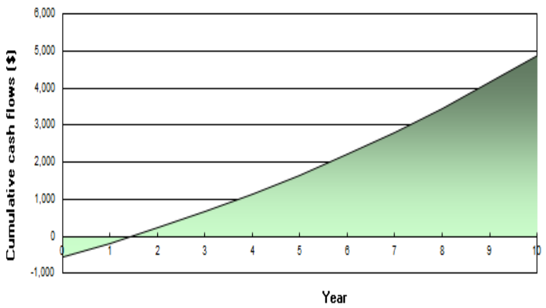

Appendix 4

Matlab code for simulate the SWHS in Palestine

```
%this script used to plot the hourly efficiency for SWHS,hourly solar fraction,hourly water temperaure inside the tank, and performance curve for
% a typical flat plate collector in Palestine.
clc
clear
close all
Ac=5.1                 % Flat Plate Collector Area(m^2).
beta=45                % Tilt Angle of Flat Plte Collector.
Cp=4186                % Water Specific Heat (J/(Kg.K)).
CP=inf                 % Bond Conductance(W/m.C).
D=12.5                 % Tube Outside Diameter(mm).
delta=0.5              % Plate Thickness(mm).
ec=0.8                 % Glass Emittance.
ep=0.8                 % plate emittance.
flow_rate=0.055        % Fluid Flow Rate.
Hfi=300                % Heat Transfer Coefficient Inside Tube(W/m^2.C).
initial_water_temp=20  % Initial Water Temperature (C).
lcap = 8               % Loss Coefficient Area Product for storage tank (W/C).
m_tank=180             % Size of Tank (L).
n=1                    % Number of Galss Cover.
ptc=385                % Plate Thermal Conductivity.
tau_alpha=0.85         % Transmitance absorbtance of the collector.
W=115                  % Distance between risers (mm)
% define the variables
qu=zeros(1,10);
T_in_water=initial_water_temp;
S=tau_alpha*Intensity;
water_temp=zeros(1,10);
collector_efficiency =zeros(1,2);
qu_n=zeros(1,365);
Ls_n=zeros(1,365);
r_n=zeros(1,365);
I_n=zeros(1,365);
collector_efficiency_n=zeros(1,365);
r=Intensity;
z=1;
loss_coefficient=zeros(1,10);
heat_removal=zeros(1,10);

% Start iteration for 8760 hours

for i=1:8760
if i>1
    % Call mean plate temperature function
[mean_plate_temp]=mean_plate_tempn(water_temp(i-1),qu(i-1),Heat_Removal_Factor,ul);
end
if i==1
    mean_plate_temp =initial_water_temp+10;
end
    % Call top loss coefficient function
[ ~,ul ] = top_loss_coefficient( n,hw(i),beta,ep,ec,ta(i),mean_plate_temp);
ul=ul*1.2;
loss_coefficient(i)=ul;
    % Call collector efficiency function
[collector_efficency_factor]=collector_efficency_factor_fcn( ul,ptc,delta,W,D,CP,Hfi);
```

```
[Heat_Removal_Factor,Flow_Factor ]=Heat_Removal_Flow_Factor( ul,Ac,collector_efficency_factor,flow_rate,Cp );
heat_removal(i)=Heat_Removal_Factor;
qu(i)=Heat_Removal_Factor*(S(i)-(ul*(T_in_water-ta(i))));

if qu(i)<0
    qu(i)=0;
end

if i==1
Ls=water_consumption*(Cp/3600)*(30-ta(i));
end
if i>1
    Ls=water_consumption*(Cp/3600)*(water_temp(i-1)-ta(i));
end
T_in_water = initial_water_temp+((1/(m_tank*(Cp/3600)))*((Ac*qu(i))-Ls(i)-(lcap*(initial_water_temp-ta(i)))));
 if T_in_water < max(ta) %to dispose from efficiency inf value
     T_in_water=max(ta)-8;
 end
initial_water_temp=T_in_water;
water_temp(i)=T_in_water;

if Intensity(i)==0
    r(i)=1;              %to dispose from efficiency NaN value
end
T_out_water(i)=((exp((-1*Ac*ul*collector_efficency_factor)/(flow_rate*Cp)))*(T_in_water-ta(i)-(S(i)/ul)))+(ta(i)+(S(i)/ul));

end
collector_efficiency=qu./r;
% ##########################################################################################
%to find the monthly qu and Ls and r
for p=1:365
I_n(p)=sum(Intensity(z:z+23));%KWH/Day
qu_n(p)=sum(qu(z:z+23));
Ls_n(p)=sum(Ls(z:z+23));
r_n(p)=sum(r(z:z+23));
collector_efficiency_n(p)=qu_n(p)/r_n(p);
z=z+24;
end


Qu=(Ac*qu_n);%KWH/Day
%###########################################################################################
%to find the daily q load
zr=1;
ta_n=zeros(1,365);
q=zeros(1,365);
for p=1:365
ta_n(p)=mean(ta(zr:zr+23));
zr=zr+24;
end
for i=1:365
q(i)=(4186*180*(55-ta_n(i)))/3600;
end
```

```
S_F=Qu./q;
for g1=1:365
   if S_F(g1) > 1
     S_F(g1)=1;
   end
end

A_S_F=mean(S_F)
%###############################################################################################
%ECONOMICAL STUDY %to find the daily solar energy
Annual_expenses_without_solar_heater = sum((q/1000)*.6)

Annual_expenses_with_solar_heater = sum(((q/1000).*(1-S_F))*.6)

%###############################################################################################
%to find the annual collector efficiency.
annual_collector_efficiency=sum(qu)/sum(Intensity)

%###############################################################################################
%to Plot solar intensity, water inlet temperature, efficiency, solar fraction
subplot(4,1,1);
plot(hor_radiation);
title('Time vs Intensity')
 axis([0 8760 0 1000]);
subplot(4,1,2);
plot(water_temp,'r')
title('Time vs Water inlet temp')
 axis([0 8760 0 120]);
subplot(4,1,3);
plot(collector_efficiency)
title('Time vs efficiency')
 axis([0 8760 0 1]);
 subplot(4,1,4);
plot(S_F,'r')
title('Time vs Solar fraction')
axis([0 365 0 1]);
%################################################################################################
% To find the performance efficiency curve
figure
x=zeros(1,10);
for i=1:500
x(i)=(water_temp(i)-ta(i))/Intensity(i);
if x(i)~=inf
    if collector_efficiency(i)~=0
plot(x(i),collector_efficiency(i),'*r');
hold on
    end
end
end
%################################################################################################
% mean plate temperature function
function [mean_plate_temp]=mean_plate_tempn(water_temp,qu,Heat_Removal_Factor,ul)
mean_plate_temp=water_temp+((qu/(Heat_Removal_Factor*ul))*(1-Heat_Removal_Factor));
end
```

```
function [ top_loss_coefficient_n,ul ] = top_loss_coefficient( n,hw,beta,ep,ec,ta,mean_plate_temp)
% beta:collector tilt
% ec:Glass emittance
% ep:plate emittance
% ta:ampient temperature(K)
% tp:mean plate temperature (K)
% hw:wind heat transfer coefficient [W/m^2.C]
ta=ta+273;
mean_plate_temp=mean_plate_temp+273;
sigma=5.66*10^-8;
F=(1+.089*hw-0.1166*hw*ep)*(1+.07866*n);
C=520*(1-.000051*beta^2);
E=.43*(1-100/mean_plate_temp);
A1=((C/mean_plate_temp)*((mean_plate_temp-ta)/(n+F))^E);
A2=(sigma*(mean_plate_temp+ta)*((mean_plate_temp^2)+(ta^2)));
A3=(1/(ep+(.00591*n*hw)));
A4=((2*n+F-1+.133*ep)/ec);
top_loss_coefficient_n=(((n/A1)+(1/hw))^-1)+(A2/((A3)+(A4)-n));
ul=top_loss_coefficient_n+2.5;
end
%##############################################################################################
% Collector efficiency factor function
function [collector_efficency_factor] = collector_efficency_factor_fcn( ul,ptc,delta,W,D,CP,Hfi)
% ul=total loss coefficient[W/m^.C] ptc=plate thermal conductivity[W/m.C]
% delta=plate thickness[mm] W=tube spacing[mm] D=tube inside diameter[mm]
% Cp=bond conductance[W/m.C] Hfi=heat transfer coefficient inside
% tube[W/m^2.C]
delta=delta*10^-3;
W=W*10^-3;
D=D*10^-3;

M=sqrt(ul/(ptc*delta));
F=(tanh(M*(W-D)/2))/(M*(W-D)/2);%Fin efficiency factor

%to find the collector efficiency factor
a=1/ul;
b=1/(ul*(D+(W-D)*F));
c=1/CP;
d=1/(pi*D*Hfi);
collector_efficency_factor=a/(W*(b+c+d));
end
%#############################################################################################
% Heat removal and flow factor function
function [ Heat_Removal_Factor,Flow_Factor ] = Heat_Removal_Flow_Factor( ul,Ac,collector_efficency_factor,flow_rate,Cp )
%ul=top loss coefficient
%Ac=Area collector
%collector_efficency_factor=collector_efficency_factor
%flow_rate=flow_rate for water (m.)
%Cp=specific heat for water
Heat_Removal_Factor= ((flow_rate*Cp)/(Ac*ul))*(1-exp((-1*Ac*ul*collector_efficency_factor)/(flow_rate*Cp)));
Flow_Factor=Heat_Removal_Factor/collector_efficency_factor;
end
```

Appendix 5

Data sheet for PV-modules 10W, 20W, 30W

PV module (10 W) data sheet:

10W Photovoltaic module

410J

Module appearance may vary.
Cells have rounded corners with either 165 or 150mm diameter.

Our latest generation of small area modules offers the following benefits:

Built to last

From mountaintops to off-shore platforms, on weather stations in the bitter cold of Antarctica and on telephone signal repeaters in the hot Australian outback, the technology has been proven in the harshest environments.

Accessible junction box for off grid connections

J-type junction box has accessible terminals for easier module interconnections in off grid applications, and it allows fitting cable glands for various cable sections.

Improved reliability with effective cooling

Cell interconnections and diode placement use well-established industry practice and are field-proven to provide excellent reliability.

Thick, durable, scratch resistant back sheet

The thick back sheet provides extra insulation and increased resistance to protect your module against rough handling. The white polyester material lasts longer and increases energy production.

Electrical characteristics

	(1) STC 1000W/m²	(2) NOCT 800W/m²
Maximum power (P_{max})	10W	7.2W
Voltage at Pmax (V_{mpp})	16.8V	15.0V
Current at Pmax (I_{mpp})	0.59A	0.47A
Short circuit current (I_{sc})	0.65A	0.53A
Open circuit voltage (V_{oc})	21.0V	19.1V
Module efficiency	8.8%	
Tolerance Pmax	± 10%	
Nominal voltage	12V	
Efficiency reduction at 200W/m²	<5% reduction (efficiency 8.3%)	
Limiting reverse current	.65A	
Temperature coefficient of I_{sc}	0.105%/ °C	
Temperature coefficient of V_{oc}	-0.360%/ °C	
Temperature coefficient of P_{max}	-0.45%/ °C	
(3) NOCT	47 ±2 °C	
Maximum series fuse rating	1A	
Application class	Class C (according to IEC 61730-2007)	
Maximum system voltage	50V	

1: Values at Standard Test Conditions (STC): 1000W/m² irradiance, AM1.5 solar spectrum and 25°C module temperature
2: Values at 800W/m² irradiance, Nominal Operation Cell Temperature (NOCT) and AM1.5 solar spectrum
3: Nominal Operation Cell Temperature: Module operation temperature at 800W/m² irradiance, 20°C air temperature, 1m/s wind speed

All solar modules are individually tested prior to shipment; an allowance is made within our factory measurement to account for the typical power degradation (LID effect) which occurs during the first few days of deployment.

SES MAPPS Solar Module Mechanical characteristics

Solar cells	36 monocrystalline silicon cut cells connected in series
Front cover	High transmission 3.2mm (1/8") glass
Encapsulant	EVA
Back cover	White polyester
Frame	Silver anodized aluminum
Junction box	IP65 with 4 terminal screw connection block; accepts PG 13.5, M20 13mm (½") conduit, or cable fittings accepting 6-12mm diameter cable.
Terminals	accept 2.5-10mm2 (8-14 AWG) wire
Dimensions	425mm x 273mm x 50mm / 16.73 x 10.74 x 1.97in
Weight	1.9kg / 4.2lbs

All dimensional tolerances within ±1% unless otherwise stated.

Warranty*

- Free from defects in materials and workmanship for 2 years
- 90% Min power output for 12 years
- Optional 25 years available *Refer to limited warranty certificate for terms and conditions

SES MAPPS Solar Module Certification

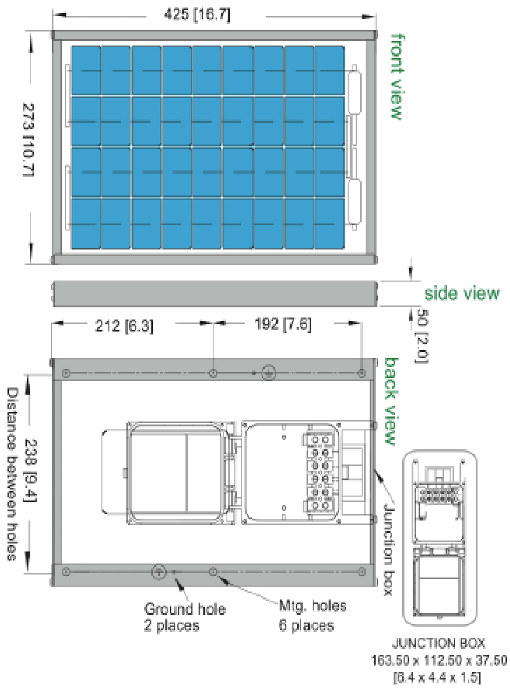

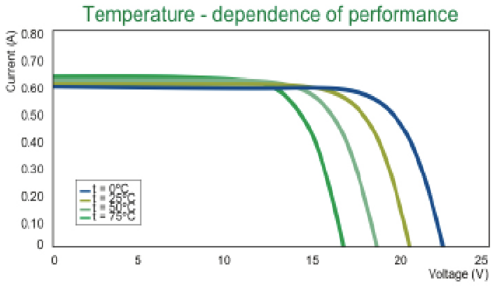

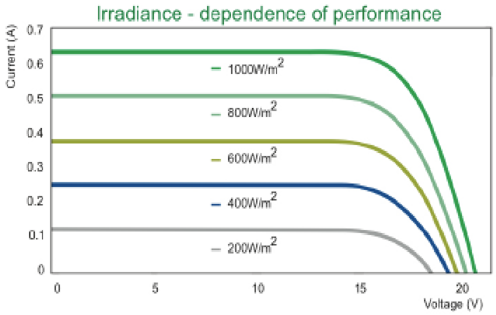

PV module (20 W) data sheet:

SOLAR ELECTRIC SUPPLY, INC.

SINCE 1998

Module appearance may vary.
Cells have rounded corners with either 165 or 150mm diameter.

20W Photovoltaic module

420J

Our latest generation of small area modules offers the following benefits:

Built to last

From mountaintops to off-shore platforms, on weather stations in the bitter cold of Antarctica and on telephone signal repeaters in the hot Australian outback, the technology has been proven in the harshest environments.

Accessible junction box for off grid connections

J-type junction box has accessible terminals for easier module interconnections in off grid applications, and it allows fitting cable glands for various cable sections.

Improved reliability with effective cooling

Cell interconnections and diode placement use well-established industry practice and are field-proven to provide excellent reliability.

Thick, durable, scratch resistant back sheet

The thick back sheet provides extra insulation and increased resistance to protect your module against rough handling. The white polyester material lasts longer and increases energy production.

Electrical characteristics

	(1) STC 1000W/m²	(2) NOCT 800W/m²
Maximum power (P_{max})	20W	14.4W
Voltage at Pmax (V_{mpp})	16.8V	15.0V
Current at Pmax (I_{mpp})	1.19A	0.95A
Short circuit current (I_{sc})	1.29A	1.04A
Open circuit voltage (V_{oc})	21.0V	19.1V
Module efficiency	9.4%	
Tolerance Pmax	± 10%	
Nominal voltage	12V	
Efficiency reduction at 200W/m²	<5% reduction (efficiency 8.9%)	
Limiting reverse current	1.29A	
Temperature coefficient of I_{sc}	0.105%/ °C	
Temperature coefficient of V_{oc}	0.360%/ °C	
Temperature coefficient of P_{max}	-0.45%/ °C	
(3) NOCT	47 ±2 °C	
Maximum series fuse rating	3A	
Application class	Class C (according to IEC 61730-2007)	
Maximum system voltage	20V	

1: Values at Standard Test Conditions (STC): 1000W/m² irradiance, AM1.5 solar spectrum and 25°C module temperature
2: Values at 800W/m² irradiance, Nominal Operation Cell Temperature (NOCT) and AM1.5 solar spectrum
3: Nominal Operation Cell Temperature: Module operation temperature at 800W/m² irradiance, 20°C air temperature, 1m/s wind speed

All solar modules are individually tested prior to shipment; an allowance is made within our factory measurement to account for the typical power degradation (LILD effect) which occurs during the first few days of deployment.

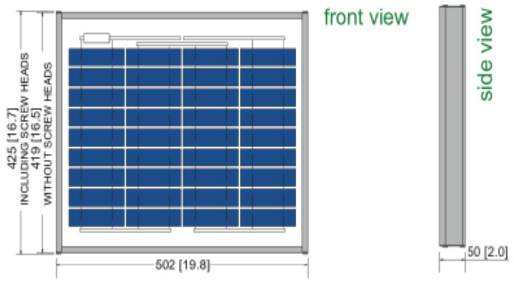

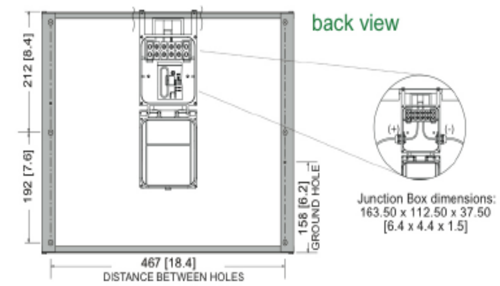

Dimensions in mm [in].

SES MAPPS Solar Module Mechanical characteristics

Solar cells	36 monocrystalline silicon cut cells in series
Front cover	High transmission 3.2mm (1/8") glass
Encapsulant	EVA
Back cover	White polyester
Frame	Silver anodized aluminum
Junction box	IP65 with 4 terminal screw connection block; accepts PG 13.5, M20 13mm (½") conduit, or cable fittings accepting 6-12mm diameter cable.
Terminals	accept 2.5-10mm2 (8-14 AWG) wire
Dimensions	839 x 537 x 50mm / 33.0 x 21.1 x 2in
Weight	6kg / 13.2lbs

All dimensional tolerances within ±1% unless otherwise stated.

Temperature - dependence of performance

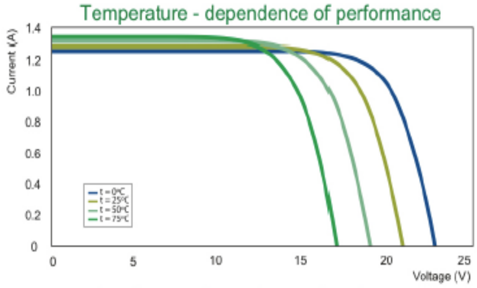

Irradiance - dependence of performance

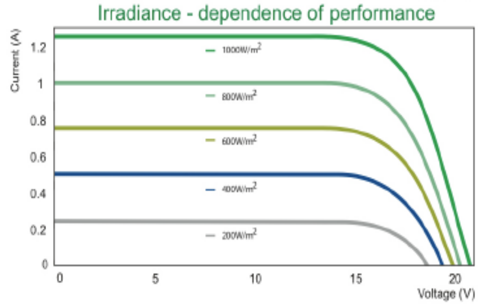

Warranty*

- Free from defects in materials and workmanship for 2 years
- 90% Min power output for 12 years
- Optional 25 years available *Refer to limited warranty certificate for terms and conditions

SES MAPPS Solar Module Certification

PV module (30 W) data sheet:

SOLAR ELECTRIC SUPPLY, INC.
SINCE 1996

30W Photovoltaic module

330J

Module appearance may vary.
Cells have rounded corners with

Our latest generation of small area modules offers the following benefits:

Built to last

From mountaintops to off-shore platforms, on weather stations in the bitter cold of Antarctica and on telephone signal repeaters in the hot Australian outback, the technology has been proven in the harshest environments.

Accessible junction box for off grid connections

J-type junction box has accessible terminals for easier module interconnections in off grid applications, and it allows fitting cable glands for various cable sections.

Improved reliability with effective cooling

Cell interconnections and diode placement use well-established industry practice and are field-proven to provide excellent reliability.

Thick, durable, scratch resistant back sheet

The thick back sheet provides extra insulation and increased resistance to protect your module against rough handling. The white polyester material

Electrical characteristics

	(1) STC 1000W/m²	(2) NOCT 800W/m²
Maximum power (P_{max})	30W	21.6W
Voltage at Pmax (V_{mpp})	16.8V	15.0V
Current at Pmax (I_{mpp})	1.78A	1.42A
Short circuit current (I_{sc})	1.94A	1.57A
Open circuit voltage (V_{oc})	21.0V	19.1V
Module efficiency	10.5%	
Tolerance Pmax	± 10%	
Nominal voltage	12V	
Efficiency reduction at 200W/m²	<5% reduction (efficiency 10%)	
Limiting reverse current	1.94A	
Temperature coefficient of I_{sc}	0.105%/ °C	
Temperature coefficient of V_{oc}	-0.360%/ °C	
Temperature coefficient of P_{max}	-0.45%/ °C	
(3) NOCT	47 ±2 °C	
Maximum series fuse rating	5A	
Application class	Class C (according to IEC 61730-2007)	
Maximum system voltage	50V	

1: Values at Standard Test Conditions (STC): 1000W/m² irradiance, AM1.5 solar spectrum and 25°C module temperature
2: Values at 800W/m² irradiance, Nominal Operation Cell Temperature (NOCT) and AM1.5 solar spectrum
3: Nominal Operation Cell Temperature: Module operation temperature at 800W/m² irradiance, 20°C air temperature, 1m/s wind speed

All solar modules are individually tested prior to shipment; an allowance is made within our factory measurement to account for the typical power degradation (LILD effect) which occurs during the first few days of deployment.

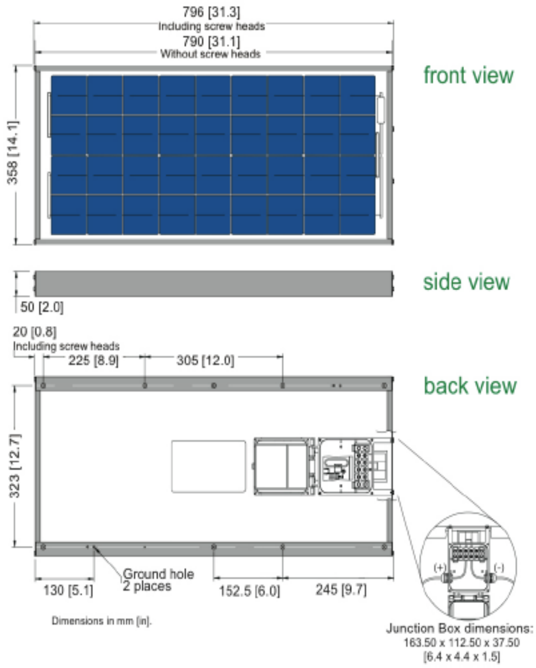

SES MAPPS Solar Module Mechanical characteristics

Solar cells	36 polycrystalline 3" silicon cells in series
Front cover	High transmission 3.2mm (1/8") glass
Encapsulant	EVA
Back cover	White polyester
Frame	Silver anodized aluminum
Junction box	IP65 with 4 terminal screw connection block; accepts PG 13.5, M20 13mm (½") conduit, or cable fittings accepting 6-12mm diameter cable.
Terminals	accept 2.5-10mm2 (8-14 AWG) wire
Dimensions	796 x 358 x 50mm / 31.3 x 14.1 x 2in
Weight	3.9kg / 8.6lbs

All dimensional tolerances within ±1% unless otherwise stated.

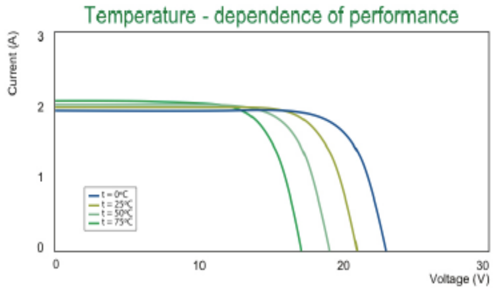

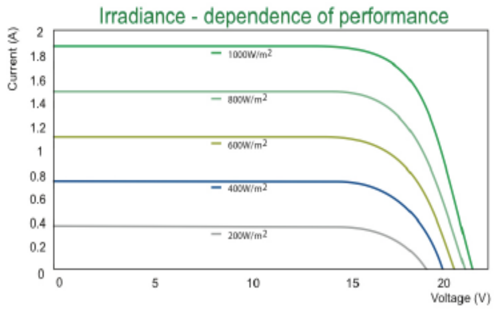

Warranty*

- Free from defects in materials and workmanship for 2 years
- 90% Min power output for 12 years
- Optional 25 years available *Refer to limited warranty certificate for terms and conditions

SES MAPPS Solar Module Certification

جامعة النجاح الوطنية
كلية الدراسات العليا

تحسين كفاءه السخان الشمسي باستخدام مضخه تعمل بالطاقه الشمسيه

اعداد
محمود عبد اللطيف محمود ابو عره

اشراف
أ.د.مروان محمود

قدمت هذه الاطروحة استكمالا لمتطلبات الحصول على درجه الماجستير في هندسة الطاقة النظيفة واستراتيجية ترشيد الإستهلاك بكلية الدراسات العليا في جامعة النجاح الوطنية، نابلس، فلسطين.

2017

تحسين كفاءه السخان الشمسي باستخدام مضخه تعمل بالطاقه الشمسيه

اعداد

محمود عبد اللطيف محمود ابو عره

اشراف

أ.د.مروان محمود

الملخص

تهدف هذه الدراسة الى تحليل أثر المضخة الشمسية اللتي تعمل على نقل السائل داخل السخان الشمسي على الكفاءه الكليه للسخان الشمسي, من اجل الوصول الى هذا الهدف تم اختيار العديد من النماذج الرياضية لكل من السخان الشمسي و المضخة الشمسية و صهريج تخزين المياه . بعد ذلك تم تحليل هذه النماذج باستخدام برنامج ماتلاب, و من الجدير بالذكر فان معظم انظمه السخانات الشمسية المستخدمة في فلسطين تعمل على مبدا دوره المياه الطبيعيه حسب درجة حراراة المياه. وبناء على ذلك تقترح الدراسه بأن يتم تزويد هذه الانظمة بمضخة تعمل على الطاقة الشمسية لنقل السائل بحيث يزيد من فعالية السخانات المستعمله وهذا يمثل المساهمة الحقيقيه لهذه الدراسة. استنتج الباحث بان اضافه مثل هذه المضخة للأنظمه المستخدمه في تسخين المياه في فلسطين يزيد من كفاءه نظام التسخين من 33 % الى 37 %. وأستنتج الباحث ايضا أن استخدام المضخة بالاضافة الى لوحي تسخين يعادل استخدام ثلاث الواح تسخين من انتاج الطاقة, و بالاضافة الى ذلك فان اضافة مضخة شمسية يزيد من فعاليه تسخين النظام الشمسي للمياه (Solar fraction) من 76 % الى 86 % خاصة في فصل الشتاء وهذا يعني الزياده في امتصاص الطاقة المنبعثه من الشمس واستهلاك اقل للكهرباء.